ニアネット成形部品の仕上げ加工のための熱モニタリングに関する研究

Doctoral Dissertation:

Research on Thermal Monitoring for Finish Machining of Near Net Shape Parts

Dongjin Wu

Muroran Institute of Technology

March.2018

Title:

Research on Thermal Monitoring for Finish Machining of Near Net Shape Parts

Name: Dongjin Wu

Supervisor: Professor Koji Teramoto

Associate supervisor: Professor Yoshihisa Aizu

&

Professor Toshiharu Kazama

School: Muroran Institute of Technology

Date:23/03/2018

Abstract

The objective of this research is to investigate an appropriate monitoring method to secure the accuracy of finish machining.

The development of complex 3-dimensional shape products for industrial applications has been one main goal for manufacturing industries over the last few decades. Conventional processes such as injection molding, forging, and casting and assembly technologies are typical processes that have contributed to achieve mass production. Recently, various small-lot near-net shape production methods such as additive manufacturing, thin-wall casting, and incremental forming are proposed and become common in industry. Because these near-net shape parts are often complex shape, these parts are finished by manual operation. Therefore, a systematic finish machining method for complex 3-dimentional parts for small-lot production is eagerly desired.

Because end-milling has advantages like efficiency, accuracy, and applicability to small-lot production, this technology is very widespread application in aerospace, automobile and other manufacturers. Therefore, end-milling is expected as a promising machining method for finish machining of near net shape parts. However, accuracy assurance of end-milling has not achieved. Especially, thermal monitoring in process has not been caught easily by traditional detect method, such as thermocouple measurement system or wireless thermographic technology.

Heat generation and heat transfer characteristics in the cutting process are strongly affected from the cutting process. As a modern technology, finite element simulation can be used to reproduce the machining process. It can be used to study the stress and strain,

temperature distribution, chip breakage and friction and heat generation characteristics of the cutting area which are difficult to be observed in processing. In this thesis, the combination method of local temperature measurement and finite element simulation is used to investigate the estimation of temperature distribution in machining process. The main contents are as follows.

Firstly, trends of recent production are summarized as a background of this research. Roles of monitoring in information driven and connected production are explained. Moreover, related researches about thermal analysis in end-milling, measurement technology development, FEM analysis, and combination of measurement and simulation are surveyed.

Secondly, a framework for temperature measurement is proposed. Based on considerations of process variety, a concept of measurement point evaluation is explained. This research presents a method to evaluate an effectiveness of each measuring points from aspects of stability of measurement and sensitivity to the process variation.

Thirdly, developed systems to evaluate the proposed framework are explained. A thermal analysis method of end-milling is explained, and details of developed simulation system are illustrated. Developed 3D finite element (FE) models are constructed based on commercial FE software to simulate the macroscopic workpiece behavior. After discussing a representation method of process variation, evaluation procedures of measurable points are illustrated. The proposed evaluation method of measuring points is evaluated based on the case studies.

Lastly, conclusion of dissertation is described.

Key words: near-net shape parts, small-lot manufacture, end milling temperature, thermal expansion, monitoring method

Acknowledgments

I would like to express my sincere gratitude to my advisor, Dr. Teramoto, for his guidance, encouragement and support during my studies at Muroran Institute of Technology. Thanks to the faculty and students of the Manufacturing Engineering Laboratory for their help and support to this research. I appreciate the partial financial support from the KAKENHI Grant Number 26420038.

Most of my daily life was support by Japan government scholarship, which I had this opportunity to contrate my focus on my research, A lot of learning gradually about end milling process with many help from my professor, he continuing gives me lectures once and once, and also I had a luck opportunity to Makino machining company for internship, I broaden my eyes to see what is happened in thermal expansion when we deal with accurate machining center, and what the bad influence to operated machines, tools and finished parts, for me, it was really good experience for my research step. I fell my burden, as researcher, do research is the backup of technology company, and also will changing our lives.

Three years passed quickly and slowly, sometimes, I felt lonely after I am leaving motherland, but their support and understanding push me walking further and further; from many good friends' encouraging around me, I known that I am a fighter. I cannot finish doctoral course without the great support of teachers, family and friends.

With thousands of thanks to everyone who helped me.

Outline of contents

1 Introduction

Near net-shape (NNS) are used in many manufacturing, the desired outcomes of manufacturability analysis for near-net-shape processes are cost and time reduction through minimization of process steps (in particular cutting and finishing operations) and raw material saving. For example, near net forming technology has advantages like high effective and low cost, this technology is very widespread application in aerospace, automobile and model manufacturers. Moreover, it is well known that additive manufacturing is widely interested and investigated as a next generation production technology. Besides the various NNS technologies are constantly improving and evolving, there still is challenge in accurately reflecting their requirements and capabilities. Therefore, a finish machining for NNS parts is still indispensable process.

Machining still remains a major industrial activity despite recent significant developments in near-net shape forming techniques[1]. We are chasing much accuracy, agile production and monitor-able in small lot manufacturing, as the manufacturing development cannot leave the advanced manufacturing technology, and advanced manufacturing technology is the core and basis of high quality, high efficiency, low consumption, clean and pollution-free technique.

Conventional workpiece has large or medium batch, the simple shape and focus on common material. Conventional requirement of machining is high quality, low cost and due date (accuracy, zero defect, agility). End-milling is satisfied with the requirement of high quality and agile production. However, when we meet the emergent workpiece, like the small batch, complex shape, hard and new material, the additional requirements are appeared. Moreover, new requirements such as traceability, environmental issues and

workers' safety are also needed to adapt..

Recently, network connected and information driven manufacturing based on modern information technologies such as IoT (Internet of Things), Cloud computing technology and CPS (Cyber-Physical System) become a realistic solution[2]. In such an emergent manufacturing system, agile and smart adaptation to changeable demands must be accomplished[3]. It is reported that a closed loop machining using on-machine shape measurement can achieve an accuracy assured machining [4-6].

With the development of new machine tools and related equipment, advanced cutting tool material development, the cutting technology towards a more efficient, practical direction. A growing concern in the aerospace, automotive and biomedical industrial segments of the manufacturing industry is to build in absolute reliability with maximum safety and predictability of the performance of all machined components [7], as we humans can pursue high precision and most perfect prediction to the machined parts.

As the finish machining methods, end-milling is a promising method because of its versatility and effectivity. Because thermal behavior influenced the accuracy of finished parts, it is important to understand and control the thermal behavior during finish process. When the thermal situation in finish machining is well controlled, components can be reliably fabricated with desired material properties.

Thermal issues in end-milling have been investigated for many years. For example, a simulation research about heat generated in end milling are reported. In the research, evaluation of a dimensional error of finish workpiece depending on experiment and analysis has been investigated[8]. After many years studying, influence of tool thermal expansion has been also investigated and summarized in many published papers. However, monitoring temperature in process is not easily caught by traditional detect method, such

as thermocouple measurement system or wireless thermographic technology.

1.1 Background

Smart manufacturing will integrate these parts of automation, enabling data sharing throughout the simulation. The convergence between machine-gathered data and human intelligence will advance manufacturing engineering, including substantial increases in economic performance, worker safety and environmental sustainability. Smart manufacturing marries information, technology and human ingenuity to bring about a rapid revolution in the development and application of manufacturing intelligence to every aspect of business. It will fundamentally change how products are invented, manufactured, shipped and sold. It will improve worker safety and protect the environment by making zero- emissions, zero-incident manufacturing possible. It will help keep jobs in this country by keeping manufacturers competitive in the global marketplace despite the substantially higher cost of doing business in the world.

Near net forming technology is through the precise mold design, strict control of hot processing technology parameters, and a reasonable forming process to produce without processing or only a small amount of processed parts of the process. It does not need or only a small amount of follow-up processing, in reducing the production cycle and save raw materials but also can greatly reducing production costs at the same time, it will effectively promote the application of small lot production. With the development of aviation and aerospace industry, the precision forming of complex shape components has replaced the traditional "multi-piece connection" structure and "forging-cutting" production mode has become an inevitable trend. New net forming technology is one of the future developments of manufacturing industry trend.

The application of near net forming will play an important role in the future

manufacturing industry. The use of near net forming technology to solve the difficult problem of alloying will be an efficient and fast way. Such as in the field of aerospace, titanium and titanium alloy because of its high strength, light density, plasticity and other characteristics, is good to meet the new materials, new technical conditions on the material requirements. However, there also has three factors of near net shape parts are looking forward to greater progress，

(1)   Laser engineered net shaping-LENS is this century in many parts of the world have developed an advanced manufacturing technology, this technology send synchronous powder laser multi-layer welding compound technology with rapid prototyping technology, can achieve high performance, compact, rapid prototyping manufacturing of complex parts. But, In the process of HIP, the powder can be compressed, deformed and the boundary is variable, and the precise simulation of complex structure is needed in the constitutive model, material parameter, and finite element solution and so on

The numerical simulation of the process temperature field is used to further understand the variation law of the forming degree field and provide the theoretical basis for the forming experiment. The study of the temperature field of the laser solvated temperature field is also helpful to establish the temperature field model of the lens process. In recent years, there are many researches on the numerical simulation of the laser coating process and the LENS process temperature field. The study of the temperature field simulation of laser salvations also helped to establish the temperature field model of the LENS process.

Research status:

In 1992，A. F. Hoadley comes from Swiss Federal Institute of Technology [9] ,who proposed the two-dimensional finite element model of powder-coated laser cladding and

4

the quasi-steady-state temperature field of the longitudinal section of the coating was obtained. The results show that the laser power and scanning speed are linearly related to the height of the cladding coating

In 2003，American corning Lasertron company's M Labudovice et al. [10], used the capabilities of ANSYS parametric design language and calculates transient temperature profiles, dimensions of the fusion zone and residual stresses, experiments showed good agreement with the modeling.

In 2004, the Italian University of Science and Technology, Palumbo, G., S et al.[11] used software to establish a three-dimensional finite element model of laser single-channel over-alloying on alloy ring parts. Calculated to solve the problem. The distribution of stress and strain in the process of the coating process was evaluated when the dilution rate and the change of the bath morphology were analyzed. Since 2004, the University of Canada, such as the University of Waterloo [12] using the laser column and the process of simulation and experimental study, pray for the pulse laser shaping process on the impact.

In 2006, University of California R. Q. Ye. et al..[13], A three-dimensional finite element model for the preparation of non-induced steel slabs was established by ABAQUS. The variation of temperature and temperature gradients near the pool was analyzed. The two-dimensional finite element model of stainless steel sheet was fabricated by Mississippi State University, and the distribution of temperature field in forming process was obtained. The influence of laser power on temperature field was analyzed. The experimental results were in accordance with the simulation results.

In 2009，Y.H. Xiong et al. of University of California, USA[14], the three-dimensional finite element model of Wc-Co ceramic metal thin-walled parts was established. The size of the solution was calculated by high-speed camera, the correctness of the model was

verified, and the temperature, cooling rate and temperature gradient near the molten pool were further studied. The simulation results explain the variation of microstructure of thin-walled parts.

In 2010, J.H. Yang et al. From Swinburne University of Science and Technology, who established a three-dimensional finite element model of laser heating alloy, analyzed the influence of different process parameters and material properties on heat influence size. The results show that with the increase of laser power, the depth and width of the heat affected zone will increase. With the increase of the spot diameter and the scanning speed, the depth and width of the heat affected zone will decrease, and the process parameters of the heat control zone size will be found by simulation.

In 2011, the United States Utah State University C Zhang and others used software to establish a laser multi-channel solution super alloy dimensional finite element die spray, to predict the multi-channel lamination process towel temperature field and stress field, pointed out that the hot crack generated. The results are consistent with the simulation results[15]. A 3-D transient finite element (FE) model has been developed and a thermomechanical analysis is performed. The developed thermal model has been applied to predict and analyze the distribution of thermal stress concentration and the tendency of stray grain formation.

(2) Additive Manufacturing (AM) is an appropriate name to describe the technologies that build 3D objects by adding layer-upon-layer of material, whether the material is plastic, metal, concrete or one-day human tissue. There are several solid freeform fabrication (SFF) techniques [16]including 3D printing, ink-jet printing, fuse deposition modeling of ceramics based on layer by layer deposition using 3D model image.

Thin-walled composite components, also better known as die casting, creates parts

that are stronger and lighter than those of other casting methods.

(3) The key to the precision forming of thin-walled composite components is that there are also a lot of hard-to-handle control of microstructure and metal flow control.

These three factors meet the high demand of produce a broad range of parts with perfect finish and astonishing detail. Many key components used in the small lot production are made of difficult machining processing and diffident materials, Alloy in the near net forming technology like the application will be greater development. Above three near net shape applications meet some problems, such as small batch, complex shape and hard material, etc. at these atmosphere, thermal issues cannot be solved by simulation only.

Finished parts from near net manufacturing need to face some problems, like complex shape from servo press, hard material from laser machining and thin wall from thin casting , and so on. In conventional approaches to solve the post processing, employing the end milling process is wildly accepted in manufactures. In the end-milling, the thermal phenomena is the common problem in finished parts. Therefore, we are considering to estimate temperature distribution in end milling is to support finish machining of near net shape parts.

1.2 Small-lot manufacturing

Quiet a large proportion of industrial products are manufactured by processes that shear and form standard shapes, largely sheet metal, into finished parts. In general, shearing and forming are all that are required some secondary operations, such as cutting, drilling, tapping and milling, or even welding, to appropriately prepare it for assembly in to wanted product. However, the near-net-shape characteristics of the results of these processes make them an extremely cost-effective alternative for producing a product or component[17].

Small-lot production is a transitional form between unit production and the

7

manufacture of products in moderate-sized lots. The sizes of the lots vary. The scale of the product is limited to existing orders or contracts. For this reason, the manufacture of a particular product ends comparatively quickly, and a new product is then introduced into manufacture. Small-lot production is used, for example, in the manufacture of some special-purpose alloys, rolled products, the production of additive manufacturing, thin-wall casting, and incremental forming in the manufacture of small lots of articles or machines intended for experimentation under various conditions. Small-lot production differs from experimental production, which is generally limited to the manufacture of a single sample.

During the cold war, the nuclear weapons complex produced thousands of components each year to support the stockpile. The manufacturing process stream had high production capacity but not always high yields[18]. As seen in Figure 1 A qualified process and what can go wrong(b), problems that can arise when one tries to develop qualified process must be compensated. In order solving a series of blind points in dynamics process which are poorly understood and not monitored, in-process monitoring and control became essential to small-lot manufacturing. To achieve in-process monitoring and control, we must employ the data reduction methods to find the key signatures that might identify the presence of specific faults. Therefore, we should introduce some signatures to develop learning algorithms that only identify the faults but also classify their causes.
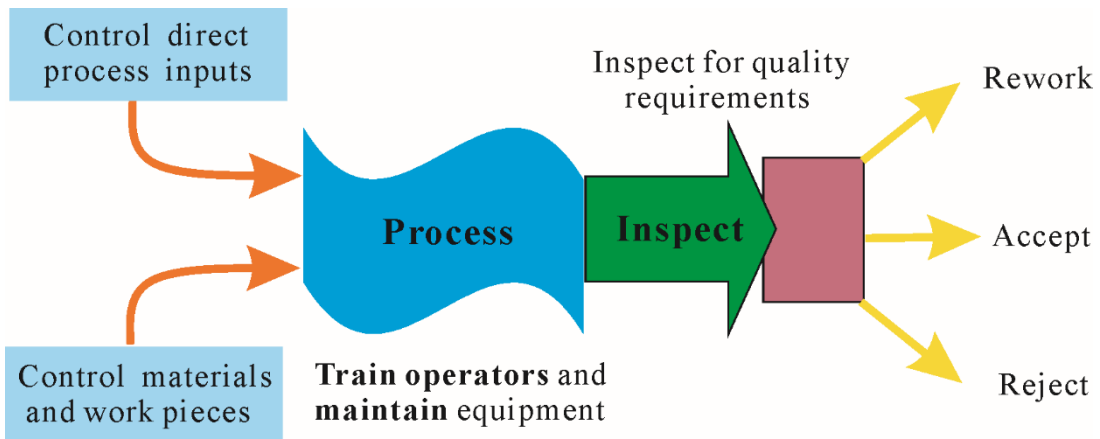
(a)
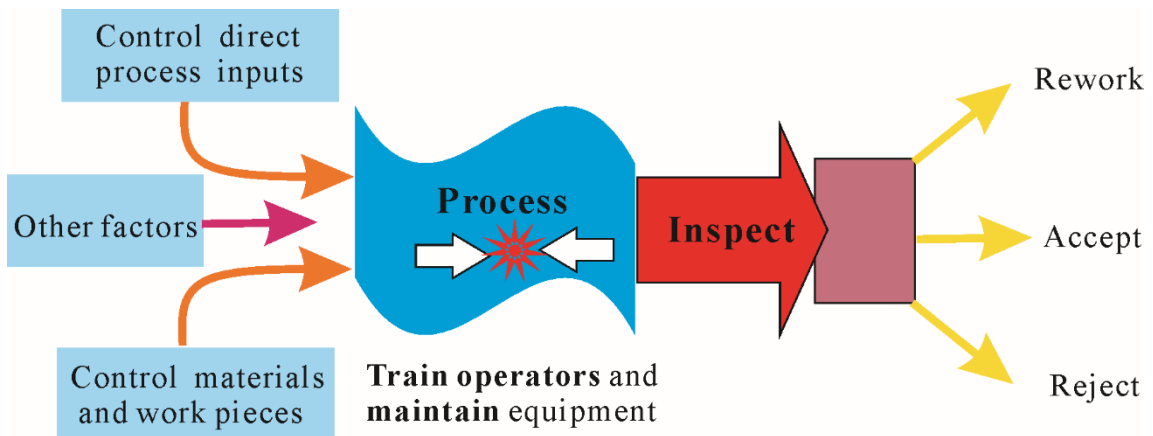
(b)

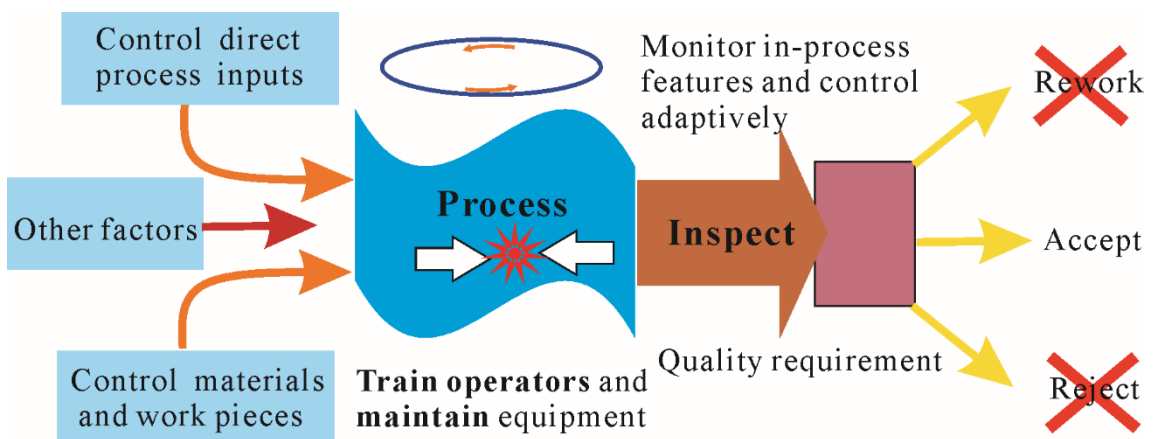**Figure 1 A qualified process and what can go wrong**

Figure 2 In process monitoring and control

In the recent years, there are increasing demands for small lot production technologies to deal with diversifying needs and rapid forming tool production technologies to survive in global competition on the development of new products. Improvements of machining technologies are necessary. For example, the sheet metal forming technique, which is typical mass-production method requires the rapid production [19].

1.3 Thermal simulations applied in machining process

Finite element (FE) simulation of machining can be used as a replacement or a supplementary to the conventional experiment allowing an analysis to be performed at a lower cost. With the rapid development of computer technology and the theory of numerical analysis, the finite element simulation is more and more widely used in machining process. Many commercial finite element software such as ABAQUS, Advantage, Deform, LS-DYNA and so on have become a powerful tool for metal cutting simulation. Thermal simulation in machining process is an active research topic in recent years, as the heat generated in the machining process has vital effect on both the quality of the workpiece and the life of the cutting tool. It also can shorten the time-to-market and reduce the cost of the machining process. However, the simulated thermal results in machining process are often unreliable due to the lack of quantitative material data, the parameters used in boundary conditions and other parameters used in the simulation process.

Maurel-pantel[20] uses DYNA software to perform 3D simulation of 304L stainless steel square shoulder milling. Man[21] proposed a three-dimensional explicit dynamic Lagrangian finite element model for predicting the overall force. Saffar[22] considered the effect of tool deformation on the cutting force in the model. The results of many researchers, such as stress, strain, temperature distribution and residual stress, can be obtained by using

finite element method in one cutting simulation, but the operation time of this method is long, especially for cutting and orthogonal milling class of the three-dimensional cutting process. This shortcoming is particularly evident. Due to the limitation of the simulation period, the finite element technology is not yet suitable for studying the influence of many different working conditions on the cutting force of 3D complex process. Cutting temperature field analysis modeling one of the pioneers Jeager[23] proposed the mobile heat source method in 1942.

The finite element method (FEM) has been employed to solve end milling dynamic models, experimental and analytical methods have been developed to estimate the values of fatigue and creak in end milling. It can reduce energy consumption for both cost saving and environmental friendliness[24]. As the rapid use of internet and simulation software,it is significately known that the simulation has played a much importment role in industry. From literatures,there are many research paper worte about the application of simulation in machining process,not only the cutter wore but also the application of workpiece thermal expansion.

Analytical modelling as opposed to the widely used FEM based modelling is much faster in computation time[25],in literautres there are provided several analytical and simulation approachs for temperature modelling in metal cutting[25], An analytical model for prediction of tool temperature fields in metal cutting processes has been developed[26].

In the field of manufacturing engineering, the computer simulation process is one of the important results, it uses the mathematical model for the required power, cutting force and chip formation. These computational models are of great value in reducing or even eliminating the number of iterations in tool design, process selection, workability estimation and chip breaking studies. In the past ten years, many studies of finite element

methods have been spent on modeling the performance of different types of diamond cutting problems. The earliest analytical model was made by Mer Chant Piispanen [27, 28], and Lee Shaffer [29]. The reason why the chip is crimped due to the contact between the tool nose and the chip is introduced[30]. Palmer proposed a model including the effect of component hardening and strain rate on the machining process [31, 32]. Doyle built a new viscoelastic model, which included the friction between the tool's rake face and the chips formed during the machining and the friction between the tool and the surface formed by the tool[33]. Trigger and Chao, the problem of heat caused by plastic deformation and friction is considered in the process in the analysis model [34]. Usui use energy methods to establish a model, this model takes into account the three-dimensional geometric conditions in the process of the impact[35].

In manufacturing engineering, using computer to simulate the manufacturing process is an important achievement, which calculates required power, cutting force and the forming of cutting by means of mathematical models. These calculated models can obviously reduce or even eliminate the repeated experiments in the design of tools, choosing of process, estimation of machinability and chip breaking research. In the past decades, the study on FEM are most about the numerical modeling of machinability of different cutting problems. The advantage of FEM is that it can be simulated the whole comlicated process automaticly. In 1973, B. E. Klameck[36] in Illinois University firstly studied the formation mechenism of chip in cutting process systematically. In 1980, M. R. Lajczok[37] in North Carolian University using FEM to analyze the major problems in maching procee in his doctoral dissertation. Usiui and Shirakashi[38], Iwata et al.[39], Strenkowsk and Carroll [40] was the prior researchers who used FEM to simulate the cutting process.

Usui and Shirakasih1[38] wanted to establish a steady-state orthogonal cutting model, the first proposed blade angle, chip geometry and streamline, etc., to predict the stress and strain and temperature of these parameters. Iwata et al. established a rigid body[39], plastic finite element model. The thickness of the chip, the shape of the crimp and the internal stress and strain distribution were calculated, and the effects of the material properties and the friction on the internal stress and strain were discussed. At the same time, the cutting test was carried out, and the test results also verified the simulation results. However, they did not consider the elastic deformation, so there is no calculation of residual stress.

In 1982, in order to build Orthogonal cutting model of the steady state, Usui and Shirakashi [38] firstly proposed cutting angle, chip geometry, flow line and et al., they predicted the parameters of stress-strain and temperature. Iwata[39], Streknows and Carroll [40] built new finite element model, which includes a chip separation criterion based on effective plastic strain. Some of the previously ignored cutting parameters are included in this finite element model, for example,they considered friction between the tool and the chip,and the tool is elastoplastic. The results show that the application of the chip separation criterion is very important and effective in the processing of finite element simulation components. In the future research, various chip separation criteria, such as K. Komvopoul and following, there were many criterion has being estimated. For example, S. A.Erpenbeck[41] "Distance tolerance" criterion, Z. E. Lln, S. Y. Lin set strain energy density criterion [42]. J. Hashemi, A. A.Tseng [43]built Separation criteria based on fracture mechanics. Huang and Black evaluated some of these criteria[44], they found that if the cutting process was stable, these criteria would not have a significant effect on the shape of the chip and the stress and strain distribution within the component. Komvopou1os and Erpenbeck used the Coulomb friction law to obtain the normal force and friction

13

between the tool and the chip by means of orthogonal cutting analysis. Komvopoulos and Erpenbeck used the Coulomb friction law to obtain the normal force and friction between the tool and the chip by means of orthogonal cutting analysis.

The elastic-plastic finite element model was used to study the effects of the side wear on the tool, the residual stress in the chip and the workpiece, and so on[41]. Furukawa and Moronuik studied The influence of finish on the surface quality of the workpiece in ultra - precision cutting of aluminum alloy by experimental method. The analysis shows that when the depth of cut is about 10^{-6}m, the minimum cutting force is in the range of about10^{-1}N[45]. Noyo Ikawa wrote the interaction between the chip formation and the depth of cutting of the red copper material was measured by a precision cutting machine. The depth of the cutting used in the experiment was 10^{-9}m[46]. Toshimichi Moriwaki et al. Used the steel-plastic finite element model to simulate the above experiments [47]. They simulated the depth of the diamond in the range of millimeters to nanometers in the process of orthogonal cutting. The effect of cutting depth and cutting speed on residual stress in orthogonal ultra-precision cutting of NiP alloy was studied by Zone Chinglin et al. of Taiwan University of Science and Technology. The model of flow stress of the material was obtained by regression analysis of the unidirectional tensile test data before the simulation, they built the thermoelastic and plastic finite element model considering the thermal effect in the cutting process[48].

But the above studies are mainly considered a number of aspects of the process, more importantly, it is based on their own research on the preparation of a model for the finite element program. And they did not form a professional business process for cutting. Because the preparation of a finite element program is a very heavy task, so the effective

14

application of existing finite element business software for cutting numerical simulation is particularly important.

1.4 Machining process monitoring

There are many reasons for installation of monitoring system in a manufacturing process. A machine tool operator performs routine monitoring tasks, for example, visually detects missing and broken tools as well as its sound characteristic. Monitoring and control of manufacturing process is becoming nowadays a driver for development and sustainability of manufacturing industries[49].The cutting force signal is considered to provide rich information for tool failure detection in end milling and drilling operations[50]

An intelligent monitoring and control of manufacturing processes is becoming nowadays a driver for development and sustainability of manufacturing industries. Process monitoring is the manipulation of sensor measurements in determining the state of the process[51]. There is an example in monitor application is Komatsu construction machines, which Komatsu not only is a maker to make construction and mining equipment but also simulation predict monitoring system to watch out fatigue or creak happened. This company focused on the monitoring during the constriction process, also inventors' development of prediction and collection information from crack date and deformation date from machine monitors, the feedback from machine to operators is a directly process that can help reducing the accident rate, monitor widely used in industries is an inevitable trend.

In the automobile industry and aerospace industry, driver monitoring system on auto driving has rapid developed in recent years, especially the monitoring has become the most validate method to improve get around easily and safely drive, the world's first driver monitoring system features a camera, using near infra-red technology, mounted on top of the steering column cover. This camera monitors the exact position and angle of the driver's

head while the cars are in motion. In 2008, the Toyota Crown system went further and can detect if the driver is becoming sleepy by monitoring the eyelids, and also there are many examples in airplane with an aircraft monitor ,such as structural health monitoring system for an airplane to determine the origin of any damage in a particular structure [52].

Monitoring cutting force in end milling is an active research, the selection of an appropriate signal and signal processing algorithm is very important. Several signals in a milling operation have been considered to monitor tool failure, for example, cutting force, torque, vibration, acoustic emission, and spindle motor current[53]. This scientific work has so far been focused mainly on the prediction of workpiece thermal damage. it was shown that thermally induced changes of workpiece surface and subsurface properties usually occurred in connection in significant changes of process quantities, especially contact zone[54].

According to the literature, a generic methodology for developing an intelligent monitoring system for machining is composed of six key issues: 1. Sensors; 2. Signal processing;3. Feature generation; 4. Feature selection/extraction; 5. Process knowledge model (a) Design of experiments and (b) AI technique[55].

1.6 Summary

1. This chapter states that end-milling is a promising machining method in the finish machining of near net shape parts.

2. The application of thermal expansion in end milling directly reflects the heat distribution in near net parts, so that the prediction of end milling thermal study can achieve the thermal prediction in near net.

3. Modern industrial monitoring system has been shipped a very wide range, the technology is more mature, and monitoring temperature in the end-milling process will be

filed in this article.

    4. The technical route of this dissertation was proposed.

2 Survey of related research

2.1 Research status

2.1.1 International and domestic research on thermal issue

The development of near net shape 3-Dimensional products for industrial applications has been one main goal for manufacturing industries over the last few decades. Processes such as polymer blow molding and its various stages of development, glass forming, extrusion, forging, centrifugal and sand casting, bulge forming, and vacuum forming are typical processes that have contributed to this development. Current practices center on surface coatings, rapid prototyping, laser forming and nanotechnology manufacture of complex 3-D shapes and assemblies[56].

The pioneering study of the field of cutting temperature analysis was initiated by Benjamin Thomason, who studied the heat generation of the cannon bore in 1798 and presented the concept of thermal equivalent[57]，or use a thermocouple to measure the temperature at a different position in the tool or workpiece[58, 59].The exact relationship equation was established by Joule in 1850[60],and found that heat had an important effect on tool wear and suggested that the cutting speed had an important relationship with tool life [61, 62], Taylor's research results have been used until now. The earliest cutting temperature analysis model was presented in the 1950s. Use a moving heat source and a heat source to approximate the temperature distribution on the shear plane and the sliding friction surface[63-68].

Rosenthat[64] and Trigger[63] made a pioneering contribution to the research of mobile heat sources, and carried out the analysis and research on the heat generation in most mechanical processes. The groundbreaking contribution of these processes to heat

18

production is the basis for many problems in the temperature of the machining process.

Boothroyd uses the semi-analytical method to calculate the maximum temperature in the cutting process and compare the results of the analysis with the experimental temperature [69]. In order to study the temperature distribution of chips, two different heat source application methods are designed: rectangular and triangular regions. An evenly distributed heat source is defined in the rectangular area where the frictional heat source is distributed along the knife-chip surface in the triangular area. The maximum temperature value of the cutting zone is obtained at the blade edge and decreases linearly from the tool nose to the knife-chip separation point along the tool nose surface temperature.

Radulescu and Kapoor have made significant breakthroughs in the use of 3D energy formulas in mathematical analysis models [26], the predicted temperature on the tool to contact surface in continuous cutting is consistent with the previous experimental data in the literature. Studies have shown that the temperature in the cutting process increases as the cutting speed increases. Maekawa uses finite element modulus materials for properties and thermal conductivity[70]. Ostafiev obtains the temperature distribution of the tool by studying the heat flow on the tool surface [71]. The temperature of the tool was measured using a thermo-sensitive coating in the experiment, and the conditions of heat transfer were studied using the measured temperature. Huang's cutting force and thermal analysis model studied the effects of cutting forces on the temperature in the process by correcting the strain, strain rate and temperature structure [72]. A uniformly moving oblique heat source simulates the heat generation in the main cutting zone, and a uniform movement zone heat source in the semi-infinite medium to simulate the heat generation in the second deformation zone.

Komanduri and Hou made a general review and summary of the previous

19

mathematical analysis model [73-76]. Evaluated the previous analytical work and presented an analytical model to eliminate the problems posed by simplicity assumptions in early work. These problems involve the heat transfer of materials and the flow of heat between different materials. In the model, the conditions of different temperature distribution of the first deformation zone, the second deformation zone and the heat source application area are superimposed, and the temperature field distribution of the whole cutting zone under different cutting parameters is obtained.

There are many researches are placed on quality and productivity in manufacturing, it becomes necessary to develop models that accurately describe the performance of machining processes[77], which shows the enhanced chip load model gives predictions of both cutting force signatures and surface error profiles that are significantly better than the rigid system chip load model developed previously.

In the end milling process, the cutting force during machining produce selection of cutter and workpiece which result in dimensional inaccuracies or surface error on finished component[78]. End milling process is one of the most important and common metal cutting operation encountered for machining parts in manufacturing industry. By utilizing this process, the material can be easily removed from the surfaces of molds and dies. End milling is an efficient operation for making mold part (articles) with Aluminum 7075-T6 that has some advantages such as small and medium series production in plastic injection molding and aircraft industry. Since end milling process is the final stage in manufacturing a product, it is important to control the performance of this process[79]. Surface roughness plays a significant role in determining and evaluating the surface quality of a product. Because surface roughness affects the functional characteristics of products such as resisting fatigue, friction, wearing, light reflection, heat transmission, and lubrication, the

product quality is required to be at the high level. While surface roughness also decreases, the product quality increases[80, 81].

Thermal generation and cutting temperatures in end milling have been long studied by many researchers. They have applied multiple analytical and numerical methods to calculate the temperature on the tool rake face, and determine the distribution of temperature on the tool rake face and workpiece. Overall, there are two methods, analytical models and numerical models.

Trigger and Chao[34] presented a steady state two dimensional analytical model to predict the average temperature in machining. They presumed that it existed two heat sources and one on the shear plane, the other one on the tool-chip interface, and they calculated the average temperature rise of the chip when it leaves the shear plane result from the average interface temperature of tool-chip in orthogonal cutting. They made assumptions that ninety percent of the heat flow into chip and ten percent flow into the workpiece, the shear plane contains heat source, the energy of friction and shear are distributed consistently, no thermal shear energy by redistributing enter the chip during the contact of a very short time. The Blok's[82] partition principle was used to calculate the distribution of heat at the shear plane. Under the same assumptions, Loewen and Shaw[66] used a similar method to compute the average temperature rise at the interface of tool-chip. They considered that the chip and the workpiece keep a relative motion at the shear plane, and the shear plane was presumed as stationary body. They also applied in Blok's heat partition principle in their analysis. And they obtained two temperature solutions for each side heat source. They also made presumption that the interface of tool-chip is adiabatic, and hence that the temperature rises in the chip only on the chip side but not on the tool. Although they used Blok's partition principle to develop a relatively straightforward

solution to predict the average temperature of the interface of tool-chip and the shear plane, but it was impossible to match the two sides' temperatures, and the two temperature distribution curves they got are nearly consistent. Another analytical model developed by Weiner[83] obtained the average temperature at the tool-chip interface. The author considered that the moving speed of heat source is equal to the cutting speed on an inclined plane, he also assumed that the chip has a normal flow to a negligible tool motion with the thermal conduction in the direction of tool motion, and the intersection between the shear plane and workpiece stayed at ambient temperature, it was no heat loss from surface to workpiece. In these consumptions, the temperature distribution in the workpiece, chip and tool could be calculated, and the temperature at any distances from the shear plane could also be calculated. Others like, analytical model of three-dimensional in continuous and interrupted machining process[26], the calculation of tool temperature in transient conditions,[84] the analytical model for combined effect of heat source of friction and shear to temperature rise distribution[75] and etc. were developed.

In order to reduce and simplify the assumptions of analytical models, there are many researches about modeling orthogonal metal cutting processes in finite element simulations. But these kinds of simulations require massive input parameters which always get from practical experimental work and mechanical property tests. Generally speaking, there are two types formulations to implement the finite element modelling in cutting processes.

Tay et al. [85]were able to obtain the temperature distribution of two-dimensional, which requires the strain-rate field. However, the input parameters should be obtained from specific combination of the tool and workpiece from machining test. Muraka et al. [86]simulated the process parameters such as cutting speed, coolant water and etc. by using the finite element method. The model needs the experimental parameters. While Dawson

22

and Malkin[87] assumed that the band heat source did not move with the shear to the workpiece, instead, it move with the cutting velocity. A thermos-viscoplastic machining model was developed by Kim and Sin[88] for the mechanics of steady-state orthogonal machining process. They assumed that the workpiece is viscoplastic and the flow stress is function of strain, temperature and strain rate, and their results matched the experiments in accordance with the workpiece and tool temperature. Moriwaki et al.[47]presented a FEM model to the analysis of the orthogonal cutting process and the role of the tool to the micro machining. And this model was just well meet low cutting speeds. More recently, Mamalis et al.[89] used the commercial implicit finite element code MARC to present a coupled thermal-mechanical model of plane-strain orthogonal metal cutting, they determined the temperature fields in workpiece, chip and tool and other parameters. Tuğrul Özel and Taylan Altan[90] developed a method to predict temperature, chip flow, tool stresses and etc. in cutting process by using finite element analysis. Regardless of cutting conditions, the highest temperatures were predicted at the primary cutting edge of the flat end milling. W. Grzesik [91]used an integrated thermal analytical and simulation models to determine the temperature distribution in the cutting zone. Their results showed that the distribution of temperature changes with heat flux transfer conditions, and they compared the simulated results with the experimental results. D. Umbrello et al.[92] used five different sets work material constants to implement the behavior of AlSi316L steel in a numerical model by using the Jahnson-Cook's(J-C) constitutive equation. They obtained temperature distribution in finite element modeling of orthogonal cutting of AlSi316L. E. G. Ng et al.[93] resented a FE model by using FORGE 2® to simulate the distribution of temperature and cutting forces when orthogonal turning a hardened hot work die steel, and the obtained a good correlation between experimental and simulated results for temperature. S. Keith

23

Hargrove and Duowen Ding[94] using a finite element method to predict the temperature distribution in the workpiece under different cutting parameters, and they determined a set of cutting process parameters through minimizing the thickness of the temperature affections. Bo Song et al.[95] simulated the temperature distribution on a three-dimensional model, they found that it exists a great temperature gradient from platform surface, and the maximum depth of molten powder layer, and the experiment date meets the simulation well. Yourong Liu et al.[96] simulated the temperature distribution of surface of Si_3N_4 and titanium ceramic tools for turning different metallic materials based on a mathematic model of heat source, and they used thermal video system to check the computed temperature distribution, the results showed a good agreement.

2.2 Measurement technology

There are many ways to measure the cutting temperature during the cutting experiment. The thermocouple method is a commonly used cutting temperature measurement method. Thermocouple temperature measurement method of the device structure is simple. According to the measurement principles and the use of different methods, temperature measurement methods can be divided into following three thermocouple methods [97].

1) Natural thermocouple method is used to measure the average temperature of the cutting area, natural thermocouple method to measure the cutting temperature is simple and reliable. The disadvantage is that the temperature of the designated point of the cutting area can not be obtained, the tool or workpiece material changes, the thermocouple calibration curve must also be re-obtained.

2) The artificial thermocouple method can be used to measure the temperature of the tool and the workpiece, and the specific artificial thermocouple material is calibrated only

once, and the thermocouple material can be selected flexibly. However, artificial thermocouple buried very difficult to embed superhard tool materials (such as PCD, ceramic), limiting the application of artificial thermocouple method.

3) The semi-artificial thermocouple method is a combination of natural thermocouple method and artificial thermocouple method. The working principle of measuring the cutting temperature is the same as that of the natural thermocouple method and the artificial thermocouple method. As a result of semi-artificial thermocouple temperature measurement using a single wire connection, do not have to consider the insulation problem.

As we known that cutting temperature measurement is an important method, metal cutting humidity research and theory predicts the results of heavy to approach. But the particularity of the metal cutting process the cutting temperature measurement is difficult, such as small cutting area, uneven temperature distribution and large temperature gradient, chip and tool contact, multiple parts in high speed moving. Temperature measurement method is commonly used in metal cutting process as shown in Figure 3, mainly includes: thermocouple method, optical radiation method, thermal radiation, metallographic structure, etc.[98]
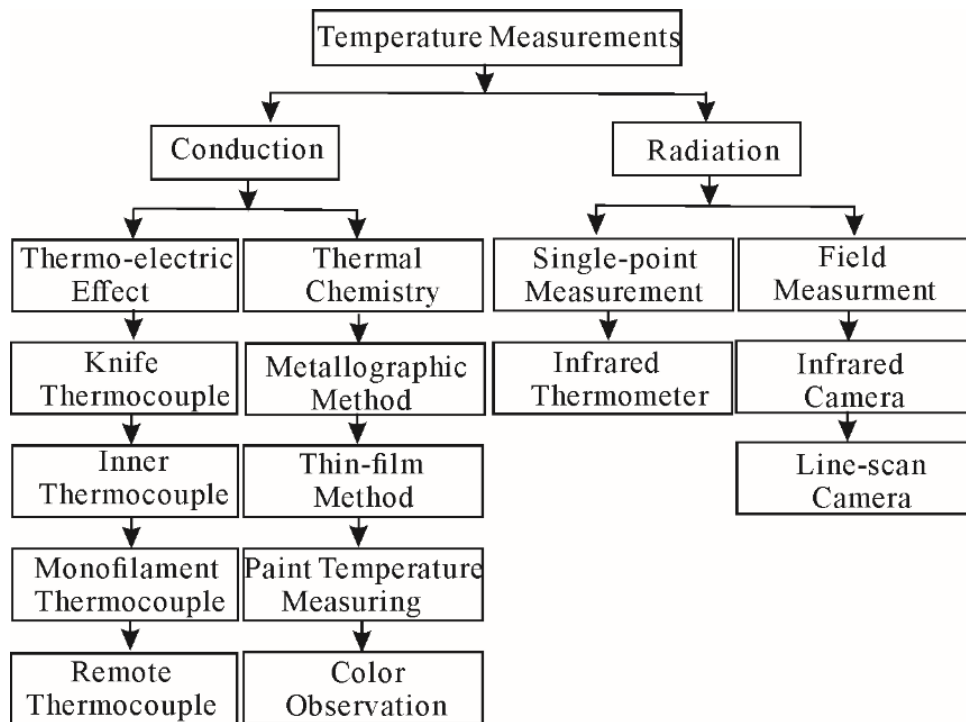
Figure 3 Method of metal cutting temperature measurement[98]

4. Sensors and sensing devices[51].

The techniques for the monitoring of machining have been traditionally categorized into two methods: Direct and indirect. The direct monitoring methods can achieve a high degree of accuracy, but due to numerous practical limitations, they are characterized as laboratory-oriented techniques. On the other hand, the indirect monitoring methods are less accurate but more suitable for practical applications, at machine shop level. Auxiliary quantities are measured and empirically correlated with machining phenomena.

Direct methods require the use of visual systems, lighting, cutting fluids, etc., which may interfere with the monitoring system and machine tools, resulting in unstable production environments. An unmeasured system has been developed for assessing tool wear using a laser sensor that measures displacement and light intensity. These methods are promising because they can measure flank tool wear greater than 40 microns [99]. Moreover, the combination of CCD cameras can be used simultaneously for the acquisition

26

of the tool images during machining[100]. Based on image acquisition and the creation of an image database, containing tools stressed under extreme conditions, an algorithm for further data processing can be created. Due to the stability issues of the direct measurement methods, other systems, using signals such as force, torque, acoustic emission, acceleration have been developed. An important factor of a monitoring system's design is the phenomenon, which data will be acquired from, and the decision of the signal characteristic to be correlated with the phenomenon. Not all the types of sensors can measure the same phenomenon, with the same accuracy. Load cells are often attached to the machine structure for the measurement of cutting forces. Expensive dynamometers are often used in laboratory settings for precise measurements; however, they are impractical for industrial applications. In [101] forces in milling operations were predicted from the current of the feed axis drive.

2.2.1 Thermal-couple and Infrared thermal-couple

Concerning measuring methods of workpiece temperature, there are two popular devices: thermocouples and infrared thermography. Thermocouples are attached on the workpiece surface. Therefore, it can measure only non-machining surface and the number of measurable points is limited. On the other hand, the infrared thermography can measure temperature distribution of surface. However, the infrared thermography is disturbed by cutting chips and coolant in the practical production environment. Therefore, thermocouples system must be employed in actual machining situation.

1) Natural thermocouple

As known dynamic thermocouple, is a widely used cutting temperature measurement method. As shown in Table 1 the natural thermocouple uses the relatively moving cutting tool and the workpiece as the poles of the thermocouple. When the insulation is insulated

27

from other parts of the machine, connect the two poles to form a closed loop and measure the thermoelectric potential using the millivolt meter. The use of the Tool-workpiece thermocouple needs to be calibrated to obtain the correspondence between the thermoelectric power and the humidity. During the metal cutting process, the cutting heat causes the temperature of the contact between the tool and the workpiece to rise, and the thermocouple is generated at the cold end of the thermocouple. The cutting temperature can be obtained by the thermoelectric potential measured by the millivolt meter.

Natural thermocouple method is a simple structure, it suitable for cutting the experimental device does not change, such as cutting speed on the cutting temperature. However, the application and accuracy of the natural thermocouple method are limited by the conductivity of the tool and the workpiece. The cutting fluid cannot be used during the cutting process. It is also controversial whether the measured temperature is the lowest temperature or the average temperature of the contact surface.

2) Built-in thermocouple

Another widely used thermocouple is a built-in thermocouple, also known as an artificial thermocouple, for measuring processing and friction temperatures. The built-in thermocouple uses two calibrated materials to form a thermocouple, place it in a turning tool or cut the workpiece to obtain the corresponding point temperature. Built-in thermocouple in the turning tool or wash the workpiece within the pre-perforated thermocouple, the size and location of the bar has strict requirements. By changing the depth of the hole, the built-in thermocouple can get the temperature of the tool or the different parts of the workpiece but cannot directly measure the tool and the workpiece surface temperature. For the tool surface and the workpiece has been processed surface cutting temperature, through the establishment of tool and workpiece heat conduction

model, based on the thermocouple measured tool and the workpiece temperature using the heat conduction reverse method to obtain.

Built-in thermocouple easy to use and good reliability. It should be noted that the use of built-in thermocouple requires pre-punching a hole, which may damage the internal structure of the tool or workpiece, affecting the tool or workpiece strength and other properties, while the hole in the tool or workpiece damage the original temperature field distribution, the temperature measurement results deviate from the original temperature. Near knife-chip contact area is generally considered not suitable for the use of built-in thermocouple, the thermocouple size requirements are more stringent.

3)Infrared thermal-couple

Infrared theory, the use of infrared cameras and lines of micro-technology to promote the use of infrared thermal imaging technology. The use of infrared thermal imager can quickly change the position of the temperature measurement point, and make timely response, electronic video signal temperature measurement results are conducive to follow-up processing analysis. It should be noted that the infrared thermal imager as a non-contact temperature measurement technology, can only get the surface temperature of the object, the cutting of metal parts and the internal temperature of the tool cannot do anything. The correct setting of the emissivity of the thermal imager is an important part of the infrared thermometer temperature measurement. Since the reading of the measured temperature is proportional to the emissivity, the irrational setting of the emissivity will lead to the measurement error.

Table 1 Measuring methods of workpiece temperature

Technology	Category	Main Advantages	Main Disadvantages	Evaluate
Thermo-paint		Cheapest	Inaccurate,	Proposed calibration
Thermocouple	Tool-workpiece	Simple build	Cannot change location of measurement point	Calibration difficult, limit on response time
	Crossed	Temperature of different positions obtained without changing the experimental device	Cannot be used for milling, drilling, grinding	
	Built in		Cannot directly measure the surface temperature, damage to the thermocouple	
Pyrometer	Infrared radiation	Quick response, Suitable for measuring surface temperature	Emissivity changes of the measured object will affect the measurement results	More sensitive to the environment temperature
Melting point powder		Quick response	Need to warm up, expensive	Cannot extract data directly
Infrared thermal imager	Optical infrared	Cheap	Inaccurate, the result is an approximate temperature range	No calibration required

Thermocouples have advantages and disadvantages, we cannot completely measure every point in the actual production, so in the following chapters, we propose a combination of simulation and production methods to predict the temperature

2.3 FEM

2.3.1 FEM used in manufacturing

In order to maximize the limited measuring points, this paper presents a method to evaluate an effectiveness of each measuring point from aspects of stability of measurement and sensitivity to the process variation. As a quantification method of an effectiveness of

the measuring point, a finite element method (FEM)–based thermal simulation is utilized.

In the 1940s, the rapid development of aviation industry for area plane machine structure is put forward more and more high demand, the engineers had to in precise design and computing, at the same time plan for the development of computer technology makes use of numerical computing method to study the cutting process is possible. In 50s ~ 60s with the finite element method (FEM) in the rapid development, limited to the early stage when the level of computer hardware and software and theory, the finite element numerical calculation method was not popular in the engineering. But at 60s~70s, there was a large general-purpose finite element program, they were good at doing calculation precisely and reliability.in the following 40 years, large number of scholar's studies the basis of FEM.

At an early stage when the level of computer hardware and software and theory, the finite element numerical calculation method is not in the engineering. They gained popularity in 60 ~ 70s a large general-purpose finite element program, and they calculated precision and reliability. Efficient computational efficiency became the analysis of the engineering structure calculation tools. In the later 40 years, scholars in a large amount of basic research. In 1973, Lee and Kobayashi of rigid-plastic finite element method (fem) is put forward for the first time Matrix column type, the extremely promoted the limited element numerical value simulation technology in the application in the process of metal volume into shape [102]. In 1974, Tay. Stevenson and Davis for the first time by finite element method to calculate the orthogonal cutting tool, cutting, work pieces the temperature distribution. Year of 1979, Mróz, Norris and Zienkiewicz Put forward the sticky plastic material such as finite element formulations and viscoplasticity is deduced Finite element of penalty function method, the high temperature molding the analysis of the problem is resolved [103]. In June 2006, The United States Net shape manufacturing

engineering research center, Ohio state university Professor Altan and others at CIRP high-speed cutting meeting, at this stage of finite element simulation of high speed cutting work made a detailed report, and puts forward the future research.[104]

The FEM is an appropriate tool to gain the necessary knowledge of manufacturing technology, the quantitative results can be obtained from a numerical analysis are important to the optimization as well. At the same time, taking all the necessary boundary conditions into consideration by the mathematical equations which describe the process is so complicated, which we can decrease some conditions make the simulation much simple to describe questions. FEM thermal analysis' target is to investigate effects in metal cutting which are not directly measurable.

2.3.2 The basic equation of heat conduction in cutting progress

As shown in Figure 4, the one-dimensional heat conduction process, the upper and lower edge of the adiabatic boundary, the left and right sides of the temperature were T1 and T0 (T1> T0), then the heat flow through the cross-sectional area A is Q, the heat flux is defined as heat flux density (Eq. 2-1)

$$\frac{Q}{A} = q \qquad\qquad \text{2-1}$$

Based on a large amount of heat transfer experimental data, Fourier concluded that in the solid thermal conduction process, the heat flux and the temperature gradient is proportional to, see equation (2-2).

$$q = -k\frac{dT}{dx} \qquad\qquad \text{2-2}$$

Where K is the thermal conductivity of the material. After substituting equation (2-2) into equation (2-1), we get the general formula (2-3) for the one-dimensional Fourier thermal law.

$$Q=-kA\frac{\mathrm{d}T}{\mathrm{d}x}$$

2-3

For H-dimensional heat conduction problems, Fourier's heat conduction law can be extended to (2-4).

$$q=-k\nabla T$$

2-4

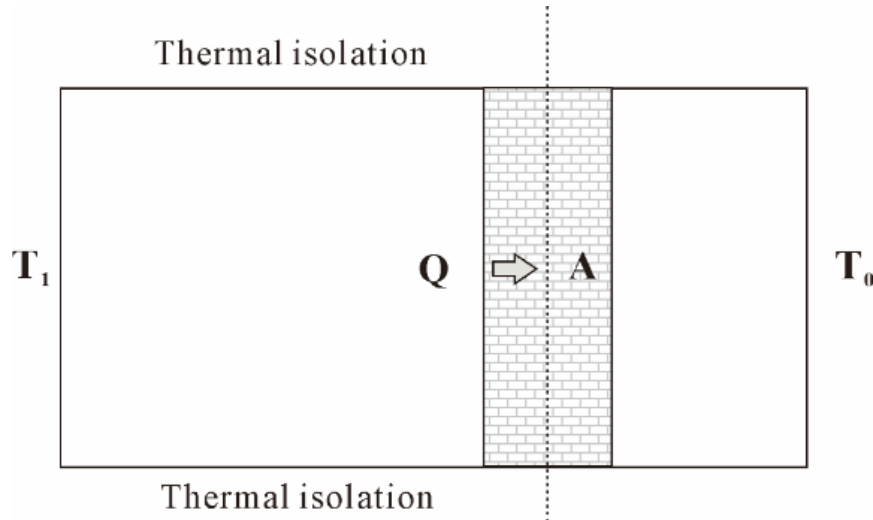Thermal isolation

T_1 Q ⇨ A T_0

Thermal isolation

Figure4 One-dimensional heat conduction process

The production and transformation of energy are always accompanied with the cutting process, the vast majority of plastic deformation work (90%) and the friction between workpiece and the tool contacted surface is converted into heat, only a small part of them is stored in workpiece in the form of elastic deformation energy, so the plastic deformation and thermal effect of friction must be fully taken into account in the thermal analysis in cutting process. According to the law of conservation of energy, the heat balance equation of heat transfer in solid is shown in Eq. 2-1.

$$-(\frac{\partial q_x}{\partial x}+\frac{\partial q_y}{\partial y}+\frac{\partial q_z}{\partial z})+\dot{q}=\rho c\frac{\partial T_x}{\partial t}$$

2-5

In Eq. 2-5. q_x, q_y, q_z is the heat flux in the direction of x, y, z, respectively, that is the energy flowing in unit time and unit area. $\dot{q}$ is the heat conducted by internal heat

33

source in unit time and unit area. ρ is the density (kg/m^3), c is the specific heat (J/kg · K),

T is the temperature, t is time.

In the research process of metal plastic deformation, workpiece and tool are normally regraded as a whole piece, and the tool is regarded as rigidity which has no deformation in machining and exists no internal heat source, furthermore, the internal plastic deformation work is considered into internal heat source, as shown in follows.

$$\left.\begin{array}{l} \dot{q}_{workpiece} = \eta \bar{\sigma} \dot{\bar{\varepsilon}} \\ \dot{q}_{workpiece} = 0 \end{array}\right\} \qquad 2\text{-}6$$

In the Eq. 2-6. $\bar{\sigma}, \dot{\bar{\varepsilon}}$ is equivalent stress and equivalent strain rate, respectively. η is Heat generation efficiency that represents the transformation ratio from mechanical energy to heat (η=0.8~0.9).

In the heat conduction of solid, it is usually assumed that heat flux is proportional to the temperature gradient, as shown in Eq2-3.

$$q_{x_i} = -\lambda_{x_i} \frac{\partial T}{\partial x_i} \qquad 2\text{-}7$$

In Eq. 2-7, λ_{x_i} is the heat conductivity coefficient in different direction, as the heat flow from high temperature to low temperature, so the left of Eq. 2-4. is minus. Consider that the analyzed material is isotropous, so $\lambda_x = \lambda_y = \lambda_z = \lambda_0$, that is

$$\rho c \frac{\partial T}{\partial t} = \frac{\partial}{\partial x}(\lambda \frac{\partial T}{\partial x}) + \frac{\partial}{\partial y}(\lambda \frac{\partial T}{\partial y}) + \frac{\partial}{\partial z}(\lambda \frac{\partial T}{\partial z}) + \dot{q} \qquad 2\text{-}8$$

Eq. 2-8 is the heat balance differential equations in the solid heat conduction process.

2.3.3 2-D heat conduction

The temperature distribution on the tool-chip interface for sharp tool edges in dry machining can be calculated with an analytical model, as proposed by Komanduri et.

al[105]. It is believed that the temperature rise in dry machining is caused by the primary heat source at the shear plane and the secondary heat source at the tool-chip interface, three heat sources/losses are considered: the primary heat source due to shear deformation, the secondary heat source due to friction, and the heat loss due to air-oil mixture cooling, as shown in Figure ,The following sections describe how the heat loss due to convection on the tool flank face and workpiece is calculated based on a stationary heat source model (for the tool) and a moving-band heat source model (for the workpiece). The temperature distribution on the tool-chip interface is then estimated by the superposition of temperature changes due to different heat sources and heat losses.

Temperature fields and subsequent heat flow into the components chip,tool and workpieceare of major significance for metal cutting.the temperature field in the tool influence for example the type of wear and the tool life and hence the temperatures evolving in the workpiece are responsible for alter product quality, and heat during metal cutting process is assumed to be generated in three areas within cutting zone.
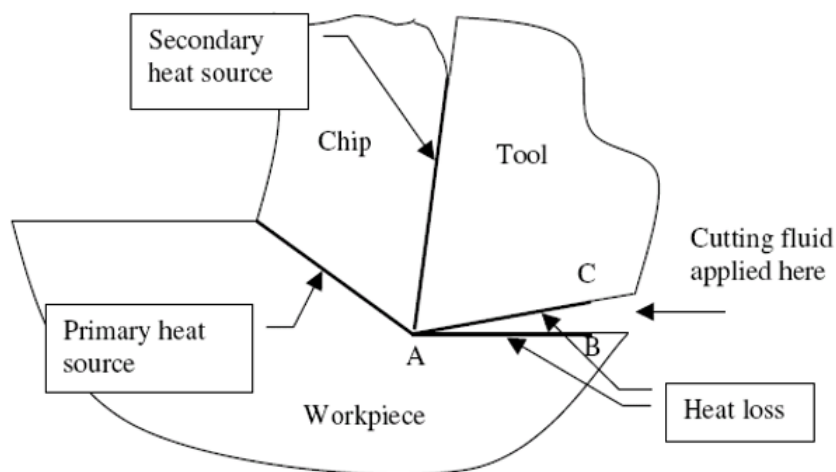
Figure 5 Heat sources and heat losses for the 2-D model

In this paper, the cutting edge is cut along with the edge of the scrubbing force, and the friction heat source of the shear zone and the flank wear zone of the main cutting zone

35

are equidistant along the milling cutter into several rectangular heat sources. The calculated thickness and cutting force of each element of the cutting heat source can be used to solve the problem that the cutting geometry is complicated, and the cutting thickness caused by the helix angle of the cutting edge is changed along the axial direction of the cutter. The influence of the instantaneous cutting heat source on the required temperature field is analyzed by dividing the machining time course, and thus the thickness of the cutting is calculated. The above Figure takes into account the main shear zone heat source, the flank face and the workpiece Frictional heat source and heat transfer model of mirror heat source. According to the above ideas, each cutting heat source is discretized into rectangular heat source element, and the angle between the heat source micro-element and the flank face wear zone heat source micro-element is $180°\text{-}\Phi_n$. The shear surface heat source element and its mirror heat source of the angle for the flank wear with heat source element and its mirror heat source coincidence. For the cutting shear surface heat source microelement in each time element, it's heat flux density,

$$q_{\delta,j}(\tau,z) = \frac{V_s \mathrm{d}F_{\delta,j}(\tau,z)}{\csc\phi_n h_j(\tau,z)\sec\beta \mathrm{d}z}$$ 2-9

Instantaneous flank wear Heat flux density is，

$$q_{\mathrm{f},j}(\tau,z) = \frac{V\mathrm{d}F_{\mathrm{tf},j}(\tau,z)}{VB\sec\beta \mathrm{d}z}$$ 2-10

2.3.4 Determination of heat proportion of heat source in flying face wear

The derivation process of the heat source heat distribution ratio of the flank wear zone is similar to that of the shear surface heat source. The average temperature rises around the flank wear zone is calculated from the workpiece side and the tool end, respectively, and then the two are equalized to obtain their analytical expression formula. The same reason,

from the workpiece side of the analysis, in a time interval, the flank wear with heat source

micro-element can be seen as the workpiece has been processed on the surface of the bevel

movement, so the use of the upper section of the ramp movement of the rectangular heat

source model can also predict the average temperature rise of the micro-element $\overline{\theta}_{f,w}$.

$$\overline{\theta}_{f,w} = \frac{B_{f,j}(\tau,z)q_{f,j}(\tau,z)\alpha_w}{\sqrt{2\pi}\lambda_w V}\overline{f}_f \qquad\qquad 2\text{-}11$$

In the equation, $B_{f,j}(\tau,z)$ shows the ratio of the micro heat powder to the amount of

heat transferred to the workpiece in the element time，$\overline{f}_f$ is based on the geometric and

kinematic relationship of the flank face heat source is based on the geometric and kinematic

relationship of the flank face heat source, the following equation is used to convert:

$$\phi_0 = \beta, \quad V_0 = V, W_0 = \frac{VB}{4\alpha_w}, \quad L_0 = \frac{V\sec\beta dz}{4\alpha_w} \qquad\qquad 2\text{-}12$$

From the tool end, the flank wear zone heat source is a rectangular heat source on the

flank face, and the relative position of the tool does not change during the cutting process.

Therefore, the temperature rise solution of the static rectangular heat source is calculated

the average temperature rise $\overline{\theta}_{f,t}$ of static rectangular heat source in the flank wear proposed

by using Trigger and Loewen et al. mentioned method.

$$\overline{\theta}_{f,t} = \frac{(1 - B_{f,j}(\tau,z))VBq_{f,j}(\tau,z)}{\lambda_t}\overline{A} \qquad\qquad 2\text{-}13$$

In the equation 2-13, the thermal conductivity of the tool material λ_t ,and $\overline{A}$ is the

dimension less area factor associated with the aspect ratio of the heat source area, given by:

$$\bar{A} = \frac{2}{\pi} \left\{ \sinh^{-1}\left(\frac{\sec\beta dz}{VB}\right) + \left(\frac{\sec\beta dz}{VB}\right)\sinh^{-1}\left(\frac{\sec\beta dz}{VB}\right) - \frac{1}{3}\left(\frac{\sec\beta dz}{VB}\right)^2 + \frac{1}{3}\left(\frac{\sec\beta dz}{VB}\right) - \frac{1}{3}\left(\frac{\sec\beta dz}{VB} + \frac{VB}{\sec\beta dz}\right)\left[1 + \left(\frac{\sec\beta dz}{VB}\right)^2\right]^{0.5} \right\}$$

<div align="right">2-14</div>

also：

$$\bar{\theta}_{f,w} = \bar{\theta}_{f,t}$$

<div align="right">2-15</div>

Hence, the simultaneous equations 2-13, 2-14, 2-15, considering the meshing discrimination coefficient, can be obtained:

$$B_{f,j}(\tau,z) = \Gamma_j(z)\frac{1}{1 + \dfrac{\lambda_t \alpha_w \bar{f}_f}{\sqrt{2\pi}VB\lambda_w \bar{A}V}}$$

<div align="right">2-16</div>

It is worth notice that the flank wear with a mirror heat source and the flank wear with heat is exactly same, the spatial position is completely coincident, it is equivalent to the effect of the original flank wear with heat source heat doubled, in the discussion below will only consider the flank wear with heat source, the mirror heat source of the calculation process is exactly the same, do not have to repeat.

2.3.5 3-D heat conduction

Internal ration at a rate q per unit volume causes an accumulation=qdxdydzdt,

It is understood that the mechanical behaviors of workpiece are sensitive to environmental conditions, such as heat conductivity, heat transfer coefficient or temperature.

2.3.6 Generated heat in end milling

Compared with turning, end milling is a discontinuous machining operation, with two totally opposite phases. In the temperature rising phase, the insert performs a cutting action and is heated by the heat source from the secondary and the tertiary deformation zone, causing its temperature gradually reach the top temperature[106].

2.3.7 The thermogenesis of plastic strain

The analysis of heat-mechanical coupling is assumed that the contribution of plastic strain in unit volume to heat flux as

$$\gamma^{pl} = \eta\sigma / \overset{\bullet}{\varepsilon}^{pl} = \frac{1}{2\Delta t}\eta\Delta\varepsilon^{pl}n / (\sigma + \sigma_t) \qquad 2\text{-}17$$

In the Eq. 2-17 , η is the non-plastic heat generation rate, Δt is the time interval of an incremental step, σ is the stress, n is the flow direction matrix. Substitute the following equation into the Eq.

$$\begin{cases} \varepsilon = \varepsilon^{el} + \varepsilon^{pl} + \varepsilon^{th} \\ \overset{\bullet}{\varepsilon}^{pl} = D(\frac{\overline{q}}{\sigma^0} - 1) \end{cases} \qquad 2\text{-}18$$

In the Eq. 2-18, W is strain energy density which is related to elastic strain and temperature, ε is total strain, ε^{el} is the elastic strain, ε^{th} is the strain induced by hot ductility, $\overline{q}$ is equivalent stress of Mises or Hill. $D(\theta)$ and $n(\theta)$ are the parameters corresponding to temperature. So, relations of plastic strain to produce heat after incremental step is finished.

$$\begin{cases} \partial\sigma = \frac{\partial^2 W}{\partial\varepsilon^{el}\partial\theta}\partial\theta + \frac{\partial^2 W}{\partial\varepsilon^{el}\partial\varepsilon^{el}} / (\partial\varepsilon - \frac{\partial\varepsilon^{th}}{\partial\theta}\partial\theta - \partial\varepsilon^{pl}) \\ \partial\varepsilon^{pl} = \partial\varepsilon^{pl}\overset{r}{n} + \partial\varepsilon^{pl}(\frac{\partial\overset{r}{n}}{\partial\sigma}\partial\sigma + \frac{\partial\overset{r}{n}}{\partial\varepsilon^{pl}}\partial\varepsilon^{pl} + \frac{\partial\overset{r}{n}}{\partial\theta}\partial\theta) \end{cases} \qquad 2\text{-}19$$

2.3.8 The thermogenesis of tool-chip friction

In the analysis of heat-mechanical coupling process, η is defined as heat generation rate which determines the ratio of the energy loss of sliding friction transfer to heat. The heat conducts to two contact surface is f_1 and f_2, respectively, and $f_1+f_2=1$. The setting of these two parameters is based on the assumption that the contacted surface has no heat capacity and the heat must be diffused by heat conduction or heat radiation. The

energy loss of friction is:

$$\begin{cases} q_A = f_1 \cdot \eta \cdot P_{fr} \\ q_B = f_2 \cdot \eta \cdot P_{fr} \end{cases}$$

2-20

In Eq. 2-20, q_A and q_B is the heat flux from major face to subordinative face. As the rising temperature of tool-chip by heat friction, the conduction and radiation of heat flux exists in the contacted surface of tool-chip. Hence, supposed the heat transfer from surface A to surface B，the two surface energy transfer to their inner, q_1 and q_2 are as follows.

$$\begin{cases} q_1 = q_A - q_k - q_r \\ q_2 = q_B + q_k + q_r \end{cases}$$

2-21

q_k and q_r is the heat generated by conduction and radiation, respectively, their formulation are as follows.

$$\begin{cases} q_k = k(h, p, \bar{\theta})(\theta_1 - \theta_2) \\ q_r = C[(\theta_1 - \theta^z)^4 - (\theta_2 - \theta^z)^4] \end{cases}$$

2-22

$k(h, p, \bar{\theta})$ is a coefficient of heat conduction which is a function about the average temperature of contact point, contacted interference and pressure. C is a parameter of radiation which is related to the radiation capacity of contacted surface and parameters of mutual view, and θ^z is the absolute zero value of used temperature unit.

2.4 ANSYS APDL

The basic idea of the finite element method is to separate the continuous structure into finite elements and set a finite number of nodes in each element. The continuum works are a set of elements that are only connected at the node. The node value of the field function is taken as the basic unknown quantity and an approximate interpolation function is assumed in each unit to represent the distribution rule of the field function in the unit and then some of the principles in the mechanics are used to establish the finite element

Equation, which makes the infinite degree of freedom problem in a continuous domain into a finite degree of freedom problem in the discrete domain. Once solved, we can use the node value of the solution and the set interpolation function to determine the field function on the unit as well as the whole assembly[107, 108]. The internal process of the finite element solution can be seen from the Figure 5.
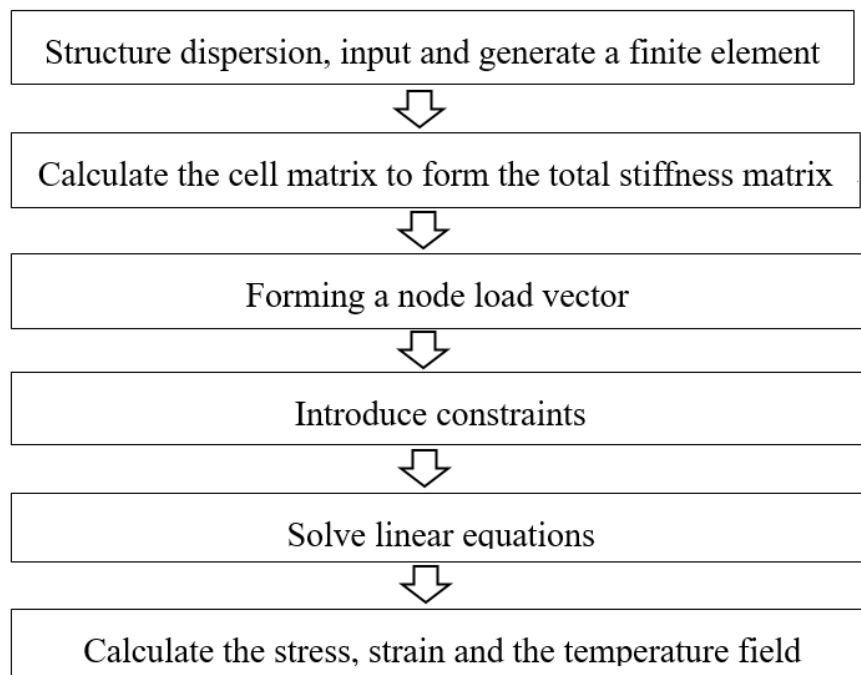
Figure 5 Flow chart of finite element

With the improvement of computer graphics and simulation technology, the simulation and optimization technique based on cutting process gradually substitute the method that obtain the parameters in cutting process by cutting experiments and empirical value in traditionally. The simulation of cutting process exists in the whole process of relative motion between workpiece with tool and display the distribution of heat flux, temperature, phase transformation and stress dynamically, which overcome the defects in traditional experimental methods and become an efficient approach to study the mechanism of cutting process. Compared to experimental methods, simulation, as an efficient assistant,

implement a function of temperature, strain and strain rate to material properties of workpiece, and fully take account into the interaction between different parameters in machining, and give a guidance to research the mechanism and optimizing of technical parameters in cutting process.

ANSYS software not only has powerful function, good generality, but also has good openness; users can accord their needs in the standard on the ANSYS version function expansion and system integration, which can be generated in accordance with the needs of user version of ANSYS program. Developmental function mainly includes three parts: ANSYS Parametric Design Language, (APDL), User Interface Design Language(UIDL) and the User program features (UPFs), among them APDL and most UIDL are popular. Generally speaking, the ANSYS software provides two kinds of working modes, namely the man-machine interactive way (Graphical User Interface, GUI) and to command flow input (BATCH) as the main form of APDL. APDL method is suitable for large, complex finite element analysis, but the other languages will not be used APDL file line by line to write, but it makes full use of GUI analysis for the first time to generate the LOG file, modification will be needed in the design of the command stream file, and then the APDL file can be got from the increasing of the APDL command control.

We introduce end milling workpiece as the research object, using the finite element model parametric language APDL programming techniques and EXCEL data visualization technology, comparing with the involved temperature parameters related temperature distribution analysis, and the contrast analysis was carried out on the simulated data and experimental data, and the characteristics and laws of S45C cube workpiece with the change of the parameter settings were explored and the visual curve were shown by EXCEL.

2.5 Combine measurement and simulation

End milling is a strong thermal coupling of the plastic deformation process, the tool and the workpiece to withstand periodic mechanical load and thermal load, the cutting process of cutting temperature research also has the following problems:

1) Cutting more continuous cutting in the cutting force and cutting heat and other aspects of the existence of significant cyclical intermittent cutting process of cutting the heat source of the cyclical changes on the tool, the workpiece temperature needs further study.

2) The traditional cutting theory is difficult to solve the problem of high-speed cutting temperature, high-speed cutting process should be for the heat convection, heat distribution ratio and heat conduction theory to study.

3) High-speed cutting process cutting tool temperature measurement technology is not yet mature, need further study.

Our laboratory has been studying monitoring temperature while end milling process for a long time. Mr.Tanaka gave an introduction about use thermal-couple to detect temperature in end milling both by experiment and computer simulation[109], and from the previous research of our group, we already had a clear illustration by combining experimental results and the simulation, the temperature distribution on workpiece could be monitored by confirmed parameters. Last year, Mr. Azhad, who was in our group proposed response surface by ANSYS workbench, which illustrated the accurate results did by Mr.Tanaka and based on all work did in these years, but the variations of machining process are generated by using the different combination of model parameters in end milling process, so I am still looking for propose a new method, which can summarize this thermal expansion based on the method to select appropriate temperature measurement

positions based on a variation conscious machining evaluation.

No matter in industries or automotive adopted Computer Aided Engineering (CAE) to decrease the number of trials of actual experiments, effective experimental mechanical tests are really need the validate CAE results, shown in Figure 6. In the previous research, the experimental setup and some of the experimental results are based on the work of Tanaka[110] . In this section, only the main points of the experiment described in detail in the mentioned research was outlined. Mr. Tanaka proposed an estimated method to monitor temperature and relative parameters by combining experimental results and simulation (see in Figure 7).
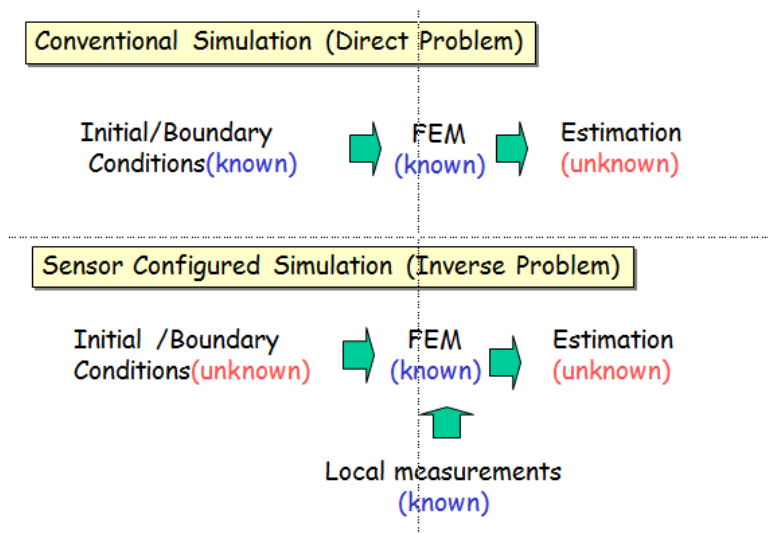
Figure 6 Comparison of conventional simulation and proposed Sensor-configured simulation
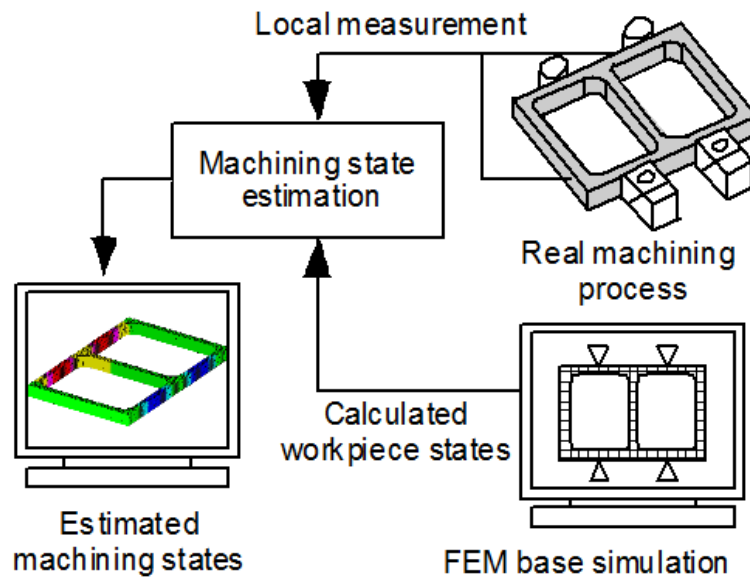
Figure 7 Combination of measurement and simulation

2.6 Summary

1. This chapter summarize conventional thermal analysis in end milling process.

2. Some theoretical issues such as the heat loss calculation formula, the results of various heat consumption are explained.

3. We consider the combination of simulations and experiments to complement each other's weaknesses.

4. Combined with the work of predecessors, we learned that simulation can predict the experimental process when the model parameters are appropriately identified.

3.Article Propose

3.1 The proposal of this subject

Advanced manufacturing technology is rapidly transforming the global competitive landscape. The companies — and nations — that act now to seize its promise will thrive in the 21st century.

We proposed a systematic monitoring method for finish machining of complex 3-dimentional parts for small-lot production. The method is to evaluate an effectiveness of each measuring points from aspects of stability of measurement and sensitivity to the process variation. As a quantification method of effectiveness of the measuring points, a finite element method (FEM)–based on thermal simulation is employed. From the results of the nominal simulation and sensitivity analysis, each measurable point is evaluated. Evaluation procedures are explained in Chapter 5. By using some case studies, feasibility of the proposed method is also confirmed in Chapter 6.

3.2 The main contents of this thesis

Small-batch, high quality and agile production methods have been required by most manufacturers. End-milling is a promising method to satisfy the requirements. In order to achieve accurate and reliable end-milling, it is necessary to understand thermal behavior in machining process. As a result of rigidity improvements of modern machine tools, a thermal expansion of workpiece becomes an important phenomenon in the precision machining [5]. Many investigations have been reported to predict thermal influence in end-milling [8, 110-112]. Furthermore, methods to identify process parameter for thermal simulation are also discussed[113, 114]. On the other hand, a concept of model based

monitoring has been expected as an important technology for advanced machining, because detailed understanding of workpiece state is considered as an effective method for machining process control[115]. Based on these technological backgrounds, a method to estimate temperature distribution of workpiece by combining workpiece measurement and thermal analysis has been proposed[110] .

```
              Introduction and Survey
                   (Chap.1 & 2)

   Measurement technology        Monitor technology
    Thermal conduction           Simulation process
              │                        │
              ▼                        ▼
                  Article Propose
                     (Chap.3)
```

```
          Combine measurement and simulation
                         │
                         ▼
                 Method and Principles
                       (Chap.4)
                  Temperature field
                         │
                         ▼
                  Thermal estimation
                       (Chap.5)
       Orthogonal tests            EoP formula
              │                        │
              ▼                        ▼
                 Applications (Chap.6)
              Case1     Case2     Case3
```

```
                         │
                         ▼
--------------------------------------------------------------------------------------------------
              Conclusion and future works
                       (Chap.7)
```
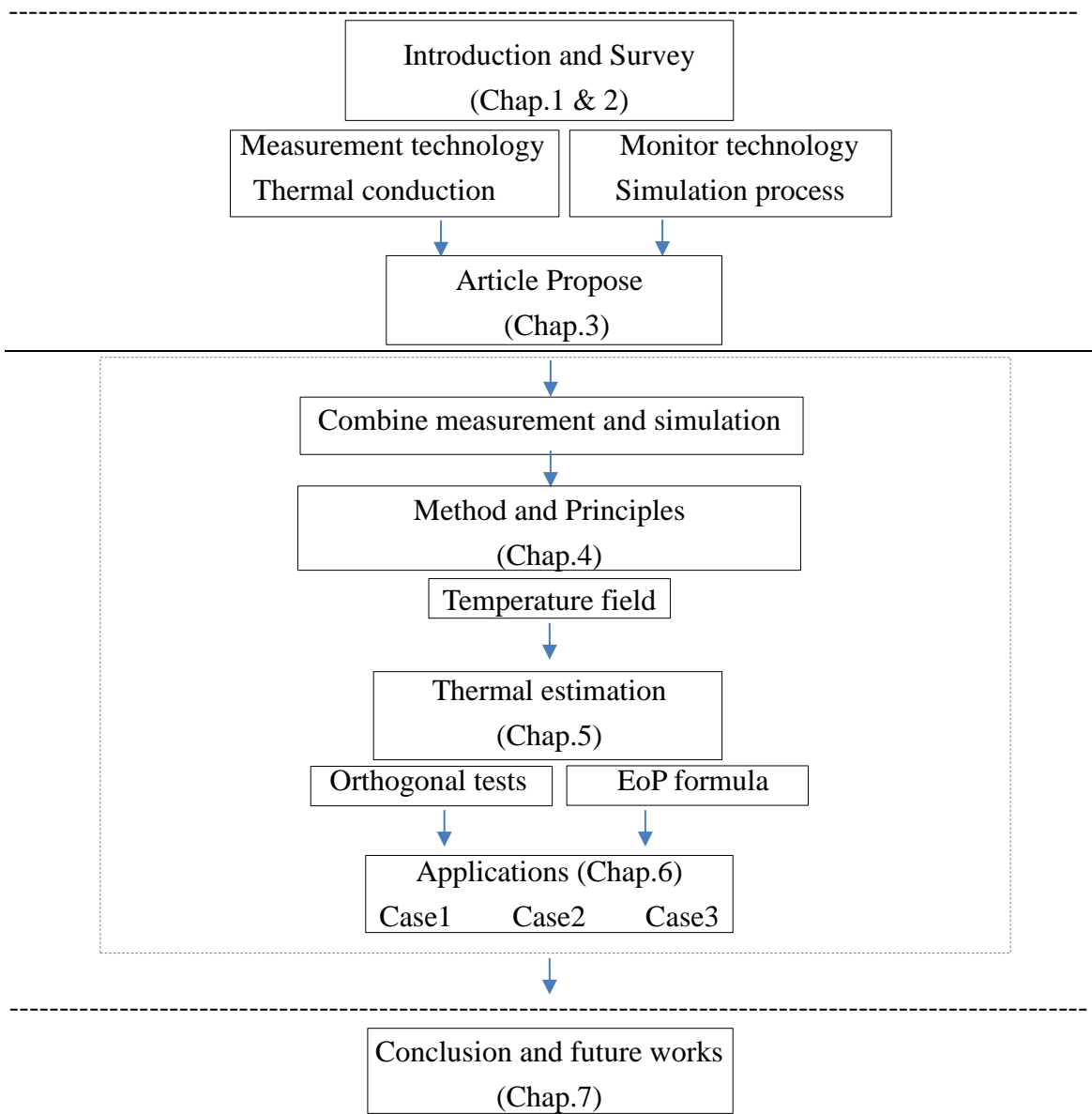
Figure 8 Organization of this thesis

4 Method and Principles

Based on the moving heat source method, this chapter establishes the cutting temperature model of the workpiece in continuous machining. The continuous heat source is substituted into the established cutting temperature model, and the influence of the temperature distribution on the cutting surface after moving the heat source is analyzed. In the case of cutting without the use of coolant, the surface of the workpiece can be considered an adiabatic boundary, that is also to say, there is no heat exchange between the workpiece and the outside, and the heat generated by the cutting heat source reaches the surface of the workpiece and is no longer conveyed.
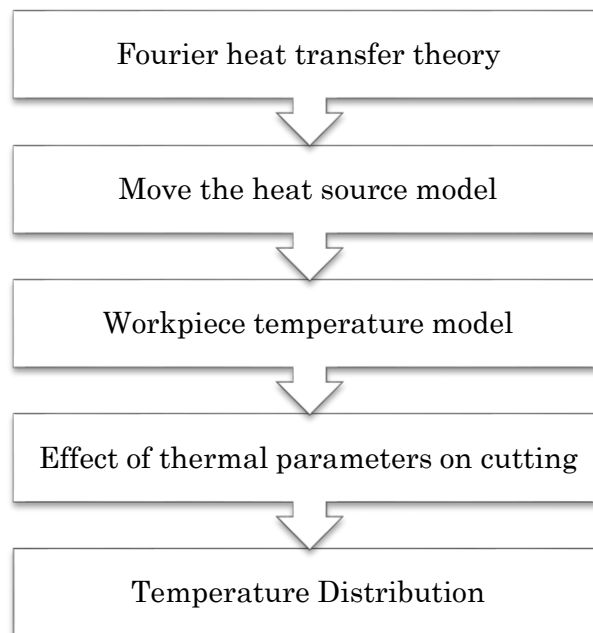
Figure 9 Flowsheet of method

4.1 Mobile heat source method based on Fourier' law heat conduction

Heat conduction in solids is the result of vibrations of the solid lattice and of the

48

motion of free electrons in the material. In metals, where free electrons are plentiful, thermal energy transport by electrons predominates. Thus, good electrical conductors, such as copper and aluminum, are also good conductors of heat. Metal alloys, however, generally have lower (often much lower) thermal and electrical conductivities than the corresponding pure metals due to disruption of free electron movement by the alloying atoms, which act as impurities.

Metal cutting process in accordance with the metal deformation cutting heat generated by different positions are mainly divided into shear zone heat, tool-chip contact surface heat and flank heat source, the three cutting heat relative to the workpiece are in the moving state, so the workpiece processing moving heat source method is widely used in the analysis of temperature [116].

To solve the three-dimensional thermal conductor in the position $P(xl, yl, zl)$ of the instantaneous heat caused Q by any moment τ, the temperature rise T at any location $A(x, y, z)$ based on Fourier heat conduction of non-steady-state heat conduction differential equation is Eq.4-1.

$$\frac{\partial T}{\partial \tau} = a\left(\frac{\partial^2 T}{\partial x^2} + \frac{\partial^2 T}{\partial y^2} + \frac{\partial^2 T}{\partial z^2}\right) \qquad 4\text{-}1$$

Fourier transform get Eq. 4-2.

$$\frac{\partial F}{\partial \tau} = -a\left(a^2 + b^2 + c^2\right)F \qquad 4\text{-}2$$

After the phase shift and integration to get the following formula

$$F(K, \tau) = Ae^{-ak^2\tau} \qquad 4\text{-}3$$

Using the Fourier transform table in the math manual, an inverse Fourier transform is applied to Eq. 4-3 using the Fourier transform of the three-dimensional Gaussian

distribution shown in Eq. 4-4. According to the law of conservation of energy, get the temperature rise T at any position at any time as shown in Eq. 4-5.

$$
\begin{cases}
f(R) = B_1 e^{-b_1^2 R^2} \\
F(K) = \dfrac{B_1 \pi^{3/2}}{b_1^3} e^{-k^2/4b^2}
\end{cases}
\tag{4-4}
$$

$$
T = \frac{Q}{c\rho(4\pi a r)^{3/2}} e^{\frac{(x-x_1^2)+(y-y_1^2)+(z-z_1^2)}{4a\tau}}
\tag{4-5}
$$

Q means the Instantaneous heat transfer energy released by the heat source, c is the specific heat capacity, ρ is density and a is thermal diffusivity.

Based on the instantaneous point heat source temperature solution, by integrating the time and space coordinates, we can deduce the temperature solution caused by the infinite heat source in an infinite heat transfer medium Eq. 4-6.

$$
T = \frac{Q_1}{2\pi\lambda} e^{-\left(\frac{v}{2a}\right)(x-v\tau)} K_0\left(\frac{v}{2a}\sqrt{(x-v\tau)^2 + y^2}\right)
\tag{4-6}
$$

Which, v is heat source moving speed and K_0 is zeroth order modified Bessel function of the second kind.

Of course, in order to avoid mass transfer heat transfer compensation issues, Hahn's[117] proposed a heat source analysis method of cutting heat source moving along the shear plane, see Figure 10, and based on the chip deformation process to establish a moving belt heat source model to solve the metal cutting process workpiece cutting temperature. During the cutting process, the material of the cut workpiece moves along the cutting plane and then generate plastic deformation to form chips, so the heat source of the cutting plane can be regarded as moving along the cutting plane inside the workpiece material.
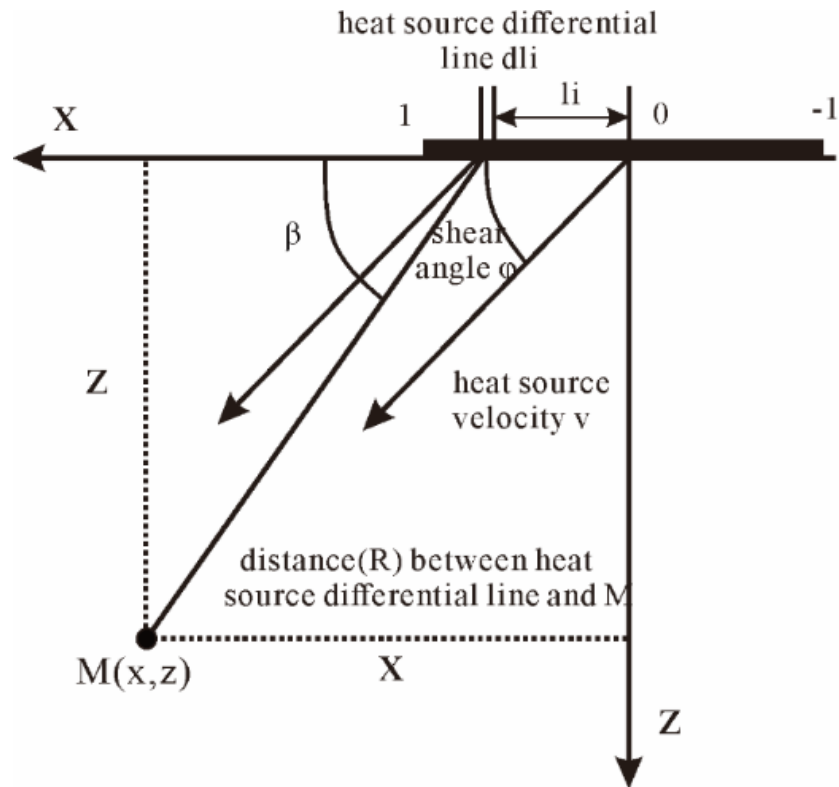
Figure 10 Hahn's moving model

From the moving heat source by pioneering works of Rosenthal on the determination of temperature distribution in a solid resulting from arc welding[118]. We got the idea if the solid is long enough in the direction of motion as compared to the penetration depth of heat transfer field, in quasi-stationary condition, the mathematically defined by setting $\dfrac{\partial T}{\partial t} = 0$ [64].

An observer stationed at the point source fails to notice any change in the temperature around him as the source moves on, this state of heat flow is called quasi-stationary. This theory of quasi-stationary sates simplifies many practical problems to the point where calculation is possible and provides a method of attack on other problems which have not yet been put on a mathematical basis.

4.2 Modeling and solving of workpiece temperature field

In this paper, in order to ignore the geometric complexity of the tool, the thickness of the cutting edge along the cutting edge of the problem，the third deformable zone heat sources are separated into several heat source micro-units. In estimating the cutting temperature with tool flank wear in dry machining, Huang and Liang [119] developed a new model to predict the heat generation due to the tool flank wear. A rubbing heat source, because of the presence of tool wear land, was added to the heat sources methods under dry machining condition. The cutting temperature distribution was thus calculated with the tool flank wear effect.

Temperature rise of tool-workpiece contact area forming in the milling process is much higher than the final machined surface owing to thicker instantaneous uncut chip thickness when the cutting tool passes by[120]. Cutting process presents periodic and non-stable, tool and workpiece to withstand periodic mechanical load and thermal load impact. This series of characteristics makes the intermittent cutting temperature theoretical model much difficult to analyze, and the cutting process of the tool and the workpiece temperature field of the unsteady state also makes it difficult to measure. Compared with the theoretical analysis and experimental study on the cutting temperature of the cutting tool and the workpiece, the finite element simulation can effectively deal with the highly nonlinear and unsteady problem of intermittent cutting. The simulation analysis method of the intermittent cutting process combines the finite element analysis theory with the metal elastic-plastic deformation and other cutting theories. Through Lagrangian and Eulerian, the differential equations of motion and the heat conduction differential equation must be solved, in order to obtain the cutting force, cutting temperature and metal cutting deformation.

The effects of heat and thermal management of structures is more and more critical for performance limits which are pushed further by the need to have lighter, smaller and more efficient designs. Convection, radiation and conduction loads are obvious to parts accuracy, but it needs including the effect of power losses and thermal energy from friction and external sources.
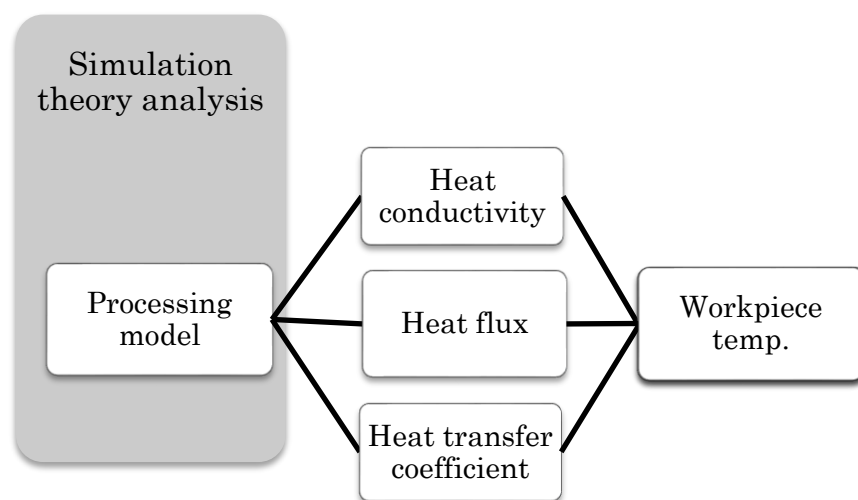
Figure 11 **Plot of this chapter**

4.2.1 Approximated simulation model

Following steps are based on this state steady thermal end-milling simulation.

Firstly, using mechanical-APDL programming method to establish model of workpiece under end milling process is not have an extremely influence to propose the new method about predict the sensitive points during cutting process.

In this study, the temperature of the workpiece at any time is obtained by integrating the instantaneous heat source element along the time axis to the temperature rise of the time required, and then the change of the temperature field of the workpiece can be described. In addition, in order to reveal the periodic variation of the temperature rise of

the workpiece during steady state, the temperature data acquisition involved in this paper is not required for the specific type of cutting. We approximate the entire workpiece cutting process as an ultra-thin cutting, so that the whole cutting process is similar in the welding process, the heat source instead of the tool after the whole process can ignore the impact of chips.

This thesis initial set is about from the heat source temperature distribution in the initial temperature atmosphere and add the same as the actual operation of simulated heat flux and constraint condition, then we calculate the temperature distribution in the workpiece.

Secondly, based on the transient thermal analysis, add heat flux in selected element, and then we use the loop orders to push the heat source moving on paths.

Lastly, from postprocessor all data can be picked out, we chose all the date which also can be detected followed easier picked criterion in actual experiment, and then export date files.

4.2.2 Simulation process

4.2.2.1 Pre-process

We take advantage of the classic ANSYS® parametric design language (APDL) to develop the simulation process. Pre-processing task is to establish various parameters under the condition of heat conduction current testing geometric model, an ultra-thin cutting setting and the transient thermal analysis estimated completed.

4.2.2.2 Modeling and meshing

This step we complete until to mesh generation, including: define material properties, modeling and mesh steps. As the properties of the workpiece and the tool material, the processing method and the processing parameters and other factors determine the heat

generation during the cutting process. In order to verify the effectiveness of the model, the S45C steel (body cubic lattice BCC) workpiece material was selected as an example for intermittent cutting.

Because the price is not too high, and it is a carbon steel which is well circulated in the market, it may be that the S45C is used for the time being in the case where the general versatility is high, and the special property is not necessary for the time being. Dimensions of the S45C workpiece (length (L), width (W) and height (H)) are illustrated in Figure 12. Top surface of the workpiece is machined by end-mill with feed rate of 600mm/min. A tool path of reference machining case is illustrated in Figure 14. The initial temperature is assumed as 20 °C (i.e. ambient temperature), Chemical Composition shows as Table 2.
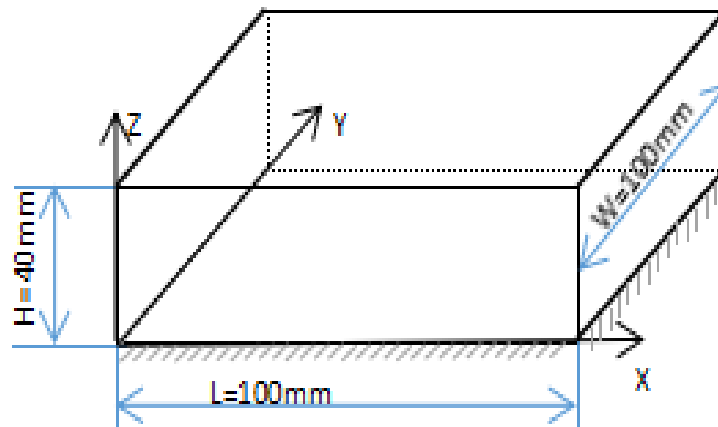
Figure 12 Dimensions of workpiece

Table 2 S45C Chemical Composition (%)

Material number	C	Si	Mn	P	S
S45C	0.42~0.48	0.15~0.35	0.60~0.90	≤0.030	≤0.035

4.2.3.4 Boundary conditions and loading

Because this simulation is focused on finish machining, this case study ignores the change of workpiece shape during machining. Therefore, movement of end-mill is modeled

as a moving heat source on the top surface. Surrounding temperature and initial temperature of workpiece is assumed 20°C. Heat transfer from workpiece to the environment is assumed in side surfaces and top surface except the end-mill position. Heat transfer at bottom surface is ignored in this case study. Reported workpiece parameters are utilized in this case study. Details of the parameters are described in Table 3. The entire model is meshed using Solid 70, which has eight nodes with a single degree of freedom.

In this paper, the influence of thermal fuels is neglected, and the physical properties of the tool material are not changed as a function of temperature. It should be noted that the establishment of the temperature model of the physical properties of the material model, the nonlinear control equation will make the calculation is extremely complex, see Figure 13. Jen [121] et al. proposed and established a nonlinear solution of the physical properties of the material with the tool's temperature field. Their results show that for the cemented carbide tool, the physical properties of the tool material are not considered to be simplified with temperature cause a large error. The properties of the cemented carbide tool material used in this paper are less affected by the temperature, so the simplified assumptions used for the nature of the tool material are acceptable. Based on the application of multiple linear regression analysis together with assumptions of moving heat source theory[122], workpiece models was defined by using finite element meshes containing linear tetrahedral elements, readily available in the software.
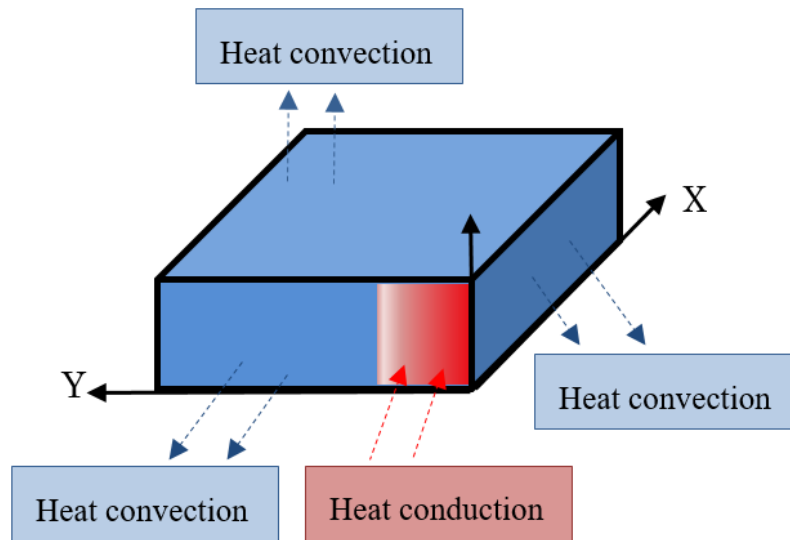
Figure 13 Cutting tool boundary condition diagram

Table 3 S45C Physics parameters

Workpiece material	Carbon steel S45C (JIS)
Density	$7.85 \times 10\text{-}6 \ kg/m^3$
Specific heat	480 J/(kg•K)
Heat conductivity	48 W/(m•K)
Surrounding temperature	20 °C
Initial temperature	20 °C

Top surface of the workpiece is machined by end-mill with feed rate of 600mm/min. A tool path of reference machining case is illustrated in Figure 14.
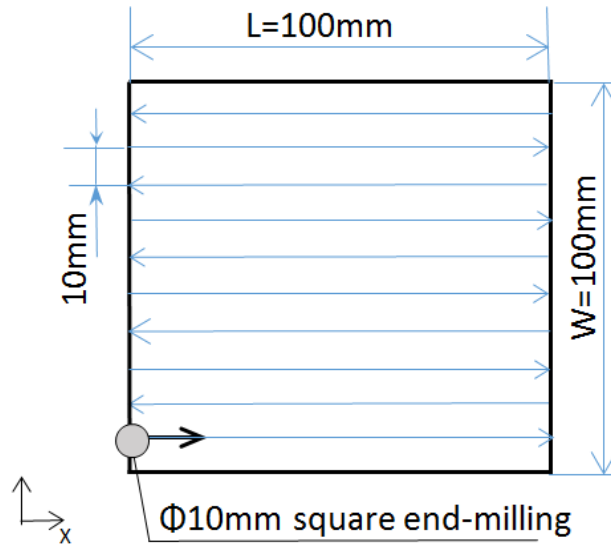
Figure 14 Tool paths of full machining

4.2.3.5 Add heat source

In machining, grinding, cutting and sliding of surfaces, the energy generated as friction heating and can be modelled as moving heat source, discussed by many researchers [123].the welding process, we consumed the heat source moving one element to another element until to the end. The computer iteratively calculates the vector temperature value of each node according to the divided cell grids, Figure 15.
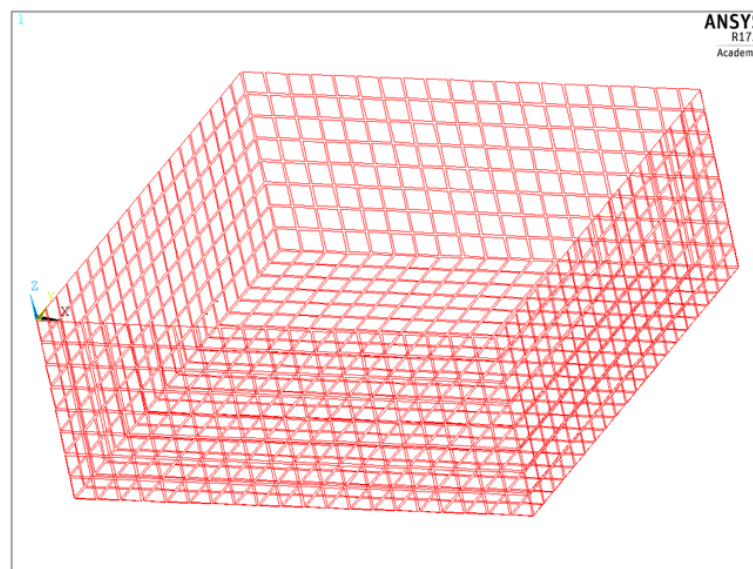
Figure 15 Cell grids

4.2.3.6 Solve and Post-process

ANSYS reprocessing module includes two parts: general post processor POST1 and time course post processor POST26. The general-purpose postprocessor is used to view the results of the analysis of the temperature field at a certain moment or the average of the parameters over time, and the postprocessor of the time history can view the results at different times.

(1) Extraction of data results: ANSYS saves each calculation result in the file with suffix rmg, which the user can extract for later analysis and modification. The analysis mainly refers to the temperature distribution of the temperature change curve according to several temperature change parameters. The modification of the APDL language is based on the experimental measurement values，through the program to save the above data into a text file in order to facilitate subsequent data visualization call data in EXCEL.

(2) Color cloud graph display: The cloud graph display can generate continuous contour lines and discontinuous contour lines along element boundaries for node results and element results. According to the needs of the analysis, you can also select a part of the model area to display the cloud image, which shows the value distribution of the relevant parameters in space. Figure 16 shows the cloud image of the temperature field on the top surface of workpiece, which also includes the type of solution (vector, node solution, etc.), excitation frequency, parameter type (H, HSUM), cell grid number, the maximum and minimum values of the parameters sought in the selected area, Color and numerical calibration scale. It also shows that the specific date saved in the cloud is available for log archiving.

Calculation of the temperature field is through the initial boundary conditions imposed, load conditions, etc., by the computer iteratively iterative calculation based on the cell grid,

get the solution of the vector temperature value of each node

Time=0.4s   Time=30s

Time=60s   Time=100s
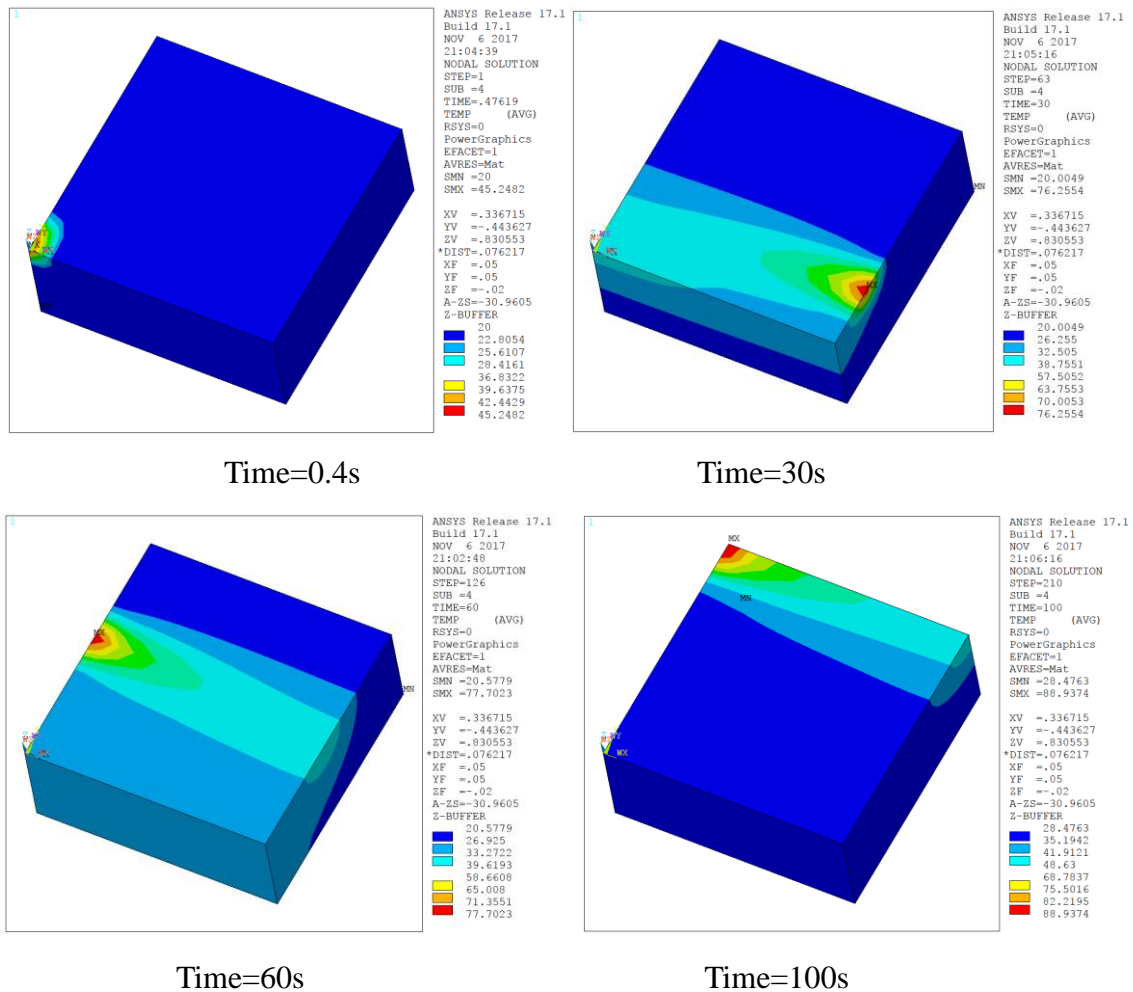
Figure 16 Temperature distribution of workpiece

4.2.3.7 Data processing and graphical visualization

In the temperature field analysis, through the APDL cycle program, the relative position of the heat source and the workpiece is changed by a small variable, and the data of the workpiece temperature is saved and stored in the text file at each position. Then change the material properties of the workpiece parameters, and then according to the above steps for analysis and data records. Finite element simulation takes a parameter as a variable, fixed other parameters to calculate.

Through the simulation of computer software, we can obtain the curve of temperature changing with time. Figure 17 illustrates temperature changes of all points include in surface I at the full machining case. From the graph, it can be seen that to complete the entire surface of cutting within 100 s, including a total of four peaks, and the highest temperature is around 65°C at 62 s. Temperatures in surface I are affected by the distance from the heat source. Points' temperatures are increasing when the end-mill is near surface I; on the other hand, the temperature is decreasing with the end-mill away. This trend is consistent to our natural understanding of the actual end-milling process. We can represent temperature's changing of points in surface I by selecting the highest temperature for each point.
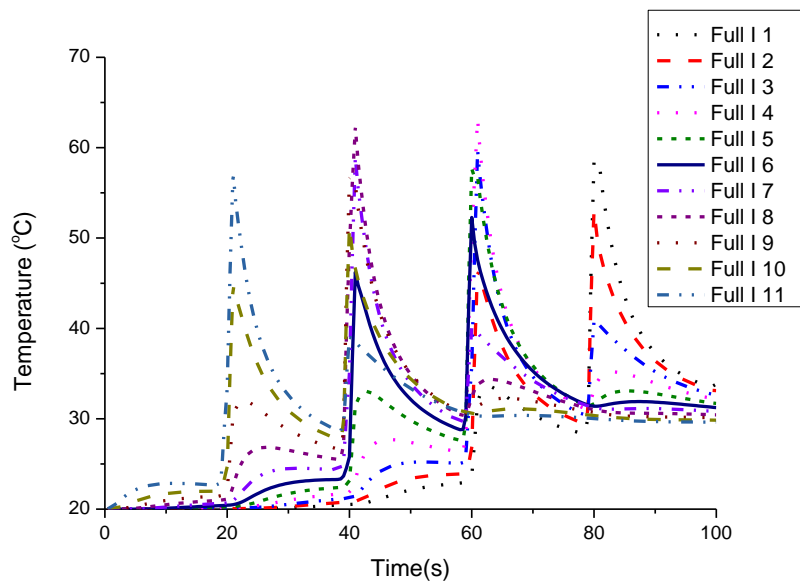
Figure 17 Temperature change of full machining

4. 3 Summary

1. The process includes five parts, modeling and meshing, boundary and conditions and loading, add heat source, solve and post-process and then data processing and graphical

61

visualization.

2. Within the allowable error, finite element analysis using ANSYS can further detect the temperature distribution.

3. There are also some shortcomings，the simulated induction heating process requires reliable and complete thermal properties of the material properties data.

5 Thermal estimation

The effects of tool wear, cutting forces and process temperature are superposed and lead to displacement between cutting edge and surface of the workpiece, thus resulting in form and dimension errors in final products[124]. To eliminate the costs associated with additional finishing processes in conventional machining, soft computing and other mathematical approaches used in CBN turning are presented[125].

As mentioned in the introduction, there have been many researches which investigate temperature distribution of workpiece. End-milling process is a thermo-mechanical coupling process in principle, nevertheless influence of elastic deformation are enough small in finish machining. Therefore, workpiece thermal analysis can be calculated without considering thermal-stress just similar to laser heating. As a numerical simulation method, most of the researches are based on the heat conduction analysis with the FEM method. To simulate the end-milling process from the thermal aspect, the process can be modeled as heat conduction problem with heat transfer surfaces and a moving heat source. To solve the problem, thermal properties such as amount of heat flux, heat transfer coefficients between the workpiece surface and environment and so on must be determined in advance.

5.1 Principle to select the nodes

Concerning the measurable points, the measurable areas of workpiece surface are selected according to the following principles.

Firstly, the hold areas cannot be selected owing to the interference with fixtures which fix the workpiece on machine tools.

Secondly, areas directly touched by coolant cannot be selected, because coolant plays a significant influence of temperature measurement.

Thirdly, working areas of end-milling are not allowed to be selected.

Finally, the temperatures of positioning reference are not preferable to measure, areas of that cannot be selected. The measurable areas are selected by above principles, and it can be simplified that selected nodes can represent surface temperatures. In order to select the nodes, it must be considered the balance, convenience of measurement, sensor availability. The data obtained from the quantification method are compared with each other, the effectiveness of the points is evaluated based on the quantified value of each point.

5.2 Evaluation of sensitivity against process variation

Sensitivity analysis is a primary approach used in mathematical modeling to identify important factors that control the response temperature in a model. As we know that there is a variety of sensitivity depends on locations of sensors, some node's temperature changes sensitively by variation of machining process, while there are stable nodes against the variation of machining process.

In order to evaluate the sensitivity to the machining process variation, it is necessary to compare several simulation trials with different thermal parameters such as the heat flux and heat transfer coefficients. Variations of the parameters are summarized in Table 4. In this study, a data set B corresponds to a nominal machining situation. A heat source is influenced by the cutting tool wear conditions and local workpiece material property. A heat transfer coefficient is also changeable depend on the air flow, surface conditions and unexpected chip accumulation. Temperature difference between the certain simulation case and the B case can indicate sensitivity to the process variation.

Theoretical basis of thermal expansion mentioned in chapter 2, in-process thermal estimation is employed in order to achieve two functions. One is evaluation of thermal

64

expansion; the other is monitoring of machining process. Thermal expansion can be evaluated based on thermal temperature analysis of nominal machining situation. Deviations of machining process such as excessive tool wear, undesirable chip accumulation and so on can be detected based on inverse analysis of heat conduction analysis[110, 113]. Based on these functional viewpoints, effectiveness of measuring points should be considered both of thermal expansion and detection of process deviations. It is well-known that thermal expansion of workpiece is proportional to temperature rise when other thermal properties are same. Therefore, comparison of temperature rise between the measurable points can be an index. Concerning deviation of machining process, it is assumed that temperature of effective points varies large according to the change of machining process.

Table 4 Analysis cases for temperature analysis

Case	A	B	C	D	E	F	G
Heat flux ($\times 1 \times 10^5$ W)	0.5	1.0	1.5	0.5	1.5	1.0	1.0
Heat-transfer coef. ($\times 20$ W/m^2•K)	0.5	1.0	1.5	1.0	1.0	0.5	1.5

5.3 Case of different machining situation (half cutting paths)

In order to inspect the ability of proposed method for selecting suitable measuring points according to the change of machining situation, a different machining situation is also investigated. A half machining process is evaluated to compare the result of the full machining process. The half machining paths for same workpiece of full machining process are shown in Figure 18. In the machining situation, heat source only moves half of top surface. Temperatures can be detected by thermo-couple in uncut region on the rest of top surface. Therefore, we can evaluate more points' temperature in top surface of workpiece. As example cases to evaluate the effectiveness of measurable points, we select measurable

surfaces. Measurable points are selected from the selected surface. In this research, 11 points are contained each surface. As the results, we have candidate points from surface I to surface IV for the full machining, from surface I to surface V for the half machining. They are illustrated in Figure 19 and Figure 20.
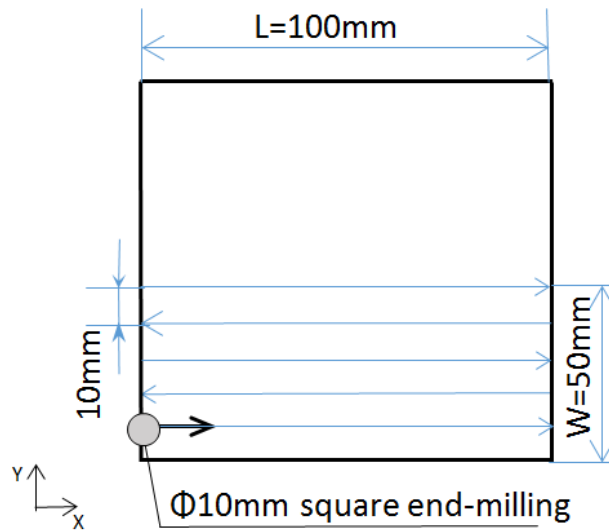
Figure 18 Tool paths in half machining
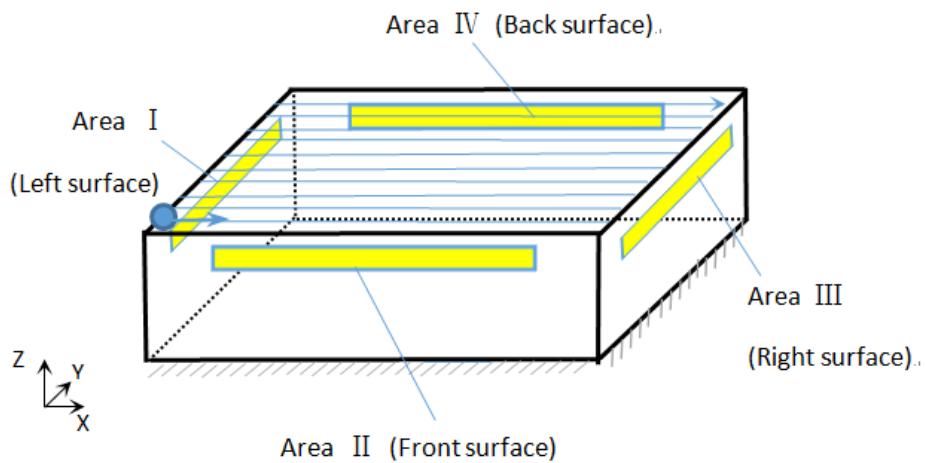
Figure 19 Selected measurable surface in full machining
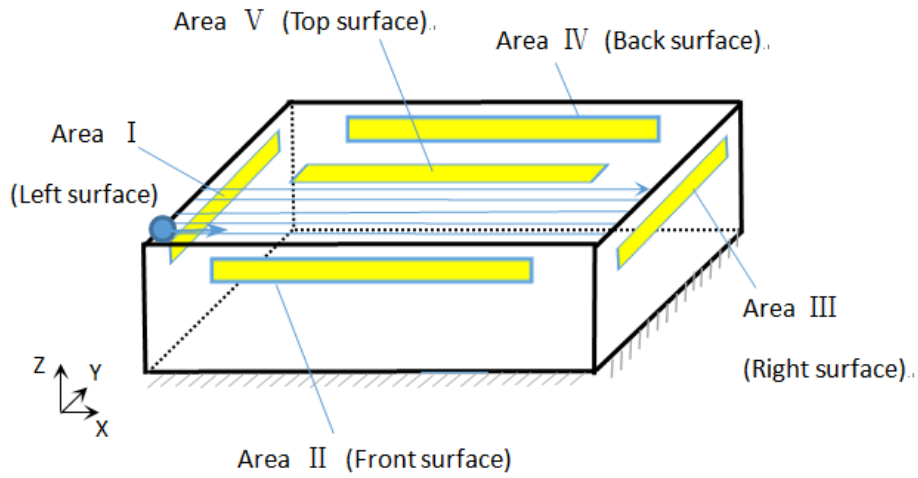
Figure 20 Additional measurable surface in half machining

5.4 Simulation results for temperature

After Figure 17 illustrates temperature changes of all points include on surface I. the differences of maximum temperature of each point are calculated, we use node 1 on surface I as example, shows in Figure 21.

The bar chart of Figure 22 illustrates the evolution of the resulting of point 1's temperature variance according the parameter set A, C, D, E, F and G in surface I. Maximum temperature difference between results of each parameter set from the result of the set B; they are $|T_B-T_A|$, $|T_B-T_C|$, $|T_B-T_D|$, $|T_B-T_E|$, $|T_B-T_F|$ and $|T_B-T_G|$. By using the maximum temperature with nominal parameter set and the maximum temperature difference among the parameter sets for measurable points, Calculate the EoP values of each point seen in the Figure 10, which illustrates most effective points in surface I is point 4.
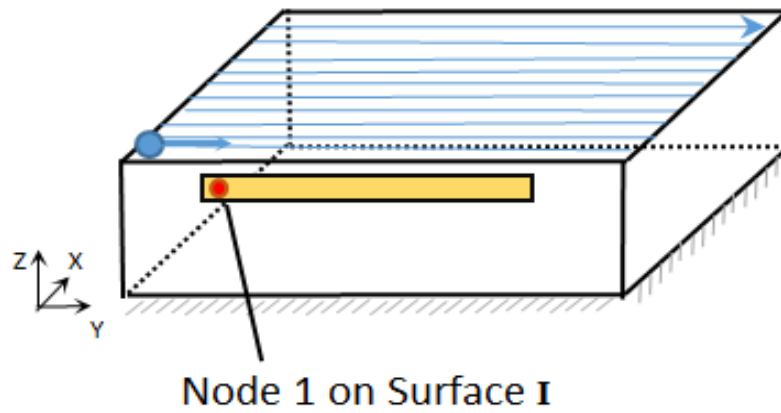
Figure 21 Node 1 on surface I of full machining
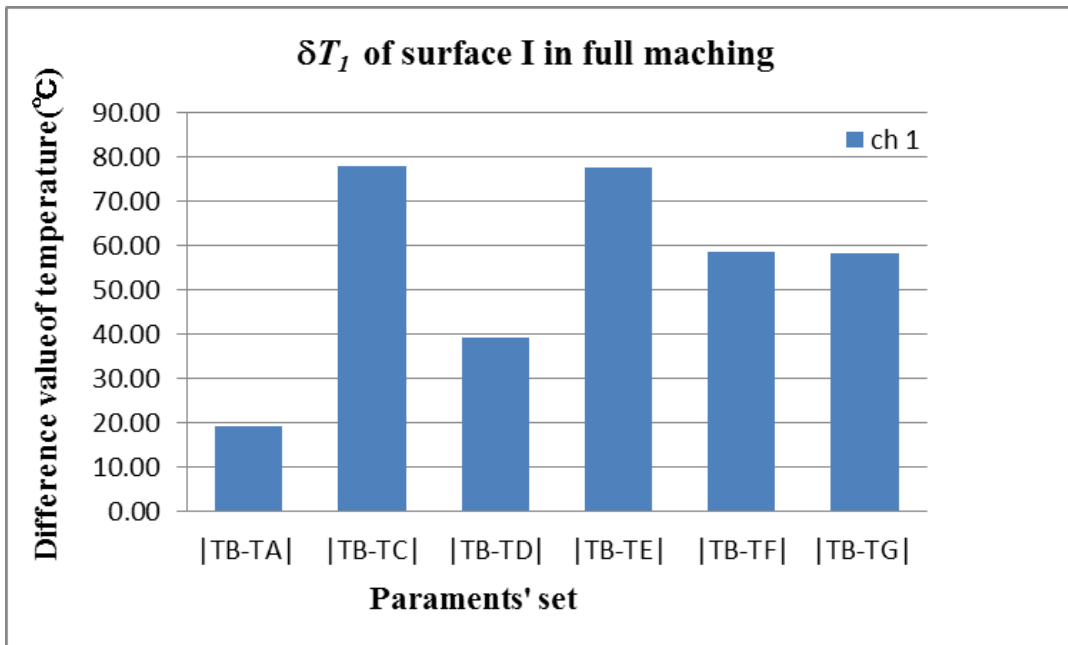
Figure 22 Variance of point 1 in 6 sets' parameters

After simulation and calculation, we known that time has distribution on each surface, we keep eyes on 11 nodes with every surface, and calculate the variance between nominal set to other sets, shows below, and discussed by five small parts.
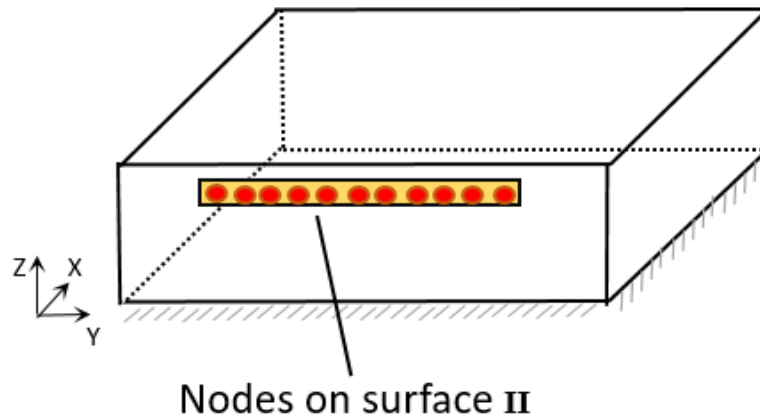
1.) Surface 1
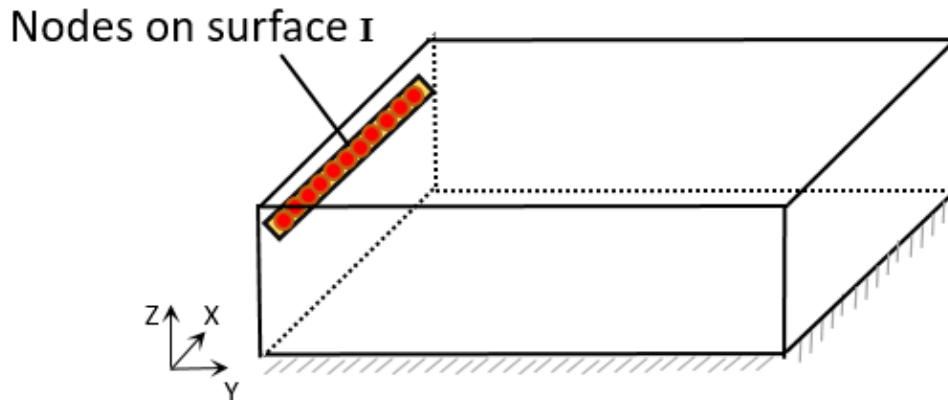
Figure 23 Nodes on surface 1

Temperature changes and nodes' temperature variances from surface I are shown in
Figure 24. Figure 25 is the variance value between parameter B to parameter A, C, D, E, F and
G.
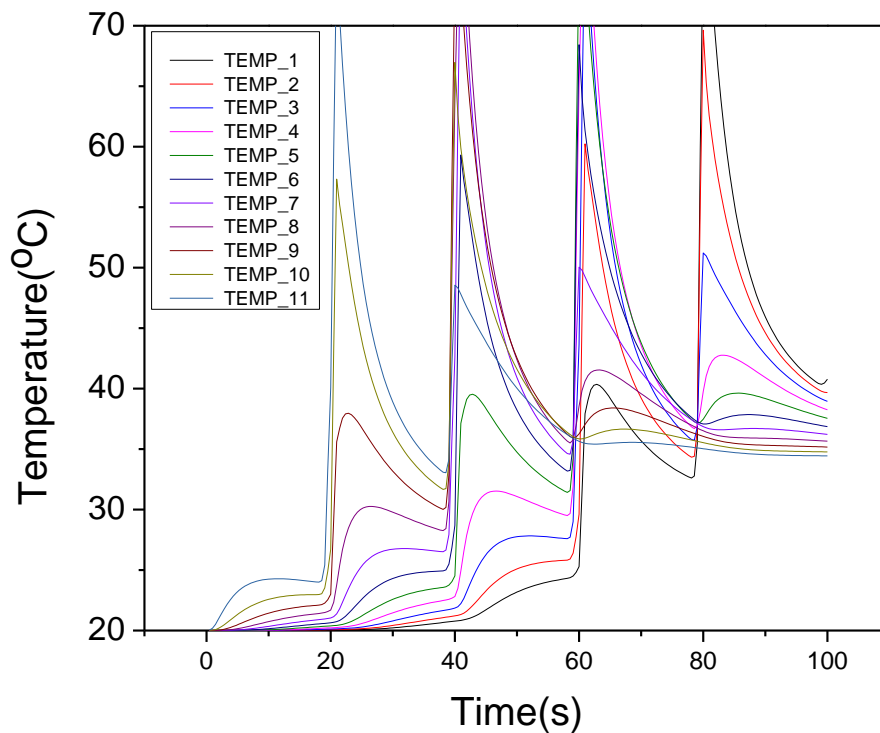
Figure 24 Temperature change of full machining on surface I

As shown in Figure 24, there are four obvious peak temperatures corresponding to its
time ranges for each node. To a certain node, the value of peak temperature increases with

the prolonging of time, because in a same cutting rate, the cutting times increase with the cutting time, and the cutting times determines the generated heat for each node. Node 1, 2 and 4 get their maximum value at the time range of 80~100s, node 3, 5, 6 and 7 get their maximum value at the time range of 60~80s, node 8, 9 and 10 get their maximum value at 40~60s, but node 11 get its maximum value at 20~40s, and the 11 nodes have their own seasonal change due to the reciprocating movement of the tool, when the tool gets close to the nodes side, the surface temperature will be raised, while the tool is far from the nodes side, the surface temperature will be reduced.
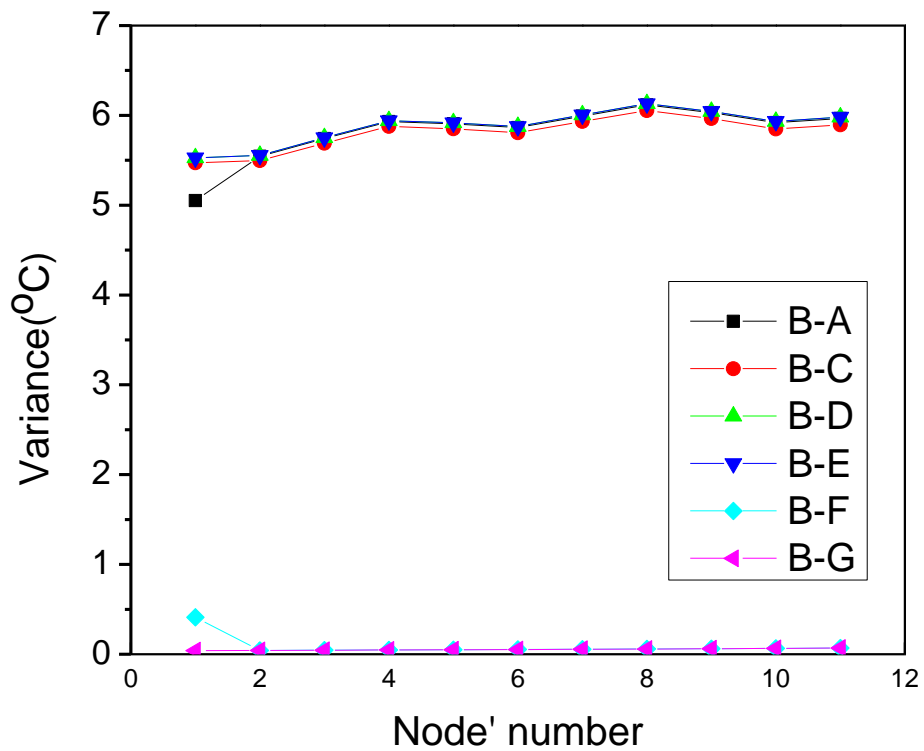
Figure 25 Variance of full machining on surface I

As seen from Figure 25, the variance value of B-A, B-C, B-D and B-E for each node has slight fluctuation, while their values are kept in the range of 5~6. However, the variance value of B-F and B-G for each node kept almost the same, while their value are kept approximately 0, except for node 1, its value is about 0.5.

Figure 26 is the temperature change of half machining on surface I, and Figure 27 is the variance of half machining on surface I.
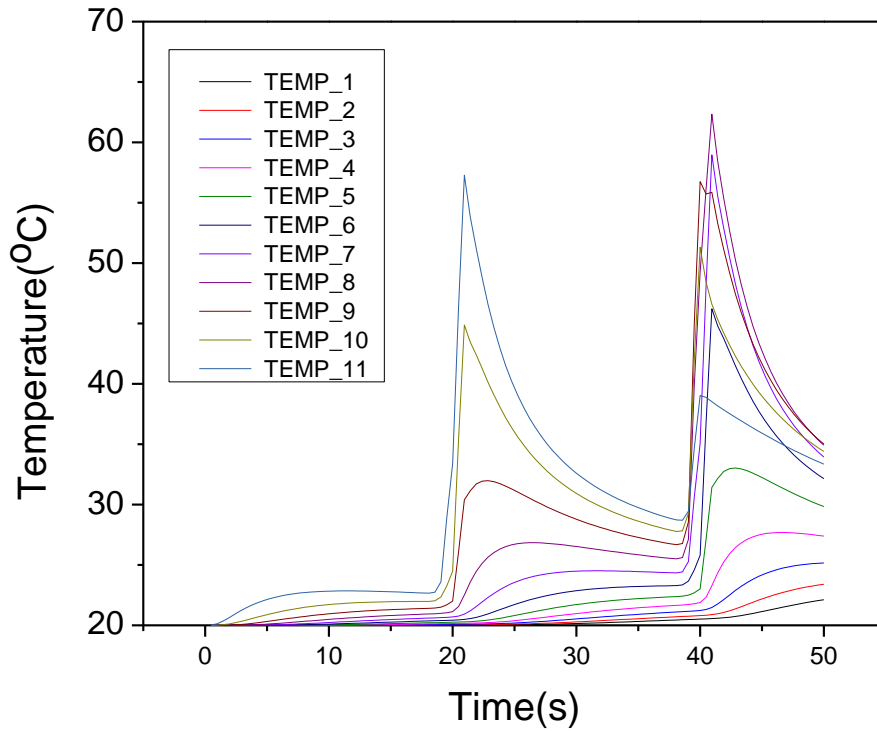
Figure 26 Temperature change of half machining on surface I

As seen from Figure 26, in the time range of 0~50s, node 1, 2, 3 and 4 do not get their peak temperature, the temperature value of each node increase with the prolonging of machining time. Node 5, 6, and 7 has one obvious temperature peak at the machining time range of 40~50s, respectively. While node 8, 9, 10 and 11 has two obvious temperature peaks at the machining time range of 20~30s and 40~50s, and node 8 and 9 get its maximum value at 40~50s, but node 10 and 11 get its maximum value at 20~30s. Overall, node 8 has the maximum temperature value of 65°C in the time range of 40~50s.
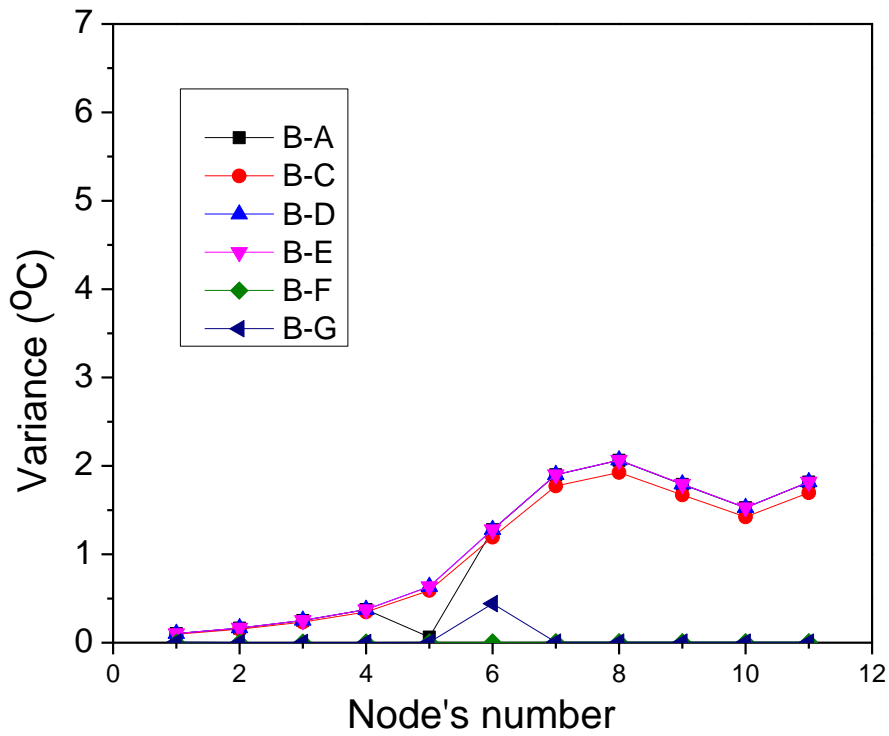
Figure 27 Variance of half machining on surface I

Figure 27, the variance value of B-A, B-C, B-D, and B-E for each node is undulate, and reach their maximum at node 8, respectively. However, the variance value of B-F and B-G stays almost the same (approximately 0) for each node, except node 6 which value reaches 0.5.

2.) Surface 2

Figure 28 Nodes on surface 2

Temperature changes and nodes' temperature variances from surface II are shown from Figure 29 to Figure 30. We can notice that temperatures do not have too huge swings either full machining or half machining on surface II.
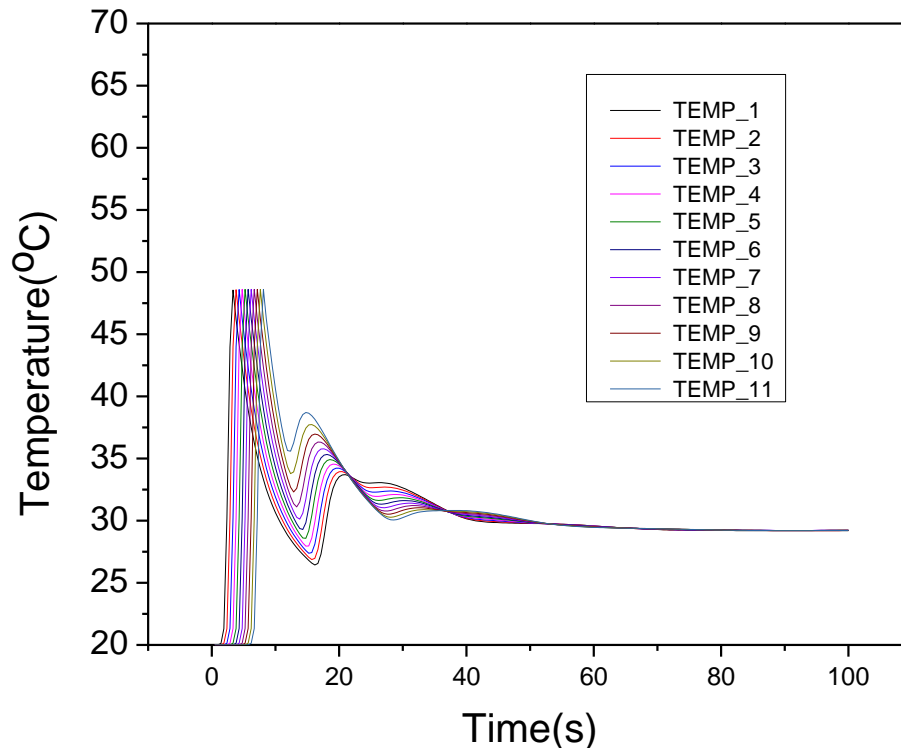
Figure 29 Temperature change of full machining on surface II

As seen in Figure 29, the temperature of each node has similar variation tendency with the extend of time, they have two obvious temperature peaks in the time range of 0~30s,

73

and the first temperature peak are their maximum of approximately 50°C. The detected nodes on surface II have similarity that the distance between the node with the tool in X direction is equal, hence the difference of their temperature change is just depended on the time.
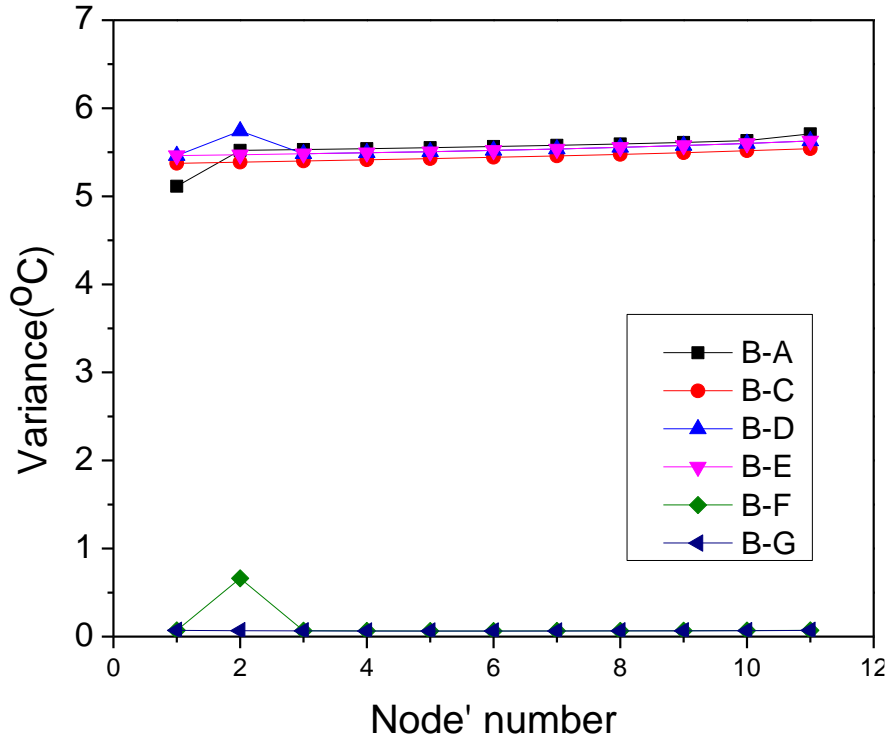
Figure 30 Variance of full machining on surface II

It can be seen from Figure 30, the variance of B-A, B-C, B-D and B-E has similar trend to each node, their variance value stays at 5~6. While the variance of B-F and B-G have similar trends, and get value of approximately 0, except node 2 to B-F.
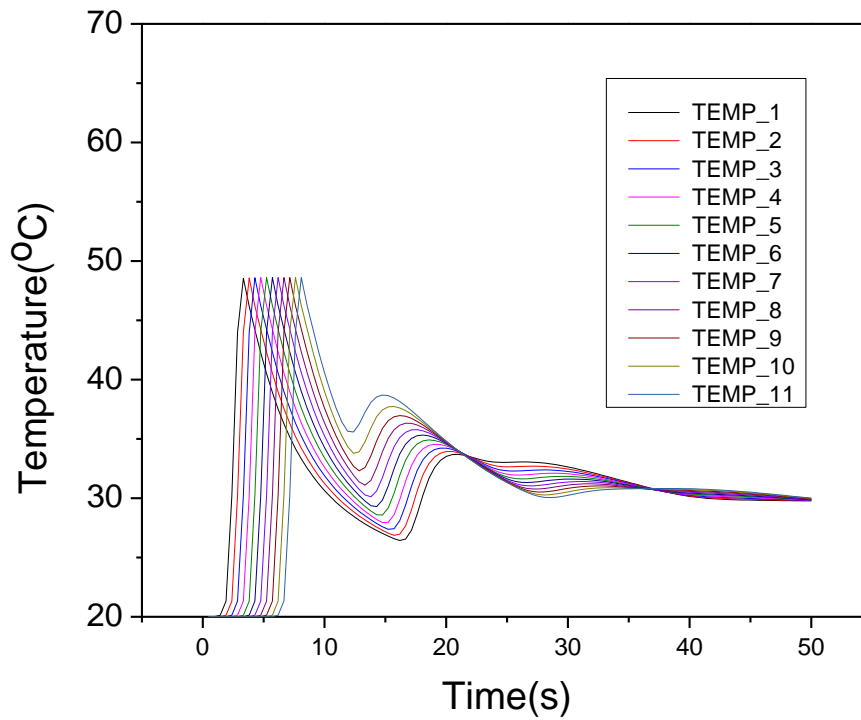
Figure 31 Temperature change of half machining on surface II

As seen from Figure 31, the temperature change of half machining is just as the first 50s of full machining on surface II, their variations are the same as the first 50s of full machining process.
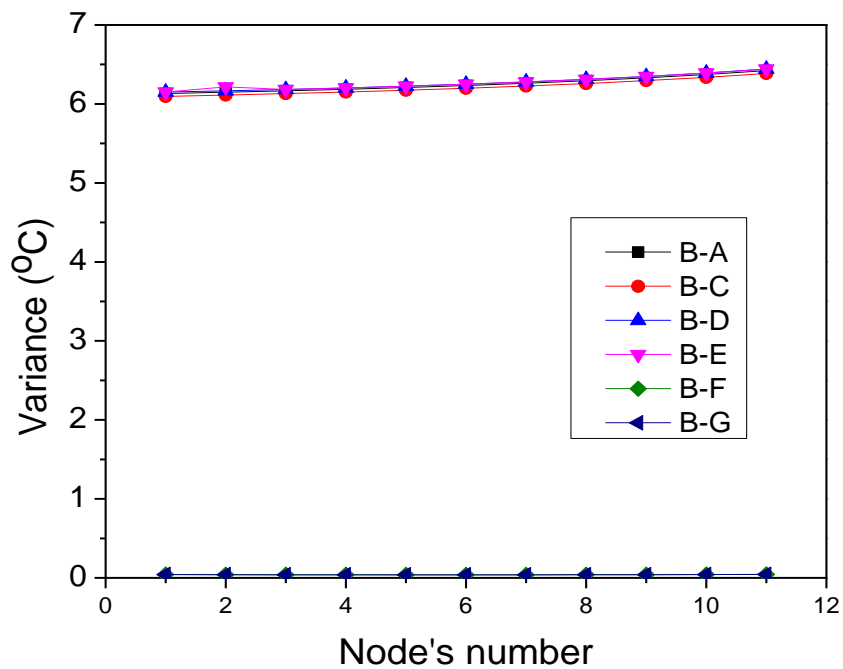
Figure 32 Variance of half machining on surface II

As seen from Figure 32 the variance values of all parameters have similar trend, almost stays the same, while B-A, B-C, B-D and B-E have the variance values of approximately 6, but B-F and B-G have the variance values of approximately 0.

   3.) Surface 3
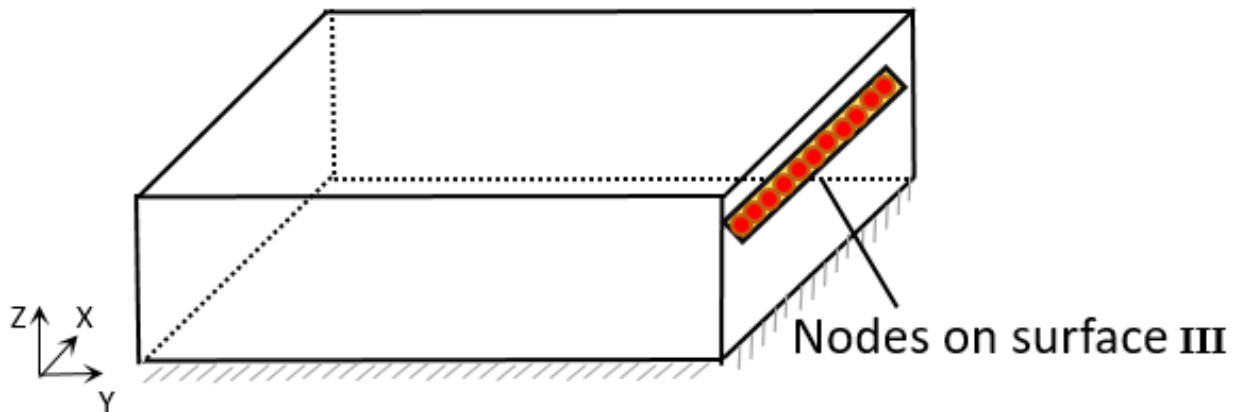
Figure 33 Nodes on surface 3

Figure 33 shows the schematic diagram of surface 3, the temperature change of full machining on surface III and the variance of parameters are shown in Figure 34 and Figure 35, respectively.
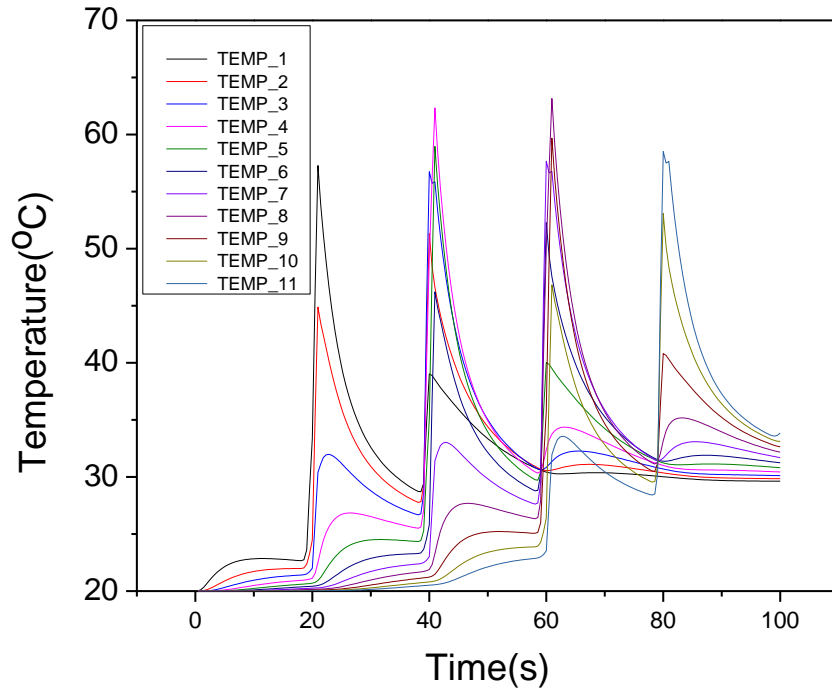
Figure 34 Temperature change of full machining on surface III

As shown in Figure 35, the variances of full machining on surface III for B-A, B-C, B-D and B-E are fluctuating as the different nodes in the value range of 5.5~6.5. However, the variances of B-F and B-G change a little almost staying at approximately 0.
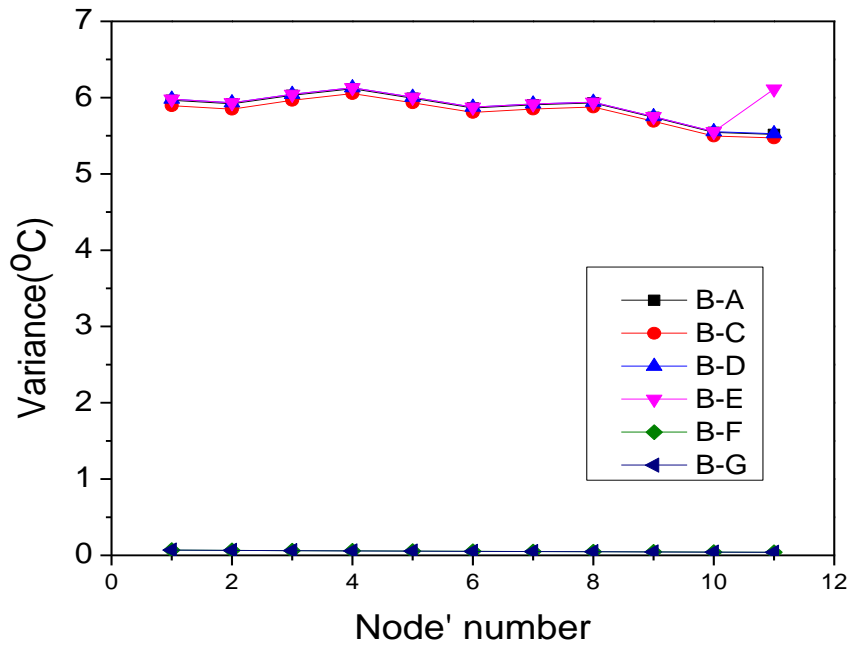
Figure 35 Variance of full machining on surface III

77

Figure 36 and Figure 37 are the temperature change of half machining and the variance of half machining on surface III, respectively.
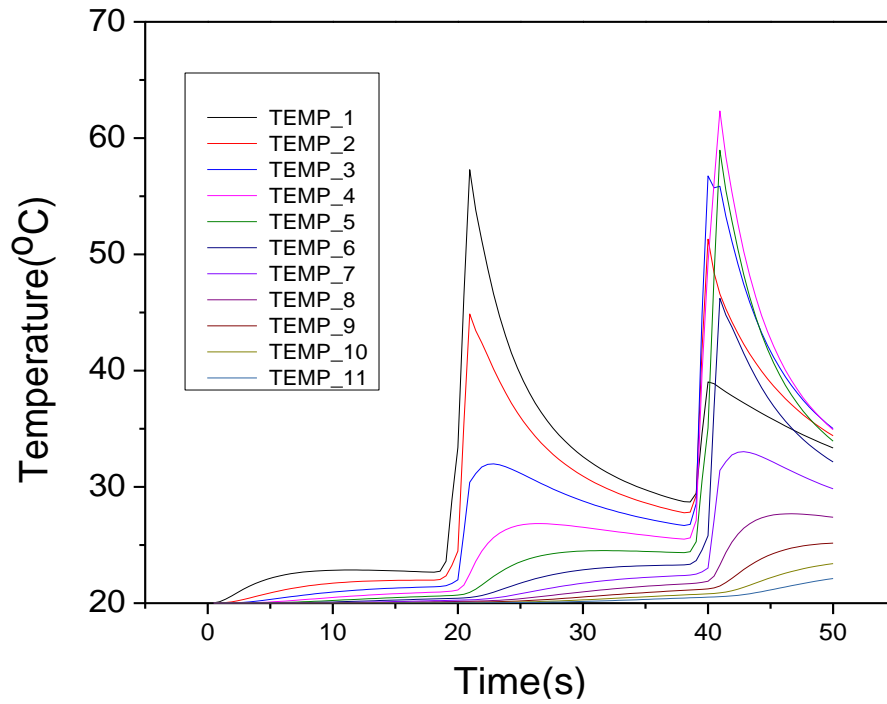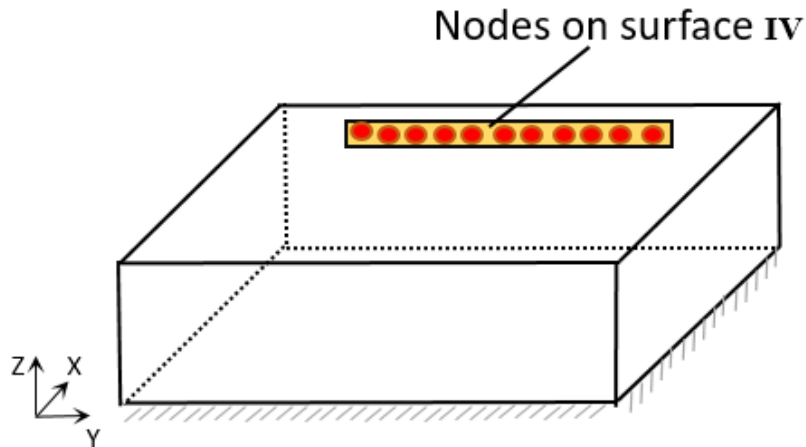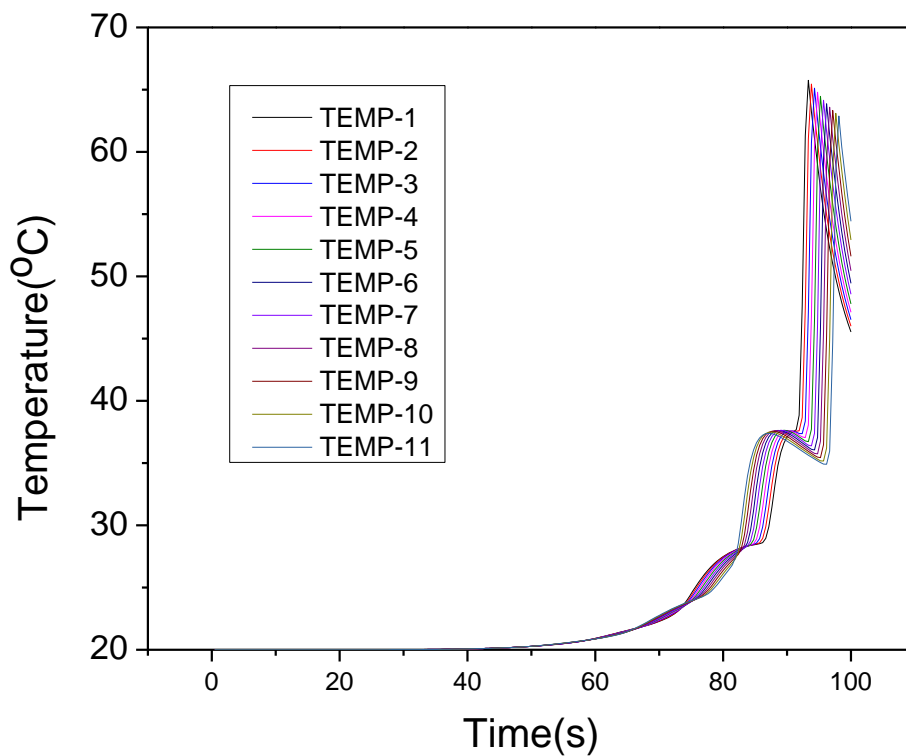

Figure 36 Temperature change of half machining on surface III

As shown in Figure 36, in the time range of 0~50s, node 1 to node 4 have no obvious temperature peak, and node 5 to node 8 have one obvious temperature in the time rang of 40~50s, while node 9 to node 11 have two obvious temperature peaks in the time rang of 20~30s and 40~50s. Overall, node 4 reaches its maximum temperature of 65°C in time rang of 40~50s.
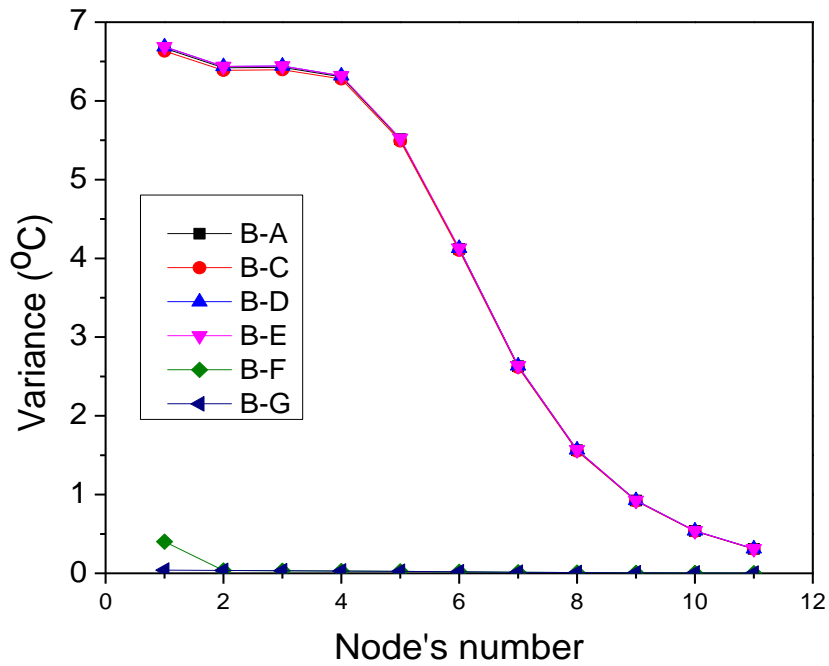
Figure 37 Variance of half machining on surface III

As shown in Figure 37, the variance value of B-A, B-C, B-D and B-E decrease with the increase of node's number, from 6.7 of node 1 to 0.4 of node 11. However, the variance value of B-F and B-G stay almost the same at 0, except node 1. Overall, parameter A, C, D and E have significant effect on the variance value, but parameter F and G have weak effect on the variance value.

4.) Surface 4

Figure 38 is the schematic diagram of surface 4. Figure 39 and Figure 40 are the temperature change of half machining and the variance of half machining on surface 4, respectively.

79

Figure 38 Nodes on surface 4

Figure 39 Temperature change of full machining on surface IV

As shown in Figure 39, there are two obvious temperature peaks on the curves for each node in the time range of 0~100s. In the first 40s, the temperature of the detected 11 nodes changes a little and their values are lower than 20°C as is the small amount of heat generated in the early cutting stage. Prolonging the cutting time, when the cutting time exceed 80s, the surface temperature increase rapidly, and then reaches their corresponding

80

maximum temperature in the time range of 90~100s. Furthermore, node 1 has the highest temperature of 67°C because of the shortest distance between node 1 with the initial cutting position.
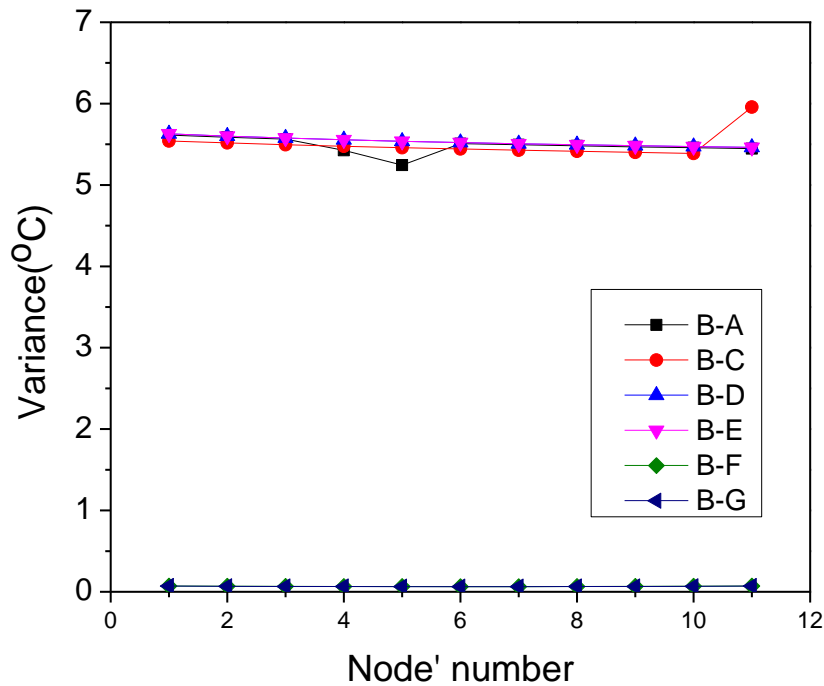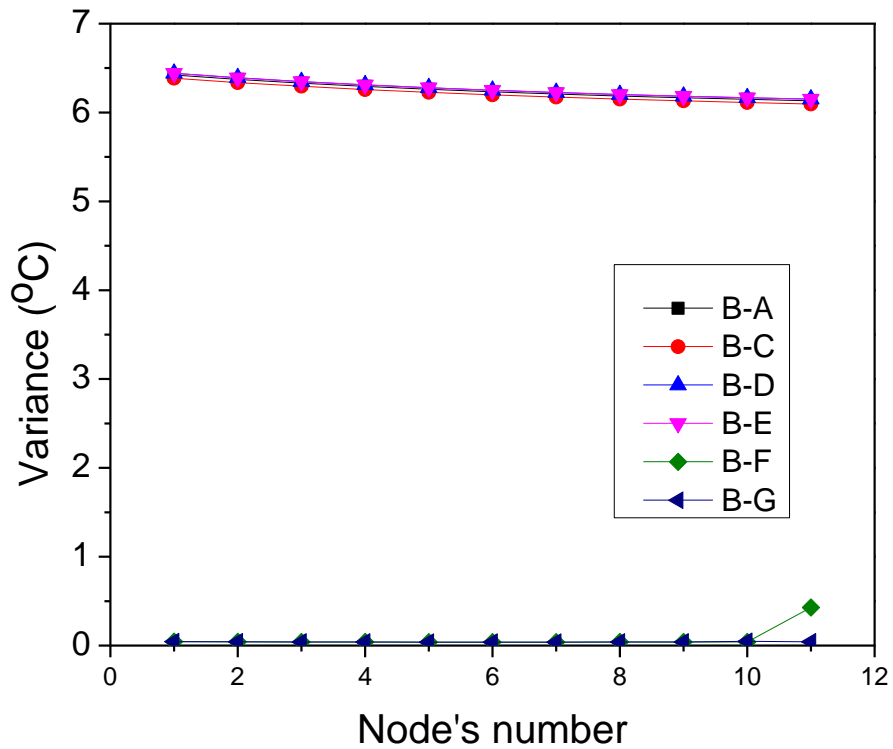

Figure 40 Variance of full machining on surface IV

As shown in Figure 40, the parameter effect of B-A, B-C, B-D and B-E have similar trend for each node, and their values are stay in the range of 5.5~6.0, except for node 11 which has a largest variance of 6.0. However, parameters of B-F and B-G have similar trend and stays almost the same at variance value of approximately 0.
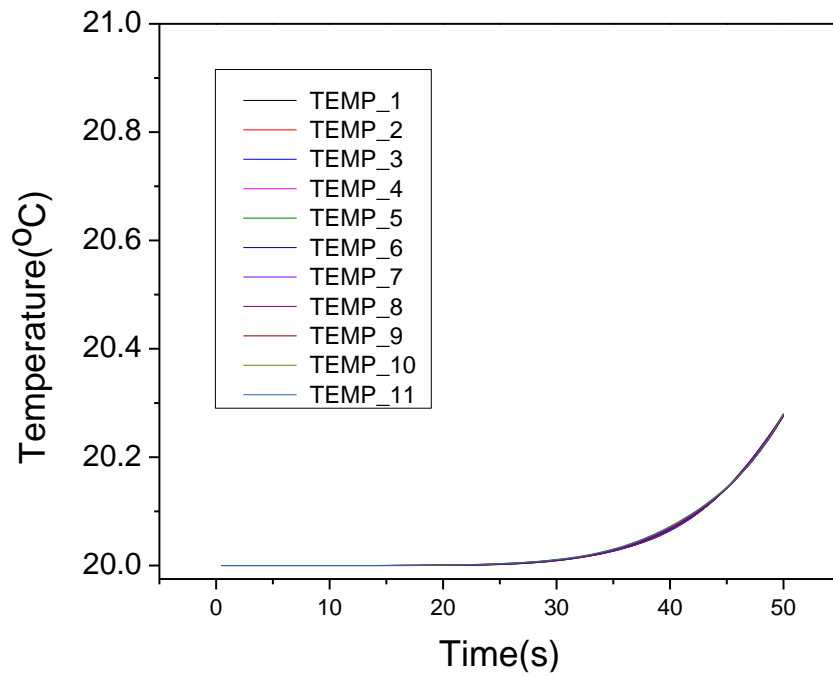
Figure 41 Temperature change of half machining on surface IV

As seen in Figure 41, in the first 30s, the surface temperature is almost the same of room temperature. After that, the increasing rate of surface temperature gets rapidly in the machining time range of 30~50s.

Figure 42 Variance of half machining on surface IV

As shown in Figure 42, the parameters effect of B-A, B-C, B-D and B-E have similar trend and their values increase with the increase number of detected node, while their values are stays in the range of 6.0~7.5. However, the parameters effect of B-F and B-G also have similar trend at the variance value range of approximately 0, except node 11 for B-F.

5.) Surface 5

Figure 43 is the schematic diagram of 11 nodes on surface 5. Figure 44 and Figure 45 are the temperature change of half machining and the variance of half machining on surface 4, respectively.
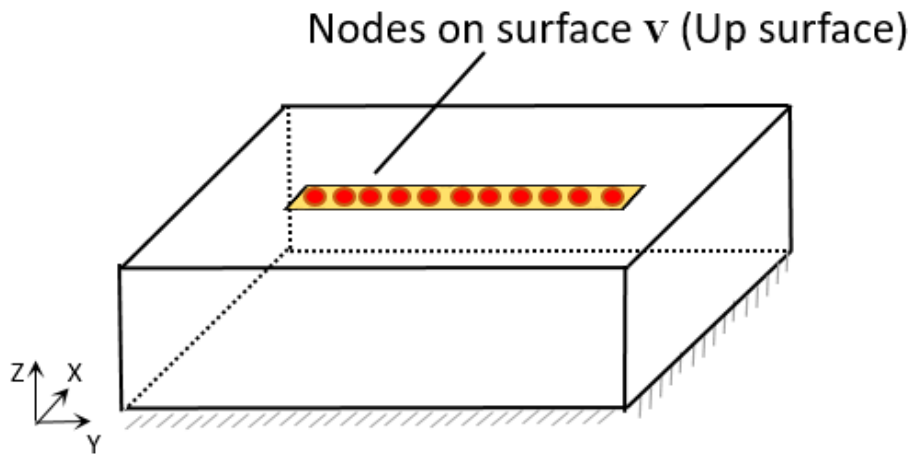
Figure 43 Nodes on surface 5
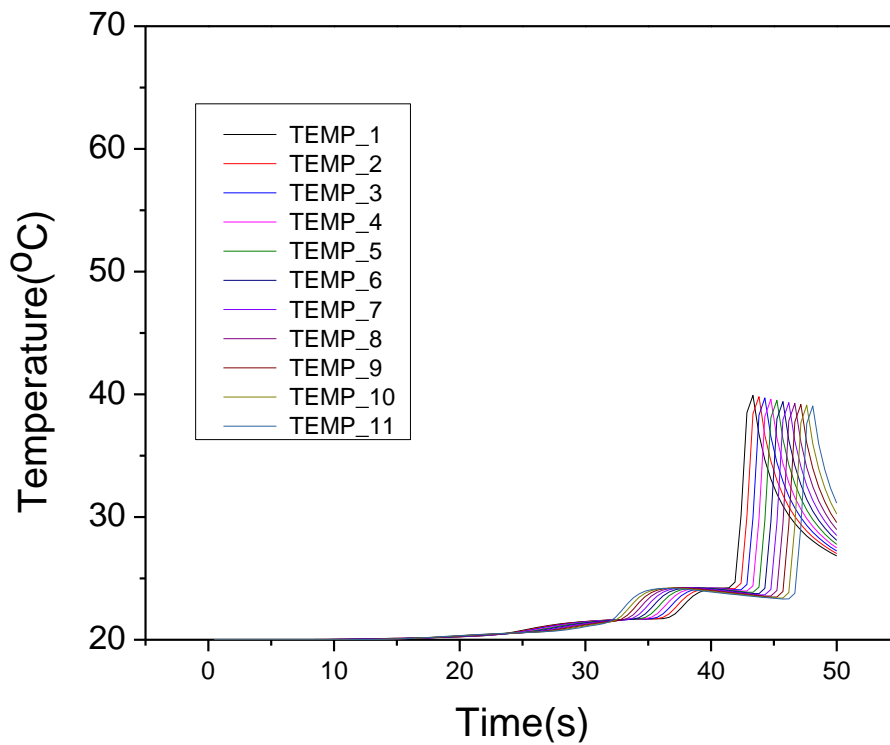
Figure 44 Temperature change of half machining on surface V

As shown in Figure 44, all nodes have similar trend with the prolonging of machining time. They have just one obvious peak temperature in the machining time range of 0~50s. And in the first 20s, their surface temperature almost stays the same, but after 30s, the increasing rate of their surface temperature get rapidly, and reaches their corresponding maximum in the machining temperature range of 40~50s. Furthermore, nodes one has the

largest temperature of 44°C due to the shortest distance between the node's position and the initial machining position.
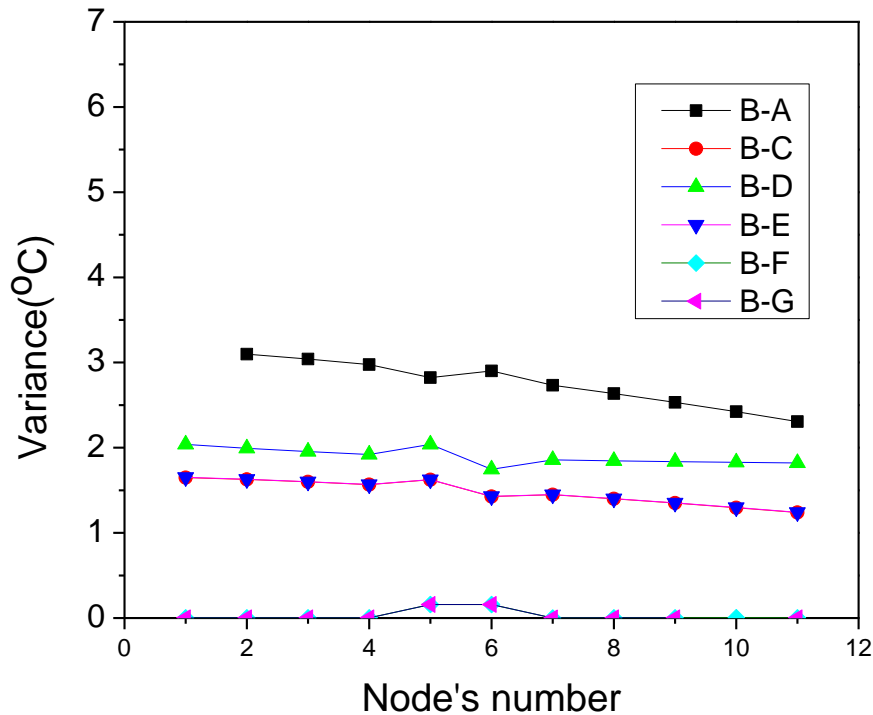

Figure 45 Variance of half machining on surface V

As seen in Figure 45, parameters B-A and B-E, B-F and B-G have same trend for 11 nodes, respectively. However, parameters B-A and B-D have different effect for 11 nodes. And the variance value of B-A is in the range of 2.5~3.2, B-D is in the range of 1.8~2.2, B-C and B-E is in the range of 1.3~1.7, B-F and B-G is in the range of 0~0.3.

5.5 Effectiveness of measurable points

5.5.1 Evaluation method for measuring points

In-process thermal estimation is employed in order to achieve two functions. One is an evaluation of thermal expansion; the other is a sensitive monitoring of machining process. Thermal expansion can be evaluated based on thermal temperature analysis of nominal machining situation. Deviations of machining process such as excessive tool wear, undesirable chip accumulation and so on can be detected based on inverse analysis of heat

conduction analysis [18-20]. In the proposed process monitoring method [18], process parameters are adjust based on the measured temperatures. Based on these functional viewpoints, effectiveness of measuring points should be considered both of thermal expansion and detection of process deviations. It is well known that thermal expansion of workpiece is proportional to temperature rise when other thermal properties are same. Therefore, comparison of temperature rise between the measurable points can be an evaluation index. Concerning deviation of machining process, it is assumed that temperature of effective points varies large when the machining process change. Figure 46 shows relations between two functions and effectiveness of the measurable point.
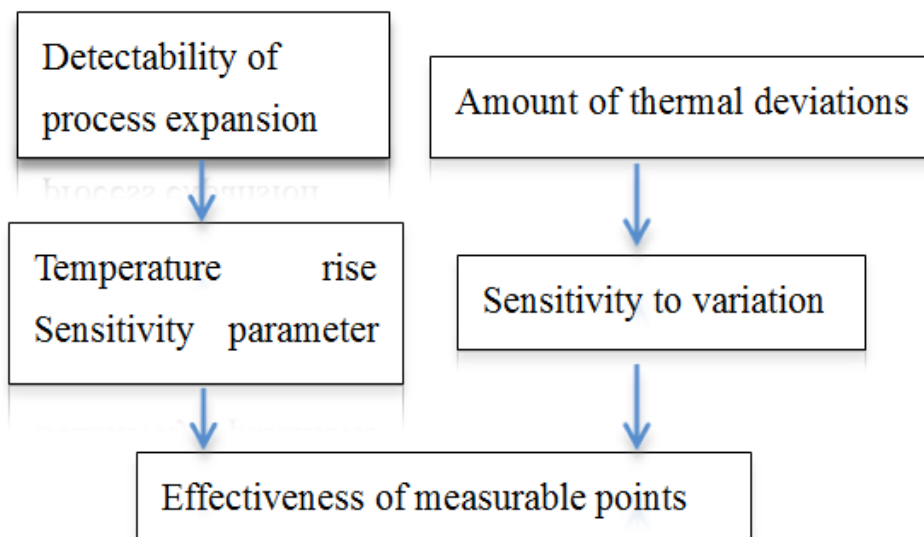

Figure 46 Constitute of EoP process

5.5.2 EoP formula

In this research, increases of heat flux caused by excessive tool wear and changes of heat transfer coefficients by chip accumulation are considered as dominant process deviation phenomena. Therefore, temperature sensitivity to the process parameters such as

amount of heat flux and heat transfer coefficients is introduced as a second index. Therefore, effectiveness of measurable points (EoP) is formalized as follows.

$$EoP_i = \frac{\Delta T_{i,n}}{\max\limits_{j\in\{1,N\}} (\Delta T_{j,n})} + \frac{\delta T_i}{\max\limits_{j\in\{1,N\}} (\delta T_j)} \qquad \text{5-1}$$

$$\delta T_i = \max\limits_{k\in\{1,M\}} (\Delta T_{i,k} - \Delta T_{i,n}) \qquad \text{5-2}$$

In Eq. 5-1, where i represents nodal number of measurable point (maximum number is N), k represents number of a thermal properties set (maximum number is M). $\Delta T_{i,n}$ indicates maximum temperature rise of i the node with nominal thermal properties set; Eq. 5-2 shows δT_i indicates variance of maximum temperature rise against the change of process parameters.

5.5.3 Result of one measurable point evaluation

Based on the results of simulation and proposed formulation, effectiveness of measurable points (EoP) for candidate nodes is calculated. Results of calculation for the full machining and the half machining are listed in Table 3 and Table 4 respectively.

This variance is a measure of how large the temperatures are affected from the process change. It can be an index of the effectiveness of measurable point.
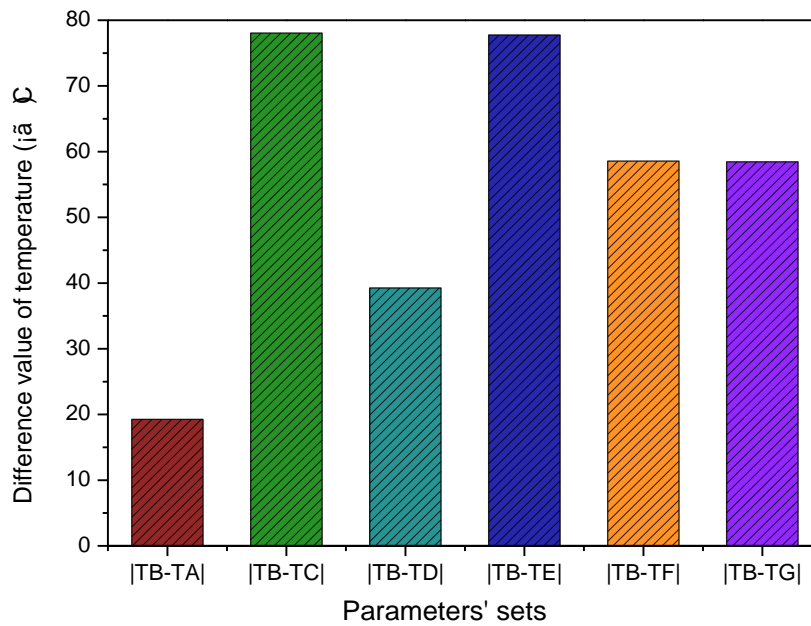
Figure 47 Temperature difference of point 1 on surface I in full machining

Figure 46 illustrates the change of temperature in machining process, and Figure 47 shows the numerator of second part of the EoP formula. In the first part, we can evaluate the effectiveness of each point based on the temperature rise. In the second part, we can evaluate the sensitivity against the process change based on the difference of temperature rise. For example, variance of point 1 in 6 sets show sensitivity against the change of the simulation parameters. The combination of the Figure 47 and Figure 48 gives enough information to calculate EoP formula. Finally, we can calculate the EoP values of each point seen in the Figure 49, which illustrates most effective points in surface I is point 4.
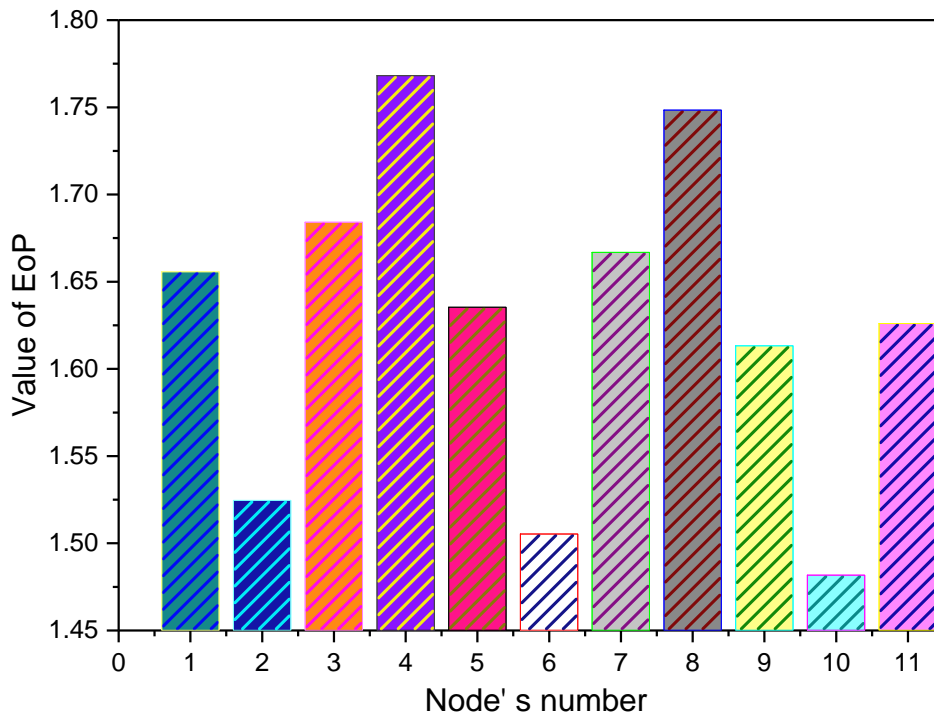
Figure 48 EoP of full machining on surface I

By the same way, we can list other surfaces' effectiveness of measurable points. By using the method mentioned above, other sensitive points can be selected in two machining cases.

5.5.4 Results of measurable points evaluation

Based on the results of simulation and proposed formulation, effectiveness of measurable points (EoP) for candidate points are calculated. Results of calculation for the full machining and the half machining are listed in Figure 49 and Figure 50 respectively.

We can know where the temperature changes hugely and fluctuates with parameters by using the EoP values. It is a quantification method of effectiveness. Figure 49 illustrates the score of point 1 of surface IV from full machining have the largest score (1.80) in all surfaces of full machining process. The score of point 2 to point 5 of surface IV scored 1.79 -1.76. At the same time, point 6 and point 10 of surface III and point 4 of surface I scored 1.76, 1.77 and 1.77, respectively.
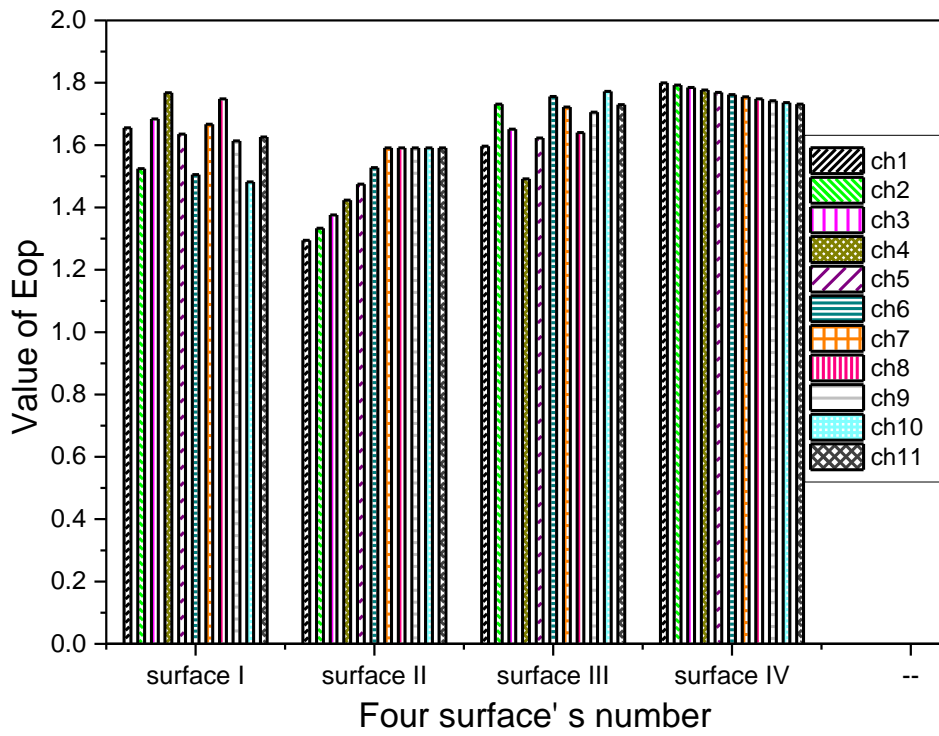
89

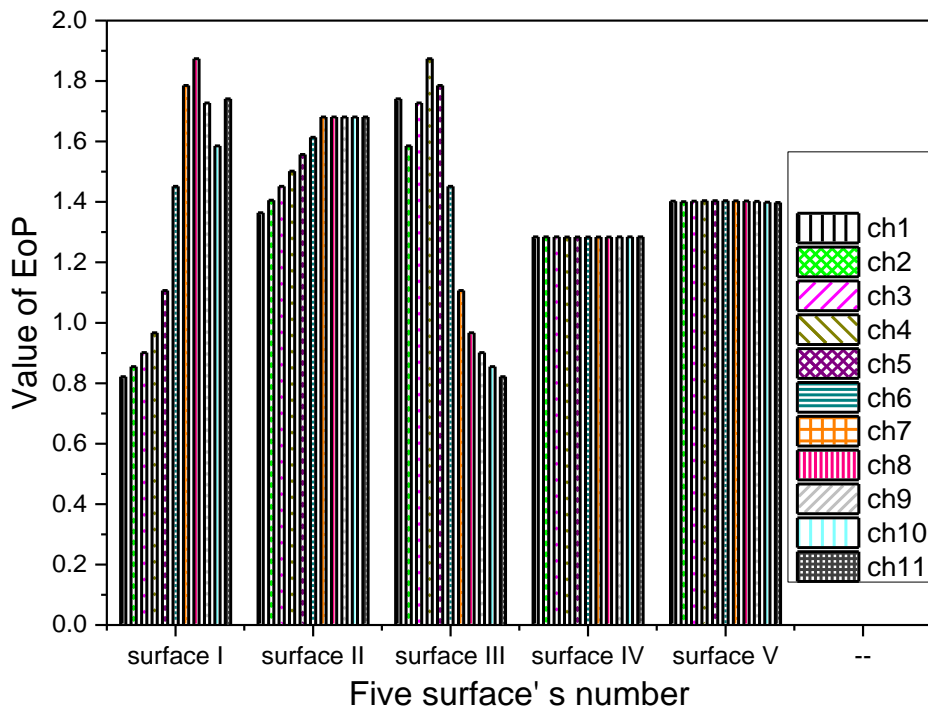**Figure 49 EoP of temperature in half machining**

Figure 50 EoP of temperature in full machining

As shown in the flowing Figure 50, we can see that 11 points on either surface IV and surface V of EoP have same temperature score (1.28 and 1.40). Point 8 on surface I and point 4 on surface III have largest score (1.87) of EoP value in half machining. Furthermore, point 7 on surface I and point 5 on surface III have second largest score (1.79).

Using this method, we can pick the effective points from 44 points in full machining and 55 points in half machining. In order to determine the effective measuring points, we also consider convenience of measurement. After the EoP analysis of two machining cases, selected measuring points based on the effectiveness of measurable points are shown in Figure 51 and Figure 52 respectively.

In the full machining case, point 4 on surface I, point 6 and 10 on surface III, and points from 1 to 5 on surface IV are selected. On the other hand, point 7, point 8, point 9 and point 11 on surface I, point 1 and point 3 to point 5 on surface III in half machining process are selected as effective points. Considering the possibility of measurement about workpiece by thermocouple in production process, we selected these surfaces and chose 8 points based on the value of EoP evaluation.

Table 5 EoP of temperature for full machining

Node	1	2	3	4	5	6	7	8	9	10	11
Full I	0.84	0.89	0.86	0.86	0.90	0.95	0.91	0.90	0.94	1.00	0.89
Full II	1.02	1.03	1.03	1.03	1.03	1.03	1.03	1.03	1.03	1.03	0.62
Full III	1.15	1.27	1.21	1.19	1.30	1.44	1.34	1.30	1.42	1.57	1.37
Full IV	1.03	1.03	1.03	1.03	1.02	1.03	1.03	1.03	1.03	1.03	0.99

We know where the temperature change hugely is the amounts of EoP largely by quantification method. The score of node 10 of surface III from full machining have the largest score in all surfaces of case of full machining process. We can see that node 1 to node 11 from half surface II of EoP have same largest temperature score (1.07) as well. Using this method, we can pick all the sensitivity nodes from 99 nodes.

Table 6 EoP of temperature for half machining

Node	1	2	3	4	5	6	7	8	9	10	11
Half I	0.82	0.83	0.85	0.88	0.73	0.89	0.82	0.84	0.90	0.97	0.94
Half II	1.07	1.07	1.07	1.07	1.07	1.07	1.07	1.07	1.07	1.07	1.07
Half III	0.96	0.98	0.91	0.85	0.76	0.84	0.89	0.89	0.86	0.84	0.82
Half IV	0.80	0.80	0.81	0.81	0.81	0.73	0.81	0.81	0.81	0.81	0.82
Half IV	0.73	0.65	0.65	0.64	0.69	0.63	0.63	0.63	0.63	0.73	0.66

Let us assume the case of available number of thermocouples are four. We select the effective measuring points from the evaluation of measurable points in full machining and half machining and convenience of measurement. Based on the principle described in section 2, four effective points are selected for both cases. They are illustrated in Figure 51and Figure 52 respectively. In the full machining situation, points III_6, III_9, III_{10} and III_{11} are selected. On the other hand, points form II_1, II_4, II_8 and II_{11} are selected in half walking process. Although we got same score in half surface II, we only chose four nodes within same scores of EoP score, because we consider balance measurement about workpiece by sensors in production process, and also it is much convenient to measure by using the separate measurements.
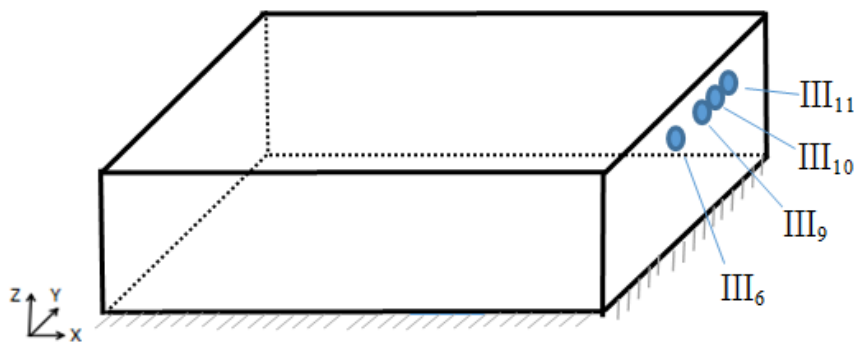

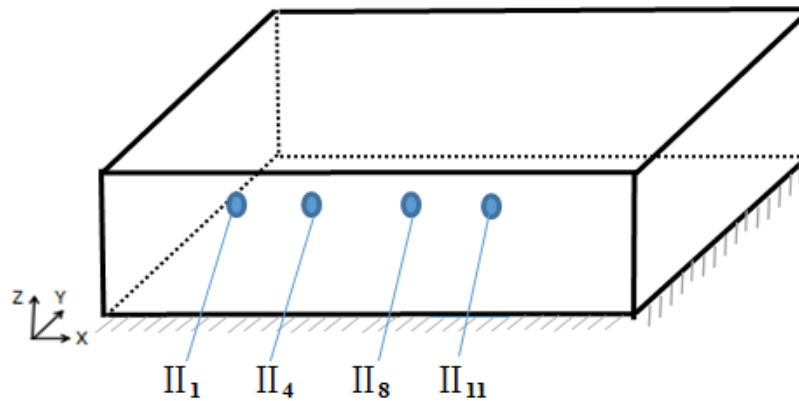
Figure 51 Effective nodes on the full machining

Figure 52 Effective nodes on the half machining

5.6 Summary

1. By using FEM-based thermal simulation, analysis of temperature distribution and sensitivity analysis are carried out.

2. Based on the results of calculation, measurable points for different machining situations are evaluated.

3. As the results, different measuring points are selected according to the change of machining situation. Furthermore, evaluations of points including sensitivity analysis can be obtained stable results at a reasonable computational cost.

6 Applications

In order to evaluate the heat flux transferred into the workpiece, some theoretical models based on FEM analysis have been investigated in the literature. For more accurate parameters by orthogonal test, we present a method to evaluate an effectiveness of each measuring points from aspects of stability of measurement and sensitivity to the process variation, based on these analysis effectiveness of measurable points (EoP) can be calculated by using thermal simulation and variation modelling.

Every machining thermal analysis is based on previous calculation or determination of temperature field during machining process, which constitutes the thermal distribution load to be applied to the overall workpiece.
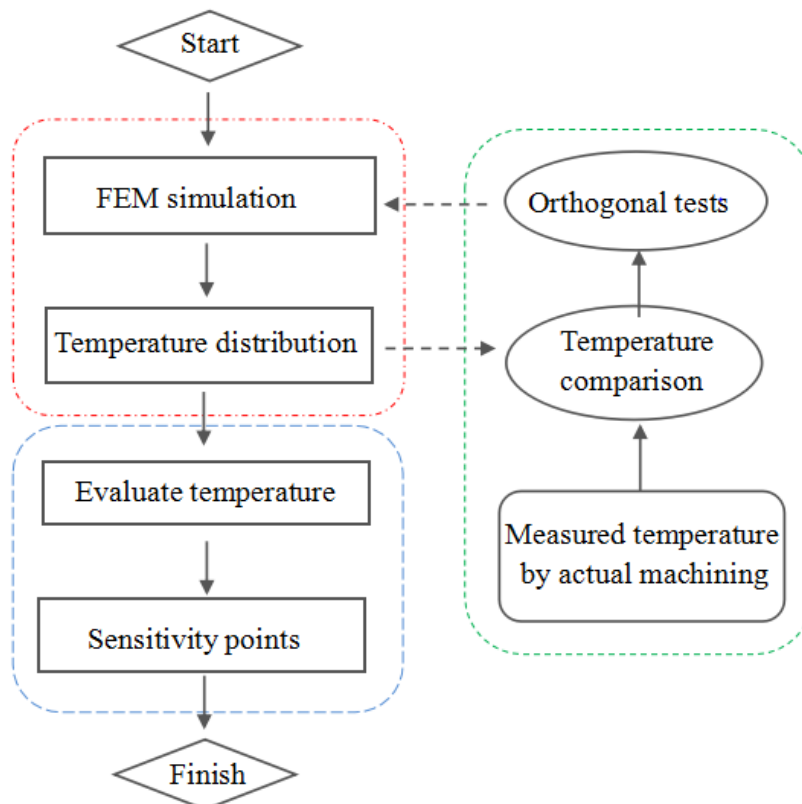

Figure 53 Detailed information flow

6.1 Simulation models

As described in chapter 4, numerical simulation of machining process has begun to be successfully simulated by FEM codes, the results of simulations can be used to explain the physical essence of some complex phenomena in various machining process, we mentioned that simulation can predict thermal distribution when cutting process exchanged, see Figure 54, by simulation software we mentioned in chapter, see the temperature distribution in Figure 55.
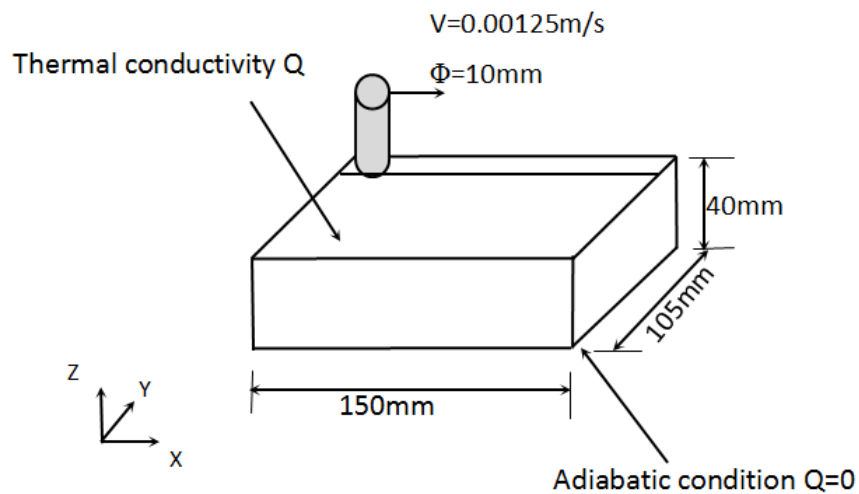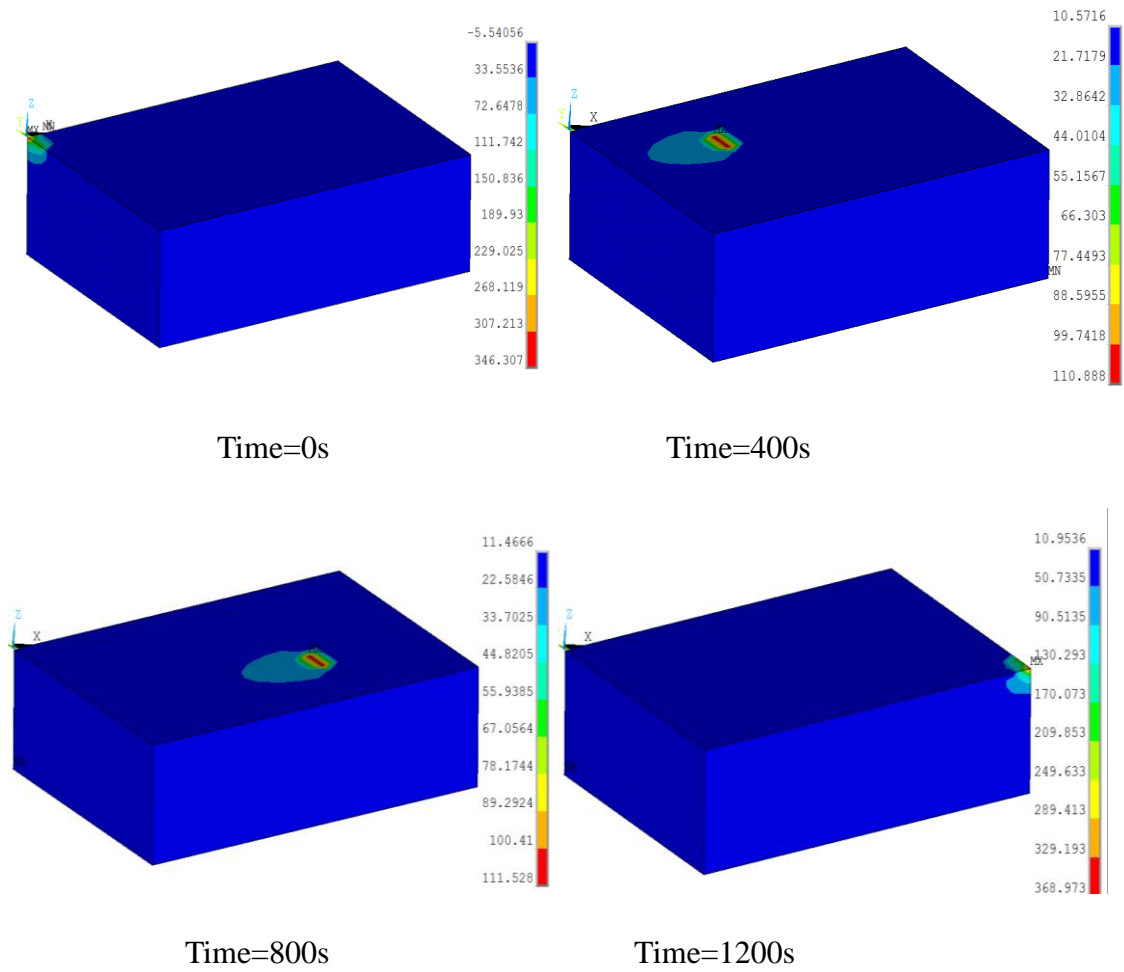

Figure 54 Parameters in end milling process

Time=0s   Time=400s

Time=800s   Time=1200s

Figure 55 Temperature distribution of workpiece

6.2 EoP application models

We consider same thermal couple as before models. There are 10 thermocouples named ch1 to ch10 shown in Figure 56, and we talk the variance by two thermocouples, name ch6 and ch8 shown in Figure 57.
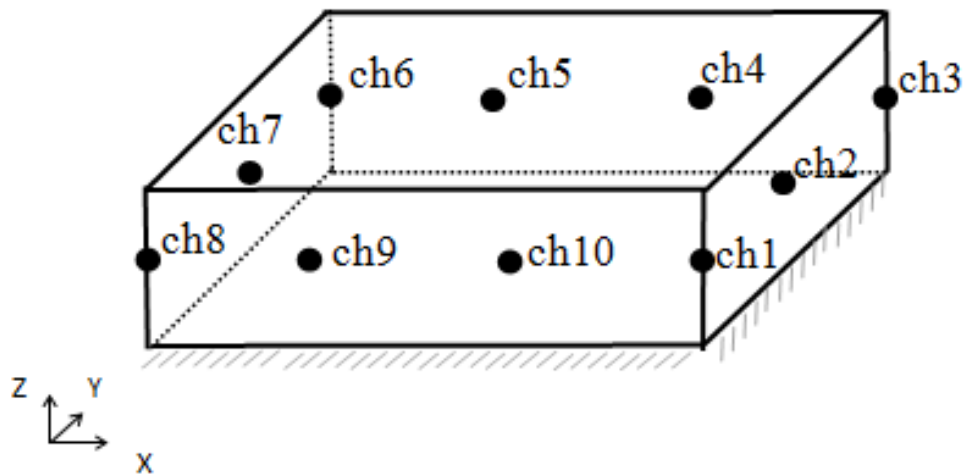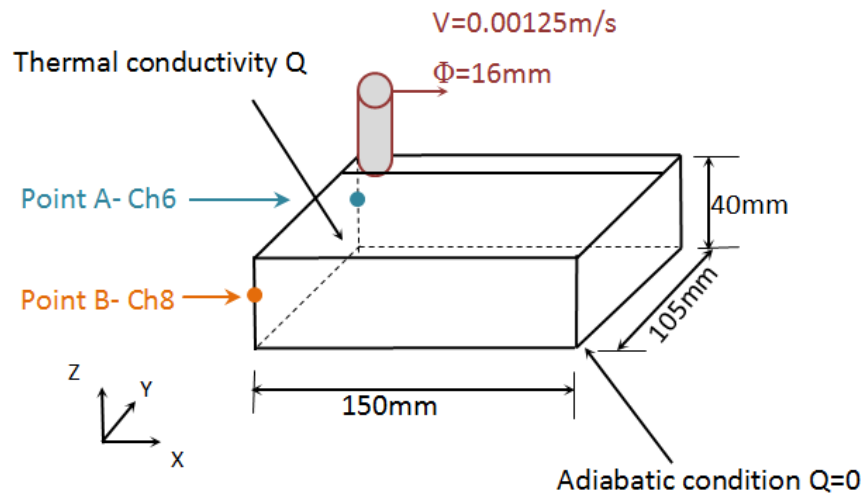
Figure 56 workpiece shape and thermocouples

Figure 57 Parameters in end milling process

6.3 Orthogonal tests

From chapter 5, the results show the two different paths go through the surface of workpiece and have a certification to EoP, but the thermal parameters are changing varies.

Orthogonal test method can reduce test times, shorten test cycles and find multi-factors optimization scheme quickly. As we all known that heat flux, heat coefficient and thermal conductivity make different contributions to thermal environment in machining process, and from orthogonal tests, we can make it clearly that which factor make

97

sensitivity effects to temperature changes. Task significant illustrated in Figure 58and orthogonal experimental design shown as Table 7.
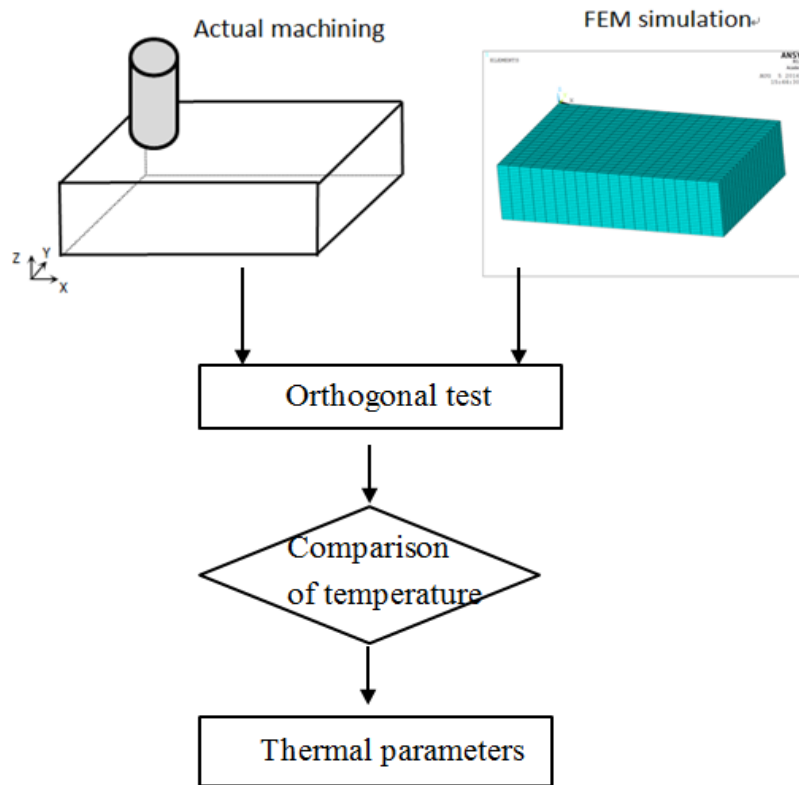

Figure 58 Orthogonal tests

Table 7 Orthogonal parameters

Set	A-Heat conductivity (W/(m•K))	B-Heat coefficient (W/m²•K)	C-Heat flux (w/m²)
1	15	194	24
2	22	278	35
3	26	361	45

In mathematics, in the area of combinatorial designs, an orthogonal array is a "table" (array) whose entries come from a fixed finite set of symbols, A variation simulation based on orthogonal array has three factors, they are thermal conductivity (HC), heat transfer coefficient (HTC) and heat flux (HF), and we named them as A, B and C, respectively. From the orthogonal arrays, we listed 10 sets by Table 8; variation simulations which are

a set of various simulations is carried out and compared with experimental results. Calculated results as a set can be considered to represent a simulated result with uncertainty. The fifth set of data (Set 5) A=22w/(m•k), B=278w/m^2•k and C=35w/m^2 as the nominal set, which is the middle set in the orthogonal arrays.

Table 8 Orthogonal arrays

Set	A	B	C
1	1	1	3
2	1	2	2
3	1	3	1
4	2	1	2
5	2	2	2
6	2	2	1
7	2	3	3
8	3	1	1
9	3	2	3
10	3	3	2

In this article, we consider 10 points of workpiece evaluated by thermocouples [10], as shown in Figure 56. By 9 sets from orthogonal arrays, we distinguished 9 sets of 10 points' temperature change with heat moving process in simulation tests and actual experiments. Use ch6 as an example, which we can see from Figure 57 that simulation test and actual test looks much similar by the date of run 3: A1B3C1.

Orthogonal test method can reduce test times, shorten test cycles and find multi-factors optimization scheme quickly. As we all known that heat flux heat coefficient and conductivity make different contribution to thermal environment by machining process, and from orthogonal test, we can understand which factor make sensitivity effects to temperature change.

1) Average temperature to test results.

We can see that value R is A>C>B, which means heat flux make biggest contribution to average temperature changing.

Table 9 Range analysis of experimental results

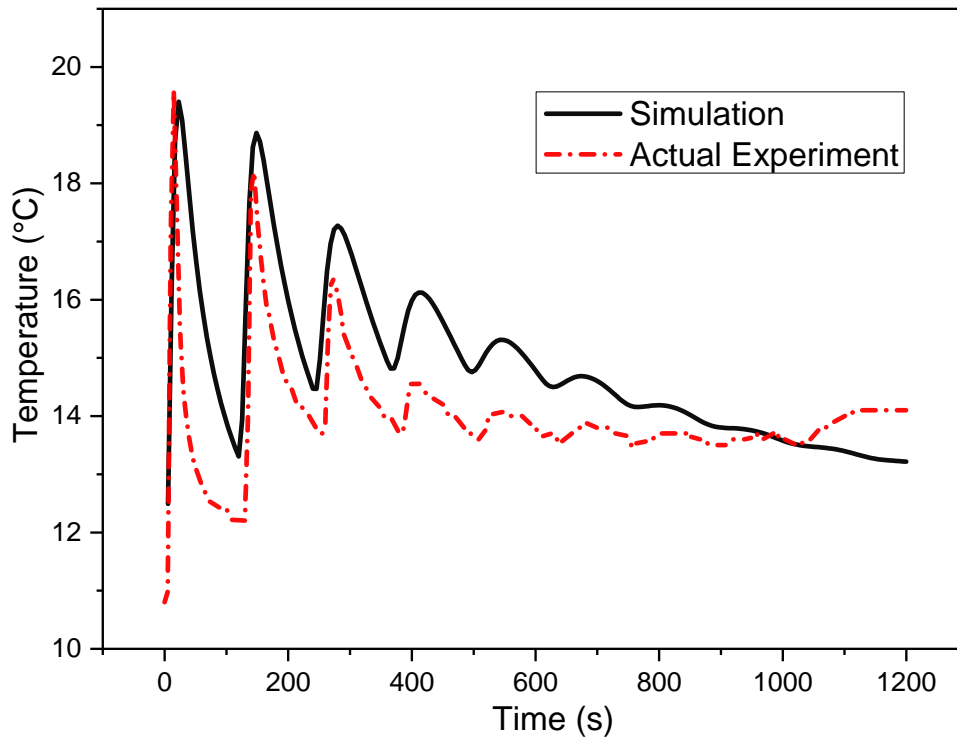|	A	B	C	variance
1	1	1	3	1.211
2	1	2	2	1.523
3	1	3	1	1.860
4	2	1	2	1.788
5	2	2	1	2.246
6	2	3	3	1.794
7	3	1	1	2.603
8	3	2	3	2.067
9	3	3	2	2.539
K1	4.594	5.601	6.709	
K2	5.827	5.836	5.850	
K3	7.209	6.193	5.072	
k1	1.531	1.867	2.236	
k2	1.942	1.945	1.950	
k3	2.403	2.064	1.691	
R	0.872	0.197	0.546	

Figure 59 Evaluation the accuracy process of ch6

2) Area difference to test results.

Temperature distribution from actual test and FEM simulation test, we can define the Area difference value under orthogonal tests, Figure 60, Which A (Heat flux), B (Heat coefficient) and C (Heat conductivity) in the form, k1, k2, k3, R. We can see that value R is C<B<A, which means thermal conductivity make biggest influence on D-value of area.

The deviation of analytical solutions as compared to the nearly constant FEM simulation results could be caused by the thermal conductivity which subsequently influences the difference area value. Simulation compares experiment，Mr. Tanaka did experiment in (22-278-35)

Table 10 **Range analysis of experimental results**

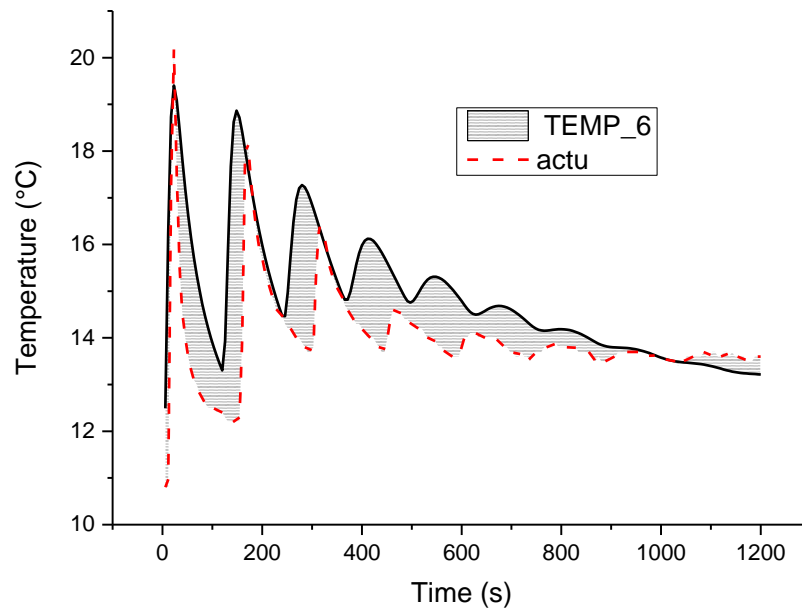|	Case number	A	B	C	ABS area
1	A1B1C3	1	1	3	1859.6
2	A1B2C2	1	2	2	1387.3
3	A1B3C1	1	3	1	941.6
4	A2B1C2	2	1	2	2690.8
5	A2B2C1	2	2	1	2139.4
6	A2B3C3	2	3	3	1843.9
7	A3B1C1	3	1	1	3492.8
8	A2B2C3	3	2	3	3103.1
9	A3B3C2	3	3	2	2559.8
K1		4188.6	8043.2	6573.8	
K2		6674.1	6629.8	6637.9	
K3		9155.7	5345.3	6806.6	
k1		1396.2	2681.1	2191.3	
k2		2224.7	2209.9	2212.6	
k3		3051.9	1781.8	2268.9	
R		1655.7	899.3	77.6	

Figure 60. Area difference

From these two orthogonal tests, we can define the value of parameters in this simulation that help us to do most similar simulation with experiment. Temperature distribution changing with thermal parameters by FEM, and then we do patterns of measurement points, which shows evaluation points are changed to the predicated points, the influence of measurement points will be different. In this article, we mentioned three cases of machining process by different paths.

6.4 Square model 1

Following two figures estimated temperatures and actual temperatures at two points, Figure 62 and Figure 63 illustrate comparisons of measured temperature and the variational simulations at point 6 and 8 in Figure 57. From the Figure 62, we can see the two points have temperature fluctuation in machining process in 1200s, and the nominal set curve (Set 5) is in the middle of 10 simulation lines, 6 raise temperatures to peaks quicker than 8, because they are in different location of workpiece, and heat source walking

through the surface as shown in Figure 54. As shown in the Figure 64, measured results can be contained within the range of the variational simulations. This indicates if we can adjust an appropriate parameter set, actual machining situation can be represented accurately.
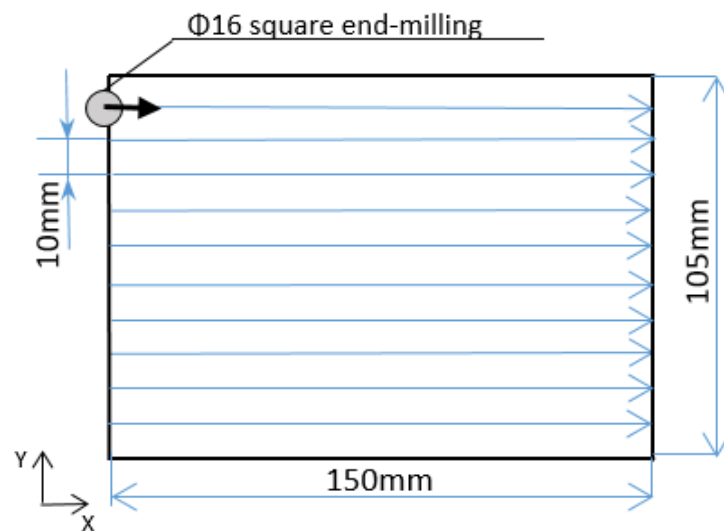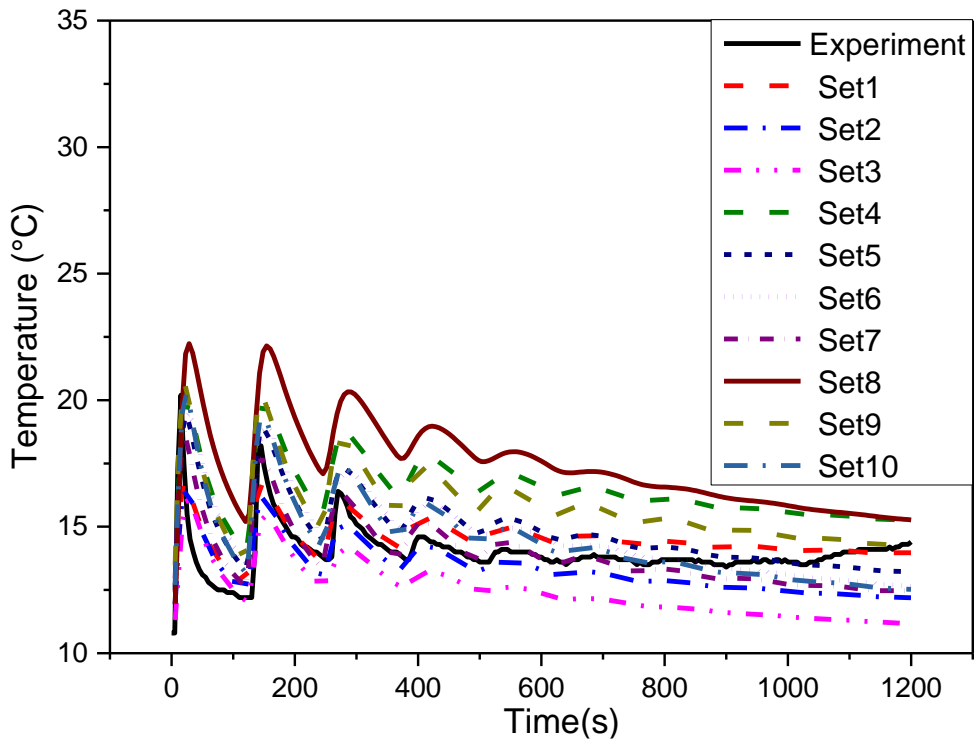

Figure 61 One-way parallel paths

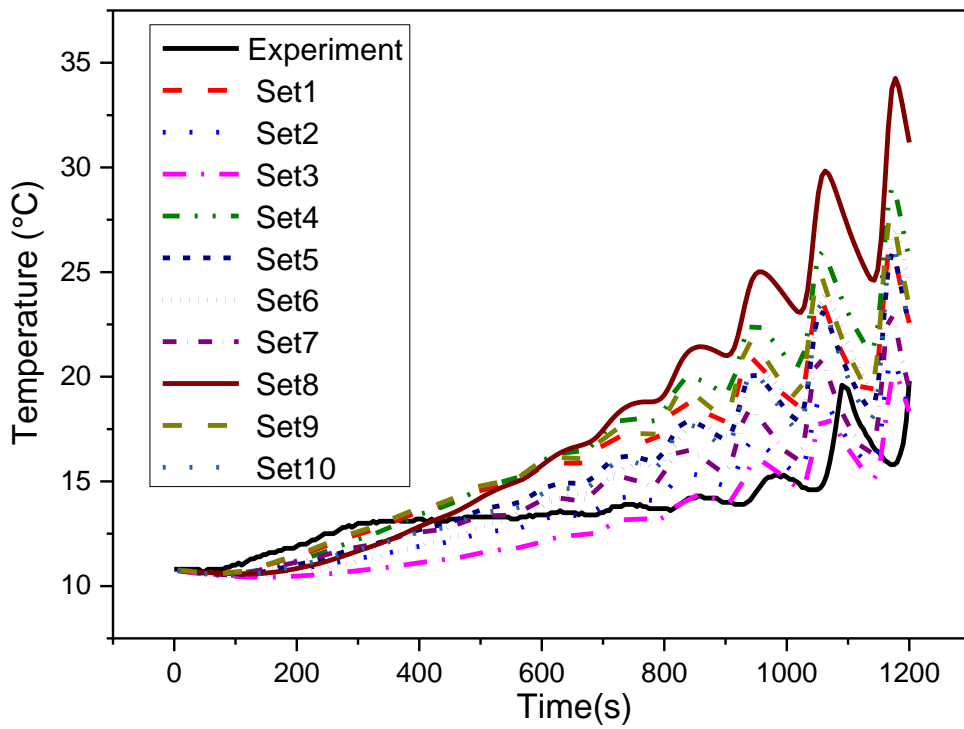**Figure 62 Temperature at point 6 in Fig.2**

Figure 63 Temperature at point 8 in Fig.2

Use ch1 in one way moving path as an example, we calculate temperatures under different experimental parameters of heat flux, heat conductivity and heat transfer coefficient shown in Table 7 Then, the differences of maximum temperature of each point are calculated. As we mentioned before that δT_i indicates variance of maximum temperature rise against the change of process parameters. In Figure 64 (b) shows the values of $\Delta T_{1,3} - \Delta T_{1,n}$ temperature difference of point 1, $|T_3\text{-}T_5|$ represents between the No.3 parameter set and nominal parameter set (No.5 set). In this case, $|T_3\text{-}T_5|$ gets the highest variance (0.647℃) in one way moving path machining. Therefore, this value becomes δT_1. At the same time, δT_2 to δT_{10} corresponding to ch1 to ch10 are also calculated based on the 9 values of $|T_1\text{-}T_5|$, $|T_2\text{-}T_5|$, $|T_3\text{-}T_5|$, $|T_4\text{-}T_5|$, $|T_6\text{-}T_5|$, $|T_7\text{-}T_5|$, $|T_8\text{-}T_5|$, $|T_9\text{-}T_5|$ and $|T_{10}\text{-}T_5|$ for each point.
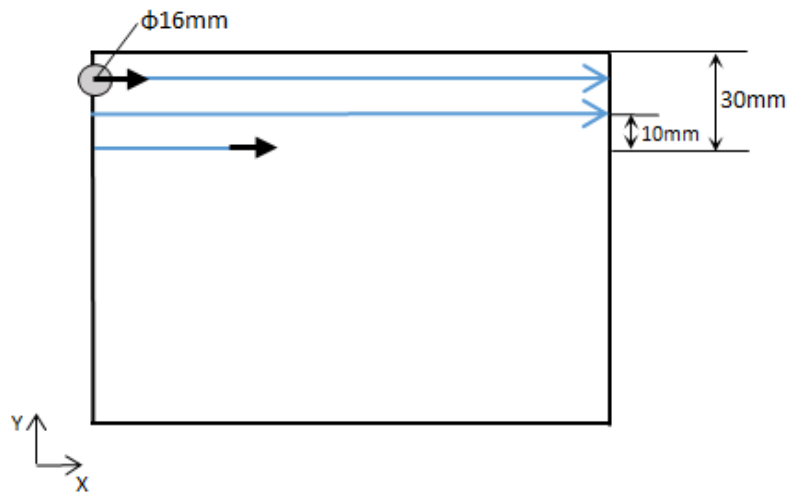
(a) One-way parallel paths in 1/4 time
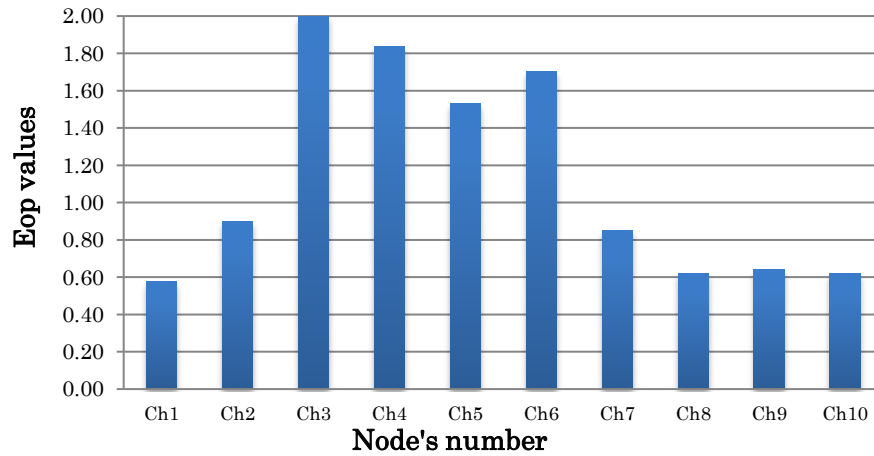
(b) EoP of one-way parallel paths

Figure 64 One-way parallel paths and EoP value

As shown in Figure 64, Ch3 is the most sensitive point by one-way movement paths. From this EoP formula, we can easily understand that some points show large variance number as sensitive parameters' change or/and thermal expansion.

To evaluate the feasibility of the EoP value, results of inverse analysis which are used different measuring points are investigated. In the reported paper [18], a relation between the measuring points and estimation error has been reported. In the research, we had a clear identification that Ch3 is the good point but not the Ch1, which illustrated in this last section of chapter 6, see from figure 64.
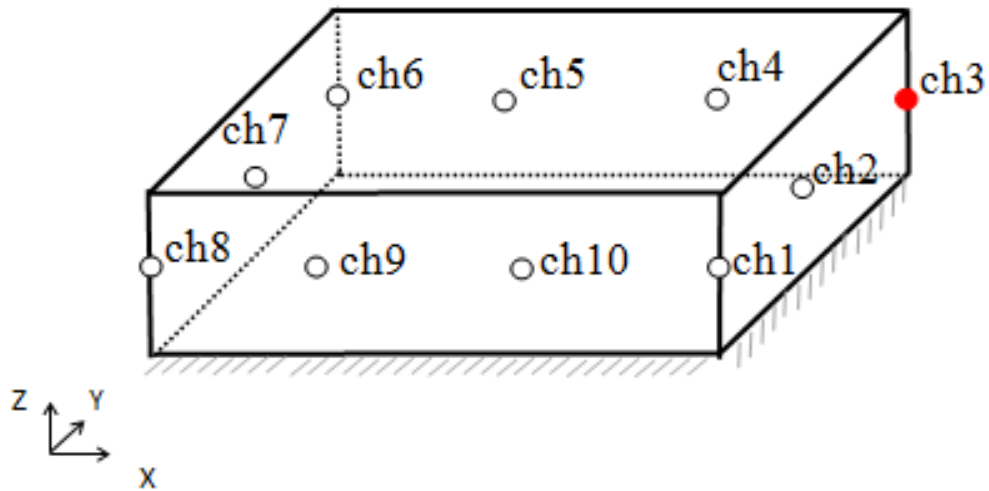
Figure 65 Sensitive point in one-way parallel path

6.5 Square model 2

From round-way parallel paths walking of Figure 66 and Figure 67 in a quarter time show the different case study, and we still use the same method the results from EoP value shows in Figure 68, we noted that EoP value of Ch3 is equal 2 ,it is still the most sensitive point not only in one-way parallel paths but also in round-way parallel paths. Then, Ch6 has larger value of EoP than other points in round-way parallel paths. We can draw Figure 69 with the sensitive point in round-way parallel paths by upper description.
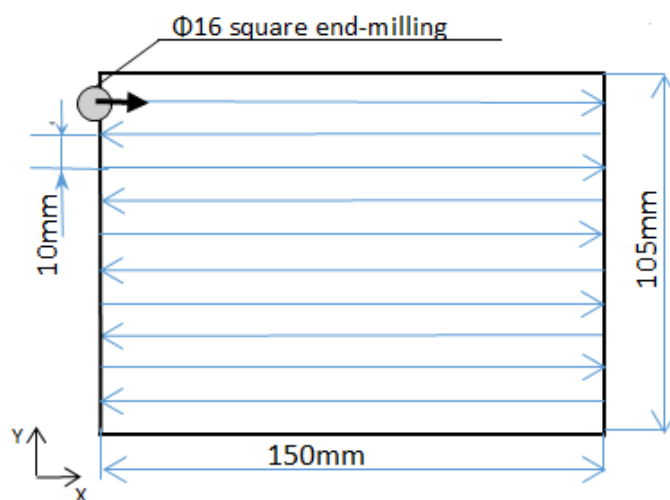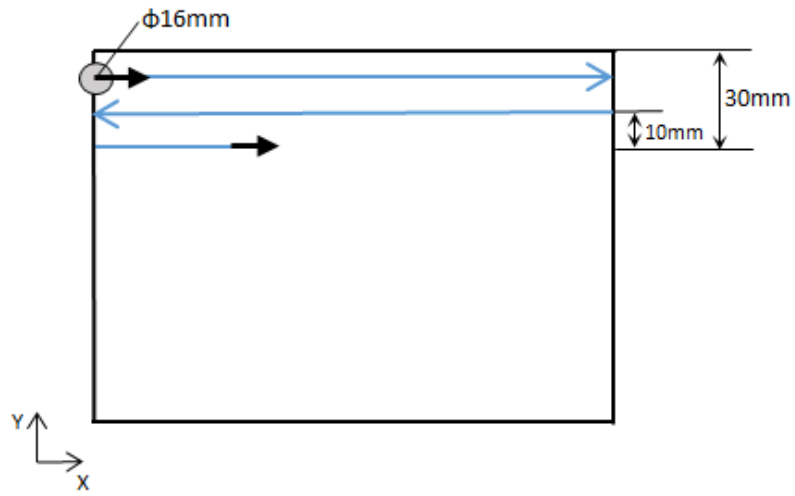

Figure 66 Round-way parallel paths

Figure 67 Round-way parallel paths in 1/4 time
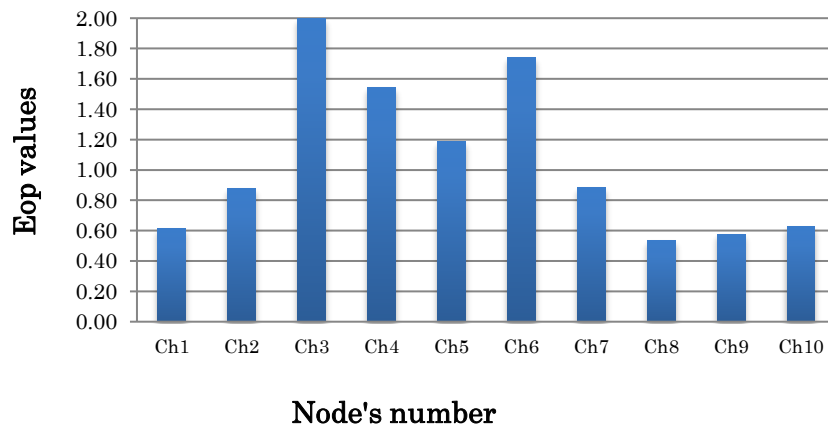
Figure 68 EoP of round-way parallel paths
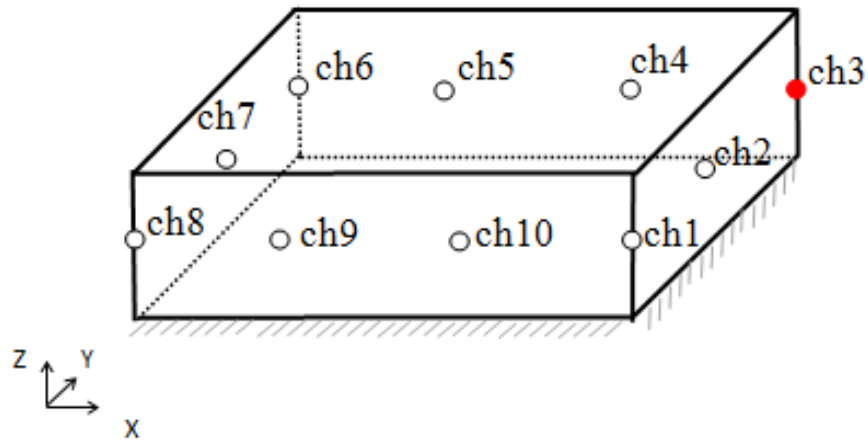
Figure 69 Sensitive point in round-way parallel paths

6.6 Square model 3

As the results shown in one-way and round-way parallel paths, the most sensitivity points found with same points, and then we proposed following walking paths in Figure 70. It is spiral moving paths from middle to side of workpiece; the dotted line means connection between two spiral paths. From the following walking paths showed in Figure 71. It is spiral moving paths from middle to side of workpiece. The dotted line shows the boundary between two spiral paths.
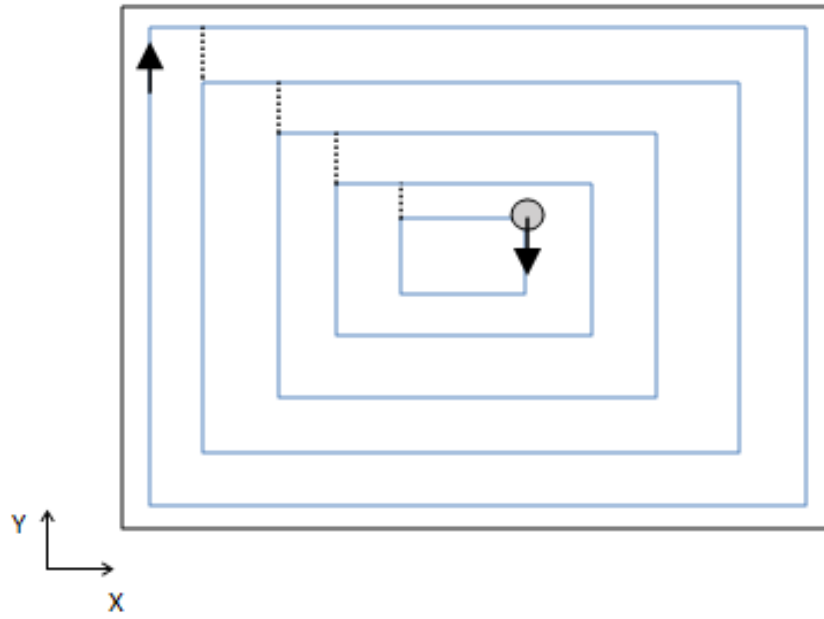
Figure 70 Spiral way Paths
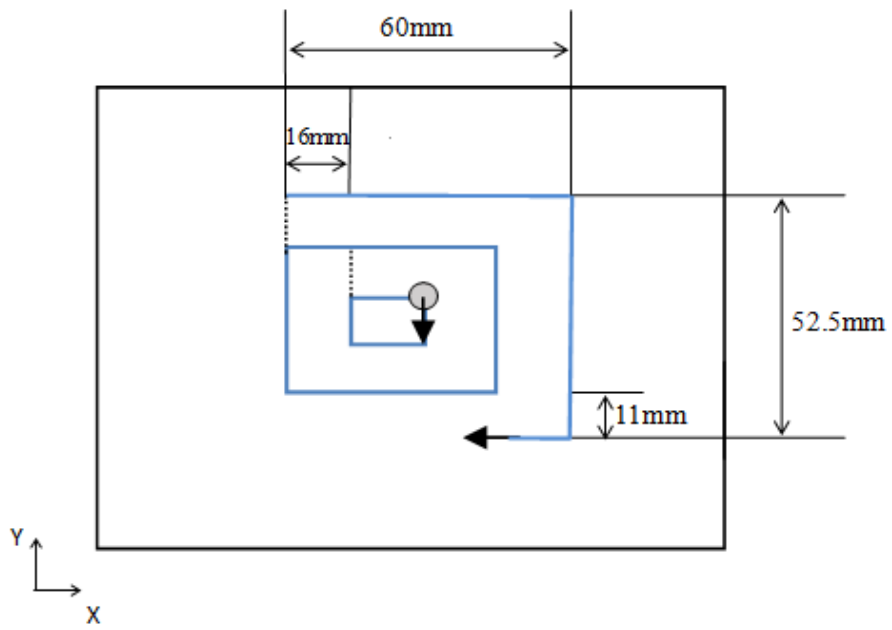
Figure 71 Spiral paths in 1/4 time
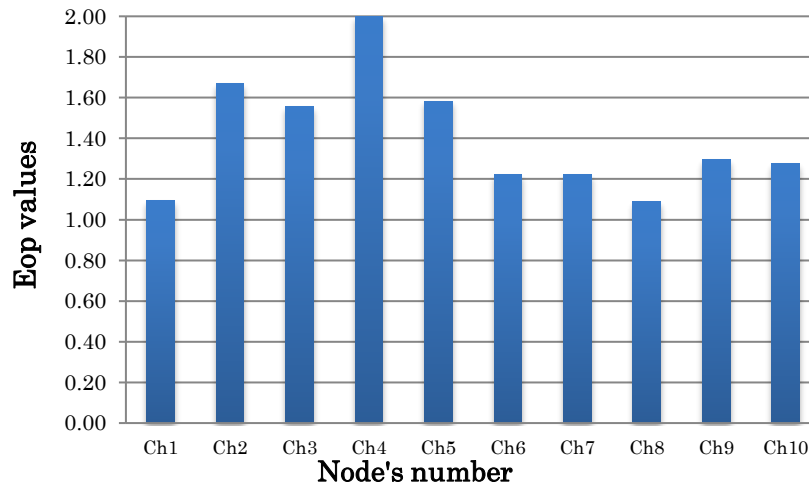
Figure 72 Maximum EoP value of spiral paths

As shown in Figure 72, Ch4 is the most sensitive point in spiral walking paths. Furthermore, Ch2 has a larger value than others in spiral paths. The sensitive point in spiral walking paths in Figure 73 is painted red solid according to the EoP results.
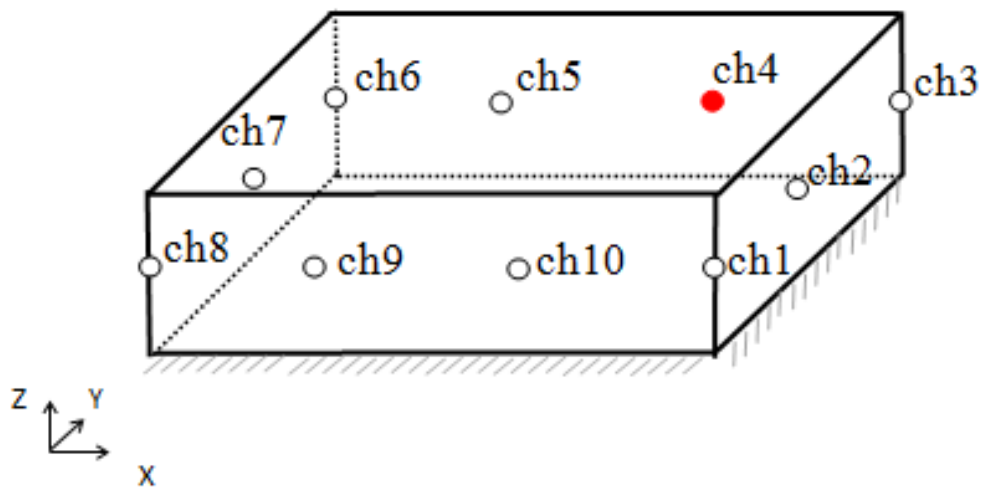
Figure 73 Sensitive point in spiral path

6.7 Calculated EoP value

To evaluate the feasibility of the EoP value, results of inverse analysis which are used different measuring points are investigated. In the reported paper[109] ,a relation between the measuring points and estimation error has been reported. In the research, we had a clear

identification that Ch3 is more sensitive than Ch1 as illustrated in Figure 74 and Figure 75. The estimated error of Ch2 and Ch7 are estimated by Ch6 and Ch3 data, which are smaller than the error of estimated by Ch6 and Ch1 data. Calculated EoP values are consistent to the relation between the measuring points and estimation error which was reported in the previous research. This implies the feasibility of the EoP value.
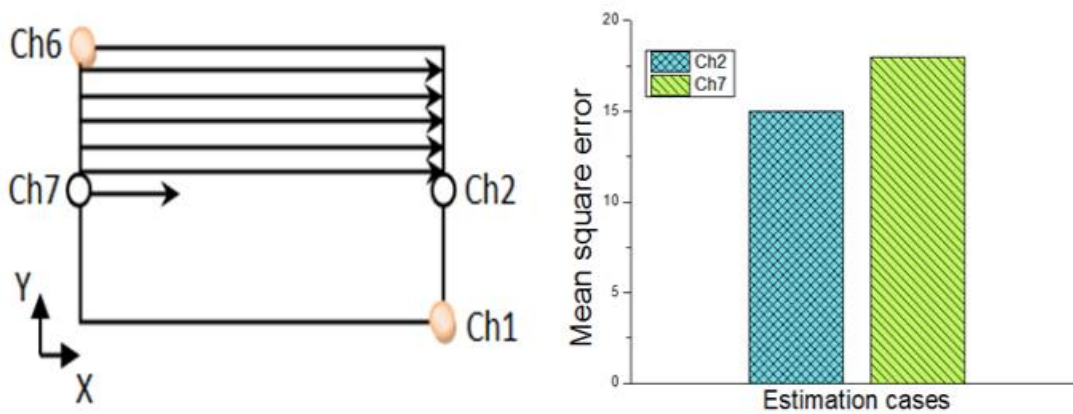
Figure 74 Ch1 and Ch6 as estimation measuring points, Ch2 and Ch7 as evaluation measuring points
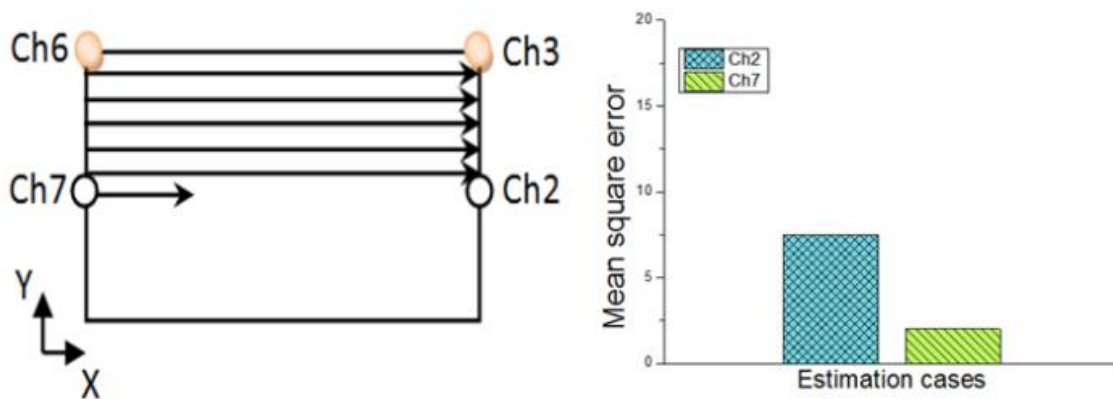
Figure 75 Ch3 and Ch6 as estimation measuring points, Ch2 and Ch7 as evaluation measuring points

6.8 Summary

1. Orthogonal table like parameter set generation was introduced as a simple representation method for process variation.

2. From the comparison of three EoP results of these three paths, three paths of the graph show that the three paths do not have the same results.

3. Results of inverse analysis which used different measuring points were investigated, this implies the feasibility of the EoP value.

7 Conclusion

In this thesis, a systematic approach to monitor the finish machining of NNS parts was discussed. The results are as follows:

1. From the survey of thermal issues in machining research, it became clear the sensor-configured simulation method which combine FE simulation and local measurement combination method is a promising solution to the process monitoring in end-milling. .

2. Thermal process simulation for workpiece temperature calculation is formalized and a FE based simulation system was implemented. Within the allowable error, developed simulation can calculate the temperature distribution of workpiece.

3. Sensitive parameters in process simulation are selected and maximum variation of those parameters are estimated. Moreover, orthogonal table like parameter set generation was introduced as a simple representation method for process variation.

4. By using FEM-based thermal simulation and process variation model, analysis of temperature distribution and sensitivity analysis were carried out. Based on the results of calculation, measurable points for different machining situations are evaluated. As the results, different measuring points were selected according to the change of machining situation. Furthermore, evaluations of points including sensitivity analysis could obtain stable results at a reasonable computational cost.

5. To evaluate the feasibility of the EoP value, results of inverse analysis which used different measuring points were investigated. Calculated EoP values are consistent to the relation between the measuring points and estimation error which was reported.

6. The three EoP results correspond to the three different tool paths were compared.

The distribution of EoP values for each path showed that appropriate measuring points were different. This implies the proposed method can quantify the appropriateness of the measuring points.

Reference

1. Ezugwu, E., *Key improvements in the machining of difficult-to-cut aerospace superalloys.* International Journal of Machine Tools and Manufacture, 2005. **45**(12): p. 1353-1367.

2. Lee, J., et al., *Industry 4.0 and manufacturing transformation.* Manufacturing Leadership Journal, 2015: p. 36-43.

3. Mori, M. and M. Fujishima, *Changeable and Reconfigurable Manufacturing Systems.* 2009, London, Springer-Verlag.

4. Kakino, Y., et al., *Study on Amendable Machining System by Using Machining and Measuring Center (1st Report).* Journal of the Japan Society for Precision Engineering, 1993. **59**(10): p. 1689-1694.

5. TERAMOTO, K., et al., A Framework of Accuracy Assured Machining for Smart Manufacturing. Muroran Institute of Technology Bulletin No. 65 All 1 book, 2016. 65: p. 39.

6. Abe, G., et al., Development of On-Machine measurement system utilizing line laser displacement sensor. Int. J. Autom. Technol, 2011. 5(5): p. 708-714.

7. Jawahir, I., et al., Surface integrity in material removal processes: Recent advances. CIRP Annals-Manufacturing Technology, 2011. 60(2): p. 603-626.

8. Toshimichi, M.E. and W. Lihui, Study on Machining Error Due to Cutting Heat in Endmillimg. Bulletin of the Graduate School of Natural Science, Kobe University. A, 1995. 13: p. 131-140.

9. Hoadley, A. and M. Rappaz, A thermal model of laser cladding by powder injection. Metallurgical transactions B, 1992. 23(5): p. 631-642.

10. Labudovic, M., D. Hu, and R. Kovacevic, A three dimensional model for direct laser metal powder deposition and rapid prototyping. Journal of materials science, 2003. 38(1): p. 35-49.

11. Palumbo, G., S. Pinto, and L. Tricarico, Numerical finite element investigation on laser cladding treatment of ring geometries. Journal of materials processing technology, 2004. **155**: p. 1443-1450.

12. Toyserkani, E., A. Khajepour, and S. Corbin, *3-D finite element modeling of laser cladding by powder injection: effects of laser pulse shaping on the process.* Optics and Lasers in Engineering, 2004. **41**(6): p. 849-867.

13. Ye, R., et al., *Numerical modeling of the thermal behavior during the LENS® process.* Materials Science and Engineering: A, 2006. **428**(1): p. 47-53.

14. Xiong, Y., et al., *In situ thermal imaging and three-dimensional finite element modeling of tungsten carbide–cobalt during laser deposition.* Acta Materialia, 2009. **57**(18): p. 5419-5429.

15. Zhang, C.S., L. Li, and A. Deceuster, *Thermomechanical analysis of multi-bead pulsed laser powder deposition of a nickel-based superalloy.* Journal of Materials Processing Technology, 2011. **211**(9): p. 1478-1487.

16. Cawley, J.D., *Solid freeform fabrication of ceramics.* Current Opinion in Solid State and Materials Science, 1999. **4**(5): p. 483-489.

17. Kalpakjian, S. and S. Schmid, *Manufacturing Processes for Engineering Materials– 5th Edition.* agenda, 2014. **12**: p. 1.

18. Davé, V.R., et al., *Strategy for small-lot manufacturing.* Los Alamos Science, 2003. **28**: p. 63-67.

19. Nakagawa, T., *Advances in prototype and low volume sheet forming and tooling.* Journal of Materials Processing Technology, 2000. **98**(2): p. 244-250.

20. Maurel-Pantel, A., et al., *3D FEM simulations of shoulder milling operations on a 304L stainless steel.* Simulation Modelling Practice and Theory, 2012. **22**: p. 13-27.

21. Man, X., et al., *Validation of finite element cutting force prediction for end milling.* Procedia CIRP, 2012. **1**: p. 663-668.

22. Saffar, R.J., et al., *Simulation of three-dimension cutting force and tool deflection in the end milling operation based on finite element method.* Simulation Modelling Practice and Theory, 2008. **16**(10): p. 1677-1688.

23. Jaeger, J. *Moving sources of hear and the temperature at sliding contacts.* in *J. Proc. Roy. Soc. NSW.* 1942.

24. Jun, M., *Modeling and analysis of micro-end milling dynamics.* 2005, University of Illinois at Urbana-Champaign.

25. Klocke, F., et al., *Analytical Modelling Methods for Temperature Fields in Metal Cutting Based on Panel Method of Fluid Mechanics.* Procedia CIRP, 2015. **31**: p. 352-356.

26. Kapoor, S., *An analytical model for prediction of tool temperature fields during continuous and interrupted cutting.* Urbana, 1994. **51**: p. 61801.

27. Mechant, M., *Basic mechanics of the metal cutting process.* ASME Journal of Applied Mechanics, 1944. **11**: p. 168-175.

28. Piispanen, V., *Theory of formation of metal chips.* Journal of Applied Physics, 1948. **19**(10): p. 876-881.

29. Lee, E. and B. Shaffer, *The theory of plasticity applied to a problem of machining.* Journal of Applied Mechanics, 1951. **18**(4): p. 405-413.

30.   Kudo, H., *Some new slip-line solutions for two-dimensional steady-state machining.* International Journal of Mechanical Sciences, 1965. **7**(1): p. 43-55.

31.   Palmer, W. and P. Oxley, *Mechanics of orthogonal machining.* Proceedings of the Institution of Mechanical Engineers, 1959. **173**(1): p. 623-654.

32.   Oxley, P., A. Humphreys, and A. Larizadeh, *The influence of rate of strain-hardening in machining.* Proceedings of the Institution of Mechanical Engineers, 1961. **175**(1): p. 881-891.

33.   Doyle, E., J. Horne, and D. Tabor. *Frictional interactions between chip and rake face in continuous chip formation.* in *Proceedings of the Royal Society of London A: Mathematical, Physical and Engineering Sciences.* 1979. The Royal Society.

34.   Chao, B. and K. Trigger, *An analytical evaluation of metal cutting temperature.* Trans. ASME, 1951. **73**: p. 57-68.

35.   Usui, E., A. Hirota, and M. Masuko, *Analytical prediction of three dimensional cutting process—Part 1: basic cutting model and energy approach.* Journal of Engineering for Industry, 1978. **100**(2): p. 222-228.

36.   Klamecki, B.E., *Incipient Chip Formation in Metal Cutting: A Three Dimension Finite Element Analysis.* 1996: UMI.

37.   LajczokM, R., *Study ofSom eAspects ofMetalCuttingByTheFiniteElem entMethod.* Ph. DD issertation, N CStateU niversity, 1980, 1~ 20.

38.   Usui, E. and T. Shirakashi, *Mechanics of machining—from descriptive to predictive theory.* On the Art of Cutting Metals–75 Years Later, 1982. **7**: p. 13-35.

39.   Iwata, K., Osakada, K. and Y. Terasaka, *Process modeling of orthogonal cutting by the rigid-plastic finite element method.* Journal of Engineering Materials and Technology, 1984. **106**: p. 133.

40.   Strenkowski, J.S. and J. Carroll, *A finite element model of orthogonal metal cutting.* Journal of Engineering for Industry, 1985. **107**(4): p. 349-354.

41.   Komvopoulos, K. and S. Erpenbeck, *Finite element modeling of orthogonal metal cutting.* Journal of Engineering for Industry(Transactions of the ASME), 1991. **113**(3): p. 253-267.

42.   Lin, Z. and S. Lin, *A coupled finite element model of thermo-elastic-plastic large deformation for orthogonal cutting.* ASME J. Eng. Mater. Technol, 1992. **114**(2): p. 218-226.

43.   Bäker, M., J. Rösler, and C. Siemers, *Finite element simulation of segmented chip formation of Ti6Al4V.* Journal of Manufacturing Science and Engineering, 2002. **124**(2): p. 485-488.

44.   Huang, J. and J. Black, *An evaluation of chip separation criteria for the FEM*

simulation of machining. TRANSACTIONS-AMERICAN SOCIETY OF MECHANICAL ENGINEERS JOURNAL OF MANUFACTURING SCIENCE AND ENGINEERING, 1996. **118**: p. 545-554.

45.   Furukawa, Y. and N. Moronuki, *Effect of material properties on ultra precise cutting processes.* CIRP Annals-Manufacturing Technology, 1988. **37**(1): p. 113-116.

46.   Ikawa, N., S. Shimada, and H. Tanaka, *Minimum thickness of cut in micromachining.* Nanotechnology, 1992. **3**(1): p. 6.

47.   Moriwaki, T., N. Sugimura, and S. Luan, *Combined stress, material flow and heat analysis of orthogonal micromachining of copper.* CIRP Annals-Manufacturing Technology, 1993. **42**(1): p. 75-78.

48.   Lin, Z.-C., et al., *The study of ultra-precision machining and residual stress for NiP alloy with different cutting speeds and depth of cut.* Journal of materials processing technology, 2000. **97**(1): p. 200-210.

49.   GHELASE, D. and L. DASCHIEVICI, *MONITORING AND CONTROL OF MANUFACTURING PROCESS.* Annals of the University Dunarea de Jos of Galati: Fascicle XIV, Mechanical Engineering, 2014(1).

50.   Xiaoli, L., *On-line detection of the breakage of small diameter drills using current signature wavelet transform.* International Journal of Machine Tools and Manufacture, 1999. **39**(1): p. 157-164.

51.   Stavropoulos, P., et al., *Monitoring and control of manufacturing processes: a review.* Procedia CIRP, 2013. **8**: p. 421-425.

52.   Notay, J.K. and G.A. Safdar. *A wireless sensor network based structural health monitoring system for an airplane.* in *Automation and Computing (ICAC), 2011 17th International Conference on.* 2011. IEEE.

53.   Choi, Y.-h., *Process monitoring in end milling.* 2003, Iowa State University.

54.   Rowe, W., *Grinding technology-theory and applications of machining with abrasives: S. Malkin Ellis Horwood Series in Mechanical Engineering, Distributed by Wiley, 1989, 275 pp,£ 49.50.* 1990, Elsevier.

55.   Kovač, P., et al., *A review of machining monitoring systems.* Journal of production Engineering, 2011. **14**(1): p. 1-6.

56.   Brosnan, D.K.a.D., *Manufacture of Near Net Shaped 3-Dimensional Components for Industrial Applications.* Conference on Materials, Tribology and Processing, MATRIB M. Grilec (ed). 2005: p. 23-25.

57.   Joule, J.P., *On the mechanical equivalent of heat.* Philosophical Transactions of the Royal Society of London, 1850. **140**: p. 61-82.

58.   Gottwein, K., *Die Messung der Schneidentemperatur beim Abdrehen von Flusseisen.*

Maschinenbau, 1925. **4**: p. 1129-1135.

59.   Shore, H., *Tool and chip temperatures in machine shop practice*. 1924.

60.   Taylor, F.W., *On the art of cutting metals*. 1907: New York, The American Society of Mechanical Engineers,[1907].

61.   Schmidt, A.O., W.W. Gilbert, and O.W. Boston, *A thermal-balance method and mechanical investigation for evaluating machinability*. 1944: University of Michigan.

62.   Schmidt, A. and J. Roubik, *Distribution of heat generated in drilling.* Trans ASME, 1949. **71**(3): p. 245-252.

63.   Trigger, K. and B. Chao. *An analytical evaluation of metal-cutting temperatures*. 1950. ASME.

64.   Rosenthal, D. *The theory of moving sources of heat and its application to metal treatments*. 1946. ASME.

65.   Leone, W. *Distribution of shear-zone heat in metal cutting*. 1953. ASME.

66.   Loewen, E. and M. Shaw, *On the analysis of cutting tool temperatures.* Trans. ASME, 1954. **76**(2): p. 217-225.

67.   Weiner, J., *Shear-plane temperature distribution in orthogonal cutting.* Trans. ASME, 1955. **77**(8): p. 1331-1338.

68.   Chao, B. and K.J. Trigger. *Temperature distribution at tool-chip and tool-work interface in metal cutting*. 1956. ASME.

69.   Boothroyd, G. and ey, *Temperatures in orthogonal metal cutting.* Proceedings of the Institution of Mechanical Engineers, 1963. **177**(1): p. 789-810.

70.   Maekawa, K., Y. Nakano, and T. Kitagawa, *Finite Element Analysis of Thermal Behaviour in Metal Machining: 2nd Report, Determination of Energy Balance and Its Application to Three-Dimensional Analysis.* JSME international journal. Ser. C, Dynamics, control, robotics, design and manufacturing, 1996. **39**(4): p. 864-870.

71.   Kharkevich, A., K. Weinert, and S. Ostafiev, *Tool heat transfer in orthogonal metal cutting.* Journal of manufacturing science and engineering, 1999. **121**: p. 541.

72.   Huang, Y. and S. Liang, *Cutting forces modeling considering the effect of tool thermal property—application to CBN hard turning.* International journal of machine tools and manufacture, 2003. **43**(3): p. 307-315.

73.   Komanduri, R. and Z.B. Hou, *Thermal modeling of the metal cutting process: part I— temperature rise distribution due to shear plane heat source.* International Journal of Mechanical Sciences, 2000. **42**(9): p. 1715-1752.

74.   Komanduri, R. and Z.B. Hou, *Thermal modeling of the metal cutting process—Part II: temperature rise distribution due to frictional heat source at the tool–chip interface.* International Journal of Mechanical Sciences, 2001. **43**(1): p. 57-88.

75. Komanduri, R. and Z.B. Hou, *Thermal modeling of the metal cutting process—Part III: temperature rise distribution due to the combined effects of shear plane heat source and the tool–chip interface frictional heat source.* International Journal of Mechanical Sciences, 2001. **43**(1): p. 89-107.

76. Komanduri, R. and Z. Hou, *Tribology in metal cutting—some thermal issues.* Journal of tribology, 2001. **123**(4): p. 799-815.

77. Sutherland, J. and R. DeVor, *An improved method for cutting force and surface error prediction in flexible end milling systems.* ASME J. Eng. Ind, 1986. **108**(4): p. 269-279.

78. DeVor, R. and I. Shareef, *The prediction of surface accuracy in end milling.* Trans, of ASME Aug, 1982. **104**(3): p. 272-278.

79. Gray, P., et al., *Comparison of 5-axis and 3-axis finish machining of hydroforming die inserts.* The International Journal of Advanced Manufacturing Technology, 2001. **17**(8): p. 562-569.

80. Oktem, H., T. Erzurumlu, and F. Erzincanli, *Prediction of minimum surface roughness in end milling mold parts using neural network and genetic algorithm.* Materials & design, 2006. **27**(9): p. 735-744.

81. Wang, M.-Y. and H.-Y. Chang, *Experimental study of surface roughness in slot end milling AL2014-T6.* International Journal of Machine Tools and Manufacture, 2004. **44**(1): p. 51-57.

82. Blok, H. *Theoretical study of temperature rise at surfaces of actual contact under oiliness lubricating conditions.* in *Proceedings of the general discussion on lubrication and lubricants.* 1937. Institution of Mechanical Engineers London.

83. Miller, T., *Effect of rake face design on cutting tool temperature distributions.* Journal of Engineering for Industry, 1980. **102**: p. 123.

84. Stephenson, D., T.-C. Jen, and A. Lavine, *Cutting tool temperatures in contour turning: transient analysis and experimental verification.* Journal of Manufacturing Science and Engineering, 1997. **119**(4A): p. 494-501.

85. Tay, A., M. Stevenson, and G. de Vahl Davis, *Using the finite element method to determine temperature distributions in orthogonal machining.* Proceedings of the institution of mechanical engineers, 1974. **188**(1): p. 627-638.

86. Muraka, P., G. Barrow, and S. Hinduja, *Influence of the process variables on the temperature distribution in orthogonal machining using the finite element method.* International Journal of Mechanical Sciences, 1979. **21**(8): p. 445-456.

87. Malkin, S., *Inclined moving heat source model for calculating metal cutting temperatures.* Journal of Engineering for Industry, 1984. **106**: p. 179.

88. Kim, K.W. and H.-C. Sins, *Development of a thermo-viscoplastic cutting model using*

finite element method. International Journal of Machine Tools and Manufacture, 1996. **36**(3): p. 379-397.

89. Mamalis, A., et al., *Finite element simulation of chip formation in orthogonal metal cutting.* Journal of Materials Processing Technology, 2001. **110**(1): p. 19-27.

90. Özel, T. and T. Altan, *Process simulation using finite element method—prediction of cutting forces, tool stresses and temperatures in high-speed flat end milling.* International Journal of Machine Tools and Manufacture, 2000. **40**(5): p. 713-738.

91. Grzesik, W., *Determination of temperature distribution in the cutting zone using hybrid analytical-FEM technique.* International Journal of Machine Tools and Manufacture, 2006. **46**(6): p. 651-658.

92. Umbrello, D., R. M'saoubi, and J. Outeiro, *The influence of Johnson–Cook material constants on finite element simulation of machining of AISI 316L steel.* International Journal of Machine Tools and Manufacture, 2007. **47**(3): p. 462-470.

93. Ng, E.-G., et al., *Modelling of temperature and forces when orthogonally machining hardened steel.* International Journal of Machine Tools and Manufacture, 1999. **39**(6): p. 885-903.

94. Hargrove, S.K. and D. Ding, *Determining cutting parameters in wire EDM based on workpiece surface temperature distribution.* The International Journal of Advanced Manufacturing Technology, 2007. **34**(3-4): p. 295-299.

95. Song, B., et al., *Process parameter selection for selective laser melting of Ti6Al4V based on temperature distribution simulation and experimental sintering.* The International Journal of Advanced Manufacturing Technology, 2012. **61**(9): p. 967-974.

96. Liu, Y.-R., et al., *The computer simulation of the temperature distribution on the surface of ceramic cutting tools.* Wear, 1997. **210**(1): p. 39-44.

97. *Metal Cutting Effective Technology. 1988: Machinery Works Edition*

98. *Jiang, F., Investigation of transient cutting temperature of workpiece and cutting tool in high speed intermittent. Shangdong University, 2015.*

99. O.RyabovK.MoriN.KasashimaK.Uehara, *An In-Process Direct Monitoring Method for Milling Tool Failures Using a Laser Sensor.* CIRP Annals, 1996. **45**(1).

100. Lanzetta, M., *A new flexible high-resolution vision sensor for tool condition monitoring.* Journal of Materials Processing Technology, 2001. **119**(1): p. 73-82.

101. Lee, B., *Application of the discrete wavelet transform to the monitoring of tool failure in end milling using the spindle motor current.* The International Journal of Advanced Manufacturing Technology, 1999. **15**(4): p. 238-243.

102. Kobayashi, C.H.L.a.S., *New Solutions to Rigid-Plastic Deformation Problems Using a Matrix Method.* Journal of Engineering for Industry, 1973. **95**(3): p. 865-873.

103. Mróz, N.a.Z., *Application of an anisotropic hardening model in the analysis of elasto–plastic deformation of soils.* Géotechnique, 1979. **29**(1): p. 1-34.

104. Taylan Altan, B.L.a.Y.C.Y., *Manufacturing of Dies and Molds* CIRP Annals-Manufacturing Technology, 2001. **Volume 50**(Issue 2): p. 404-422.

105. Hou, R.a.Z.B., *Thermal modeling of the metal cutting process — Part III: temperature rise distribution due to the combined effects of shear plane heat source and the tool–chip interface frictional heat source.* International Journal of Mechanical Sciences, 2001. **43**(1): p. 87-107.

106. Baohai, W., et al., *Cutting tool temperature prediction method using analytical model for end milling.* Chinese Journal of Aeronautics, 2016. **29**(6): p. 1788-1794.

107. El-Ali, J., et al., *Simulation and experimental validation of a SU-8 based PCR thermocycler chip with integrated heaters and temperature sensor.* Sensors and Actuators A: Physical, 2004. **110**(1): p. 3-10.

108. Capriccioli, A. and P. Frosi, *Multipurpose ANSYS FE procedure for welding processes simulation.* Fusion Engineering and Design, 2009. **84**(2): p. 546-553.

109. Koji Teramoto, R.T., Tohru Ishida and Yoshimi Takeuchi, *Thermal State Visualization of Machining Workpiece by Means of a Sensor-Configured Heat Conduction Simulation.* JSME International Journal Series C Mechanical Systems, Machine Elements and Manufacturing,, 2006. **Vol. 49.** (No. 2 (2006)): p. 287-292.

110. Teramoto, K., et al., *Thermal State Visualization of Machining Workpiece by Means of a Sensor-Configured Heat Conduction Simulation.* JSME International Journal Series C Mechanical Systems, Machine Elements and Manufacturing, 2006. **49**(2): p. 287-292.

111. Denkena, B., et al., *Prediction of temperature induced shape deviations in dry milling.* Procedia CIRP, 2015. **31**: p. 340-345.

112. Joliet, R., et al., *Validation of a heat input model for the prediction of thermomechanical deformations during NC milling.* Procedia CIRP, 2013. **8**: p. 403-408.

113. Bäker, M., *A New Method to Determine Material Parameters from Machining Simulations Using Inverse Identification.* Procedia CIRP, 2015. **31**: p. 399-404.

114. Wernsing, H. and C. Büskens, *Parameter identification for finite element based models in dry machining applications.* Procedia CIRP, 2015. **31**: p. 328-333.

115. Van Houten, F. and F. Kimura, *The virtual maintenance system: a computer-based support tool for robust design, product monitoring, fault diagnosis and maintenance planning.* CIRP Annals-Manufacturing Technology, 2000. **49**(1): p. 91-94.

116. Ozisik, M. and D. Tzou, *On the wave theory in heat conduction.* Journal of Heat Transfer, 1994. **116**(3): p. 526-535.

117. Hahn, R.S. *On the temperature developed at the shear plane in the metalcutting*

process. in *Journal of Applied Mechanics-Transactions of the ASME.* 1951. ASME-AMER SOC MECHANICAL ENG 345 E 47TH ST, NEW YORK, NY 10017.

118. Mass, D.R.a.C., *The Theory of Moving Sourcesof Heat and Its Application to Metal Treatments.* Transactions of ASME, 1946. **68**: p. 849–866.

119. Huang, Y.a.L., S.Y., *Modelling of the cutting temperature distribution under the tool flank wear effect.* Proceedings of the Institution of Mechanical Engineers, Part C: Journal of Mechanical Engineering Science, 2003. **217**(11): p. 1195-1208.

120. Lin, S., et al., *An investigation of workpiece temperature variation in end milling considering flank rubbing effect.* International Journal of Machine Tools and Manufacture, 2013. **73**: p. 71-86.

121. Jen, T.-C., S. Eapen, and G. Gutierrez, *Nonlinear numerical analysis in transient cutting tool temperatures.* TRANSACTIONS-AMERICAN SOCIETY OF MECHANICAL ENGINEERS JOURNAL OF MANUFACTURING SCIENCE AND ENGINEERING, 2003. **125**(1): p. 48-56.

122. Jermolajev, S., C. Heinzel, and E. Brinksmeier, *Experimental and analytical investigation of workpiece thermal load during external cylindrical grinding.* Procedia CIRP, 2015. **31**: p. 465-470.

123. Outwater, J. and M. Shaw, *Surface temperatures in grinding.* Trans. Asme, 1952. **74**(1): p. 73.

124. Zhou, J., M. Andersson, and J.-E. Ståhl, *Identification of cutting errors in precision hard turning process.* Journal of Materials Processing Technology, 2004. **153**: p. 746-750.

125. Dogra, M., et al., *Tool wear, chip formation and workpiece surface issues in CBN hard turning: A review.* International Journal of Precision Engineering and Manufacturing, 2010. **11**(2): p. 341-358.